ILLUMINATING THE BLACK BOX: ASPECTS OF *ELIZABETHKINGIA* EPIDEMIOLOGY AND ANTIMICROBIAL RESISTANCE

By

WILLIAM L. JOHNSON

Master of Science in Biology
New Mexico State University
Las Cruces, New Mexico
2014

Master of Public Health in Epidemiology
University of Colorado, Denver
Denver, Colorado
2016

Submitted to the Faculty of the
Graduate College of the
Oklahoma State University
in partial fulfillment of
the requirements for
the Degree of
DOCTOR OF PHILOSOPHY
May, 2020

ILLUMINATING THE BLACK BOX: ASPECTS OF

ELIZABETHKINGIA EPIDEMIOLOGY

AND ANTIMICROBIAL

RESISTANCE

Dissertation Approved:

Dr. John E. Gustafson

Dissertation Adviser

Dr. Patricia Canaan

Dr. Donald Ruhl

Dr. Charles Chen

Dr. Erika Lutter

ACKNOWLEDGEMENTS

First and foremost, I would like to thank Dr. John E. Gustafson, my mentor and advisor. Without his invitation to join his laboratory as an undergraduate at the lowest point in my academic career, I would not be writing the dissertation you are now reading. Words will never adequately convey the profound gratitude I have for the many years of sound advice he has provided me.

I would also like to thank the fantastic members of my committee, all of whom have provided invaluable advice over the years, and have made this process as close to painless as such things can be. I will continue to value your wisdom and advice long after I depart OSU. I would also like to thank all of the many friends and colleagues I have met while a member of the Biochemistry and Molecular Biology Department.

I would like to thank the current and former members of the Gustafson laboratory, particularly Dr. Nathanial Torres.

I would like to thank my family, particularly my parents Bill and Emily for their patience and encouragement as I navigated a winding and frequently rocky academic career. Without their support none of this would have been possible. Finally, I would like to especially thank my brother Peter, who has been my best friend, supporter, ear for cathartic complaining, and source of encouragement trough this journey.

Name: WILLIAM L. JOHNSON

Date of Degree: MAY, 2020

Title of Study: ILLUMINATING THE BLACK BOX: ASPECTS OF

ELIZABETHKINGIA EPIDEMIOLOGY AND ANTIMICROBIAL RESISTANCE

Major Field: BIOCHEMISTRY AND MOLECULAR BIOLOGY

Abstract: *Elizabethkingia* are emerging Gram negative opportunistic pathogens and the etiologic agents of community- and hospital-associated outbreaks in immunocompromised patients. These organisms are notable for the multiply-antibiotic resistant phenotypes all known members express. While vancomycin is normally ineffective against infections caused by Gram negative organisms, this antibiotic has been reported to effectively treat *Elizabethkingia* infections. Despite increasing interest in these organisms, the epidemiology, along with mechanisms by which antimicrobial agents, particularly vancomycin, may act on these organisms, and how these organisms might acquire resistance to vancomycin, remains poorly understood.

I initially investigated the genomic and antimicrobial profiles of two *Elizabethkingia anophelis* isolates associated with horses. Next, to better understand the interaction of antimicrobial agents, particularly vancomycin, with *Elizabethkingia*, I challenged a collection of 21 isolates, including 2 isolates from horses in Oklahoma, representing the 6 currently described species with vancomycin alone and in combination with other antibiotics. I then assessed how vancomycin challenge impacts the type strain of *Elizabethkingia anophelis*, R26, using RNAseq. Finally, I investigated the mutations underlying vancomycin resistance and the physiological consequences of these mutations by selecting 8 vancomycin-resistant mutants from 2 different *Elizabethkingia* species.

Whole genome sequence analysis revealed that the two horse-associated isolates are clonal and closely related to human clinical *E. anophelis isolates*. These isolates displayed antimicrobial susceptibility profiles that were similar to *E. anophelis* isolates from human infections in the United States, including susceptibility to fluoroquinolones and resistance to all tested cell wall active antimicrobials. The other projects revealed that vancomycin acts as a bactericidal agent, and likely kills *Elizabethkingia* through an inhibition of peptidoglycan biosynthesis, and induces a stress response that shares many characteristics of the oxidative stress response. Mutations associated with resistance to vancomycin rapidly arose after a single vancomycin challenge, and these mutants demonstrated altered susceptibility to other antimicrobials and antimicrobial combinations. These mutations uncovered in the vancomycin-resistant mutants occurred in an array of genes, suggesting that vancomycin resistance can arise via multiple pathways. This dissertation represents a collection of research that produced data to allow for multiple courses of future research.

TABLE OF CONTENTS

LIST OF TABLES

Table Page

LIST OF FIGURES

Figure Page

CHAPTER 1

INTRODUCTION AND REVIEW OF THE LITERATURE

1.1 The *Elizabethkingia*

1.1.1 Overview

Elizabethkingia are Gram-negative opportunistic pathogens and the etiologic agents of hospital- and community-acquired infections worldwide [1-4]. These organisms are widely distributed and have been found in diverse environments including the surface of corn leaves [5], condensation on the Mir space station, soils [6], the digestive systems of multiple organisms [7-12], contact lens solutions, and water supply systems such as faucets and reservoirs [13]. *Elizabethkingia* have been associated with infections in dogs [14], frogs [15, 16], fish [17], and humans [1, 2, 18-26].

Originally described by Elizabeth King in 1959, *Elizabethkingia* were initially placed within the genus *Flavobacterium* as *Flavobacterium meningosepticum* [27]. New isolates were initially grouped by serum agglutination assay, although this technique was subsequently displaced by DNA – DNA hybridization studies which added 4 new species in addition to *F. meningosepticum* [28]. New isolates were frequently described as new species without reference to the existing genomospecies [29], which further confused the

taxonomy of the *Elizabethkingia* and led to the final revision, where the *Elizabethkingia* genus was formed with *Elizabethkingia anophelis* and *Elizabethkingia endophytica*, along with *E. meningoseptica* and *E. miricola*. Doijad *et al.* [30], and Nicholson *et al*. [29] utilized whole genome sequencing and the average nucleotide identity measurement to further refine the taxonomy of the *Elizabethkingia*, with the former determining that *E. endopyhtica* was a subspecies of *E. anophelis* while the latter characterized the original genomospecies which were transferred to the six species that currently comprise the genus (Figure 1). A proposed seventh species consisting of a single isolate identified by whole genome sequencing [31].

From a clinical prespective, the speciation of *Elizabethkingia* is complicated as these organisms do not show consistent phenotypic differences that can be used to differentiate these species, and similar problems are encountered when using common molecular identification techniques such as 16S rRNA sequencing or MALDI-TOF mass spectrometry [29, 32, 33]. All *Elizabethkingia* isolates sequenced to date contain five 16S rRNA genes which can demonstrate considerable differences from each other in the same organism, and can even harbor 16S sequences that are more related to completely different species [29]. The manufacturer's libraries that are provided with most MALDI-TOF machines are presently only able to distinguish *E. meningoseptica* at the species level [29, 32]. The Centers for Disease Control and Prevention (CDC) has released updated MALDI-TOF libraries that are able to differentiate *E. anophelis* from *E. meningoseptica*, but accurate identification of the remaining four species remains a

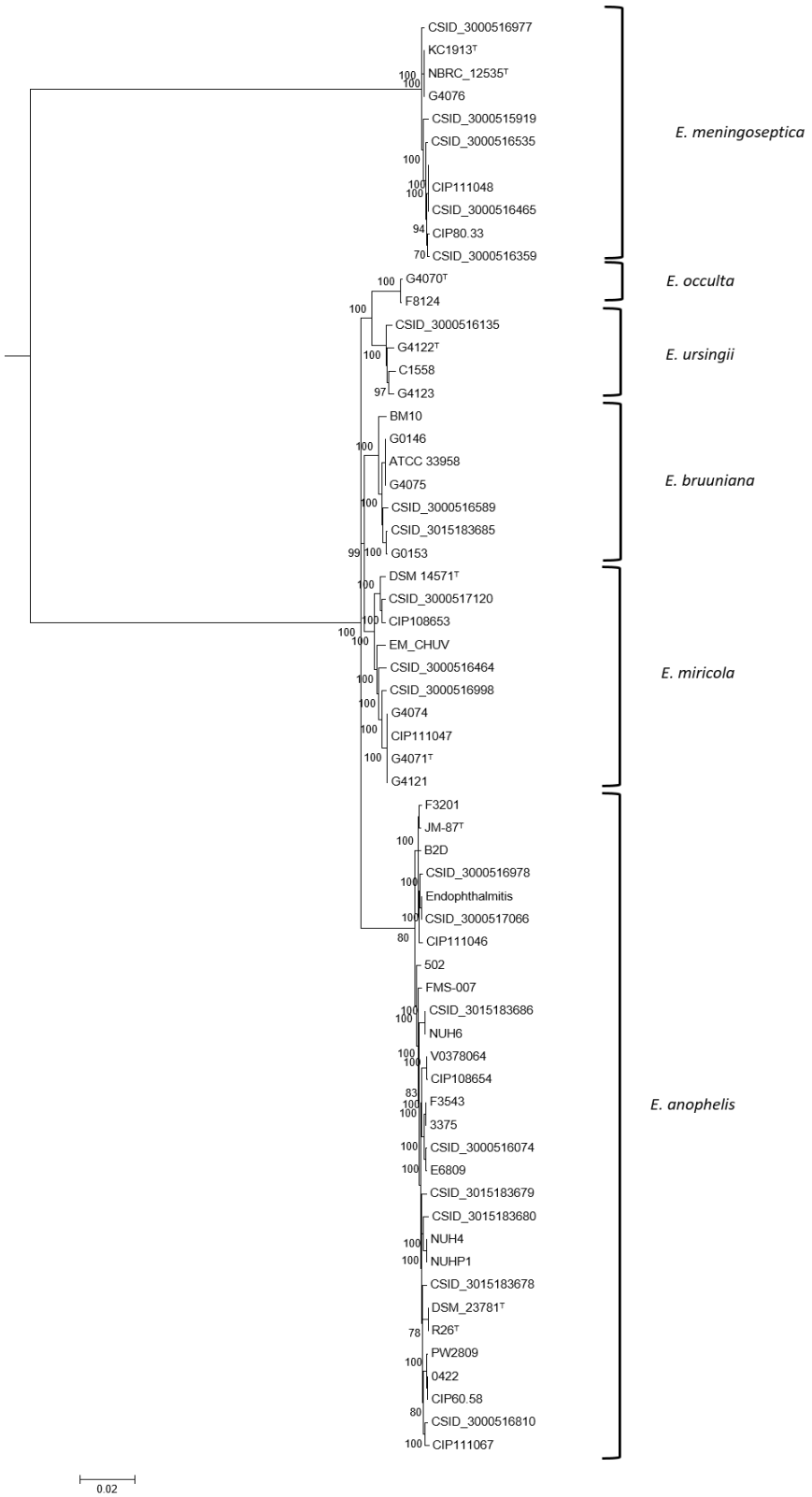

Figure 1. Whole genome single nucleotide polymorphism phylogenetic tree showing the six *Elizabethkingia* species from Nicholson *et al.* [29]. Reprinted by permission from Springer Nature Publishing (Appendix A).

challenge [29]. *RpoB* sequencing is more reliable, and was able to accurately identify all six species, although some difficulties were reported within *E. bruuniana*, and the CDC has released an updated *rpoB* alignment package to aid in better identification of *Elizabethkingia* isolates by Sanger sequencing [29].

1.1.2 Epidemiology of *Elizabethkingia*

All six currently described species of *Elizabethkingia* are known to cause infections in humans [2, 18, 19, 21, 22, 26, 34-37]. These organisms typically infect immunocompromised individuals, particularly neonates [2]. Infections primarily manifest as meningitis, although sepsis, endophthalmitis, necrotizing fasciitis, and pneumonia have been reported [18, 21-24, 26, 36, 38-63]. Infections caused by *Elizabehtkingia* result in high mortality rates, with reports ranging from 25% to as high as 75% [1, 35]. *Elizabethkingia* infections can manifest as isolated cases that typically occur in hospitals and can also occur as larger scale outbreaks in both the community and hospital settings [4, 35]. The largest outbreak of *Elizabethkingia* to date was reported in Wisconsin during 2015 to 2016 and would eventually grow to a total of 65 cases including one case each in Illinois and Minnesota and resulted in 20 deaths [4]. Both incidence and prevalence of *Elizabethkingia* infections are poorly understood, although there are reports that suggest the incidence of infection is increasing [21, 44, 64-66]. Hsu *et al.* [44] have conducted the most complete epidemiological survey to date, and report that the incidence of infection in Taiwan has increased significantly from 7.5 cases per 100,000 admissions in 1996 to 35.6 cases per 100,000 admissions in 2006, a five-fold increase in 10 years. Similar results were reported in South Korea by Choi *et al.* [21],

with the incidence increasing from 2 per 100,000 admissions in 2009 to 88 per 100,000 admissions in the first half of 2017.

1.1.3 Antimicrobial resistance in *Elizabethkingia*

The most widely used classification scheme has β-lactamases divided into 4 major classes, with Class A, Class C, and Class D containing active site serine β-lactamases, while Class B contains the metallo-β-lactamases which have at least 1 Zn^{2+} atom in their active sites [67]. These groups are differentiated by conserved amino acid sequences in the case of Classes A, C, and D, or by sensitivity to Zn^{2+} chelation in the case of Class B [68]. These enzymes can be further differentiated into enzymes that are narrow spectrum or extended spectrum, which reflects the ability of the enzyme to hydrolyze multiple classes of β-lactam ring containing antibiotics, and all 4 Classes have both narrow and extended spectrum β-lactamase enzymes [67-69].

Elizabethkingia are known to be resistant to the majority of β-lactam antibiotics as well as most cephalosporins and carbapenems, and are notable in that they express three different β-lactamases: Class A serine β-lactamase *C. meningosepticum* Extended Spectrum β-Lactamase (CME) [70], along with two metallo-β-lactamases, the Class B1 BlaB [71], and the Class B3 GOB [72]. All of these β-lactamases demonstrate broad specificities for different β-lactam antibiotics, and differences in the expression of these enzymes within *Elizabethkingia* have been reported [71-73]. In addition to the three characterized β-lactamases, bioinformatics suggests that these organisms may also contain Class D and Class C serine β-lactamases [4, 5, 7, 9, 10, 12, 37, 61, 74-81], although due to the significant similarities between β-lactamases and penicillin binding

proteins it is unclear if these are functional β-lactamases or are penicillin binding proteins or other serine hydrolases [82].

While all characterized *Elizabethkingia* isolates demonstrate resistance to aminoglycoside antibiotics, resistance to other antibiotics is variable, with a higher prevalence of resistance to fluoroquinolones reported from countries in Asia than elsewhere [4, 18, 21, 25, 26, 36, 44, 46-48, 52, 62, 76, 83-85], although the lack of large scale studies in other areas severely limits our understanding of antimicrobial susceptibility in this genus. Variable levels of susceptibility are also reported for trimethoprim + sulfamethoxazole (6% susceptible to 92% susceptible), piperacillin and piperacillin in combination with tazobactam (15% - 100% and 5% - 100%, respectively), and tigecycline (5% - 55%) [4, 18, 19, 21, 25, 26, 36, 44, 46-48, 52, 62, 76, 83-89]. *Elizabethkingia* are frequently reported to be susceptible to amikacin, minocycline, and rifampin, although isolates resistant to these antibiotics have also been reported [4, 18, 19, 21, 25, 26, 36, 44, 46-48, 52, 62, 76, 83-89]. Efflux can play a key role in antibiotic resistance and function by transporting antibiotics from the cell cytoplasm or periplasm to the outside of the cell [90-92]. Efflux pumps are characterized depending on the specific organization of the genes in the system as belonging to five families: ATP-Binding Casette (ABC) [93], Major Facilitator Superfamily (MFS) [94, 95], Multidrug and Toxic compound Extrusion (MATE) [96], Resistance-Nodulation-cell Division (RND) [97], and Small Multidrug Resistance (SMR) [98]. Whole genome sequencing of *Elizabethkingia* isolates reveals putative genes encoding for all of these systems, although to date there

has been no biochemical confirmation of these systems functioning as drug efflux pumps in the *Elizabethkingia*.

Despite the well-established inability of vancomycin to inhibit Gram-negative bacilli *in vitro* [99], the drug has been used clinically to treat serious *Elizabethkingia* infections with variable success. Based on Kirby-Bauer disk diffusion susceptibility data, George *et al*. [100] used vancomycin to treat six infants with *Elizabethkingia* infections and three of these infants died. Plotkin and McKitrick [55] also described a case of neonatal meningitis that was treated successfully with vancomycin. More favorable results were reported amongst *Elizabethkingia* infections in non-neonatal patients, where all three cases treated exclusively with vancomycin survived [48, 54, 101]. When used to treat *Elizabethkingia* infections vancomycin is more frequently used in combination, with rifampin and ciprofloxacin being the most common partners. Like treatment with vancomycin alone, combination therapy seems to show some clinical efficacy, with 16 out of 20 reported cases surviving when treated with vancomycin combination therapies [49, 89, 102-104]. It should be noted, however, that any assessment of vancomycin as a stand-alone treatment or in combination is complicated by the small number of reported cases along with potential bias among those cases that are reported.

The assessment of vancomycin susceptibility in *Elizabethkingia* is complicated by the lack of uniform standards for interpreting the results of Kirby-Bauer or minimum inhibitory concentration (MIC) assays [105]. As a result, both Kirby-Bauer disk diffusion assays and MIC assays have been interpreted using guidelines established by the Clinical

and Laboratory Standards Institute (CLSI) for *Staphylococcus aureus*, which in turn has led to contradictory susceptibility results. In 1971, for example, the first report suggesting that the Kirby-Bauer assay significantly underestimated the resistance of *Elizabethkingia* to vancomycin was published by Aber *et al*. [86], and several other reports confirming this discrepancy followed [105-107]. Even with these reports, vancomycin remains a drug of choice to treat *Elizabethkingia* infections as recently as 2018 [102].

1.2 Companion and food animals as a source of antimicrobial-resistant organisms

It has been well documented that both food and companion animals may serve as reservoirs for antibiotic-resistant bacterial pathogens [26-34]. Matyi *et al.* [26] isolated a methicillin-resistant *S. aureus* (MRSA) strain from a dairy cow undergoing antibiotic treatment that was virtually identical to a clinical MRSA strain isolated from a human at the genomic level. Voss *et al.* [27] demonstrated a much greater prevalence rate for MRSA carriage among pig farmers and Lozano *et al.* [28] reported carriage of identical MRSA clones by pigs and pig farmers. Bates *et al.* [29] isolated vancomycin-resistant *Enterococcus faecium* strains from pigs that shared the same ribotype as isolates from hospital patients. With regard to companion animals, Guardabassi *et al.* [30] detected similar antibiotic-resistant clones of *Staphylococcus intermedius* in humans and dogs, while Damborg *et al.* [33] detected quinolone-resistant *Campylobacter jejuni* with identical pulsed-field gel electrophoresis signatures in a young patient and her dog. In addition, Bordelo *et al.* [34] isolated *E. meningoseptica* from a dog suffering from

bacteremia, and it is possible that farm and/or companion animals can also act as reservoirs for *Elizabethkingia* that cause infections.

1.3 Vancomycin

1.3.1 History of vancomycin

Vancomycin was isolated from *Streptomyces orientalis* in 1955 and quickly noted for the strong inhibitory effect exerted on Gram-positive cocci [99]. Preliminary investigation suggested that vancomycin functioned as an inhibitor of RNA synthesis in *S. aureus* [108], however subsequent investigations rapidly identified peptidoglycan biosynthesis as the primary target of vancomycin [109, 110]. It is now well established that vancomycin inhibits the transpeptidation reaction linking new peptidoglycan polymers to the existing cell wall by binding the terminal D-Ala-D-Ala residues on the pentapeptide stem [111-114]. Fairbrother and Williams [99] tested the activity of vancomycin against 1,350 bacterial isolates by Kirby-Bauer disk diffusion assay and noted that while all of the Gram-positive organisms tested were inhibited by vancomycin, it was only marginally effective against Gram-negative cocci, and completely ineffective against Gram-negative bacilli.

The cell envelope of Gram-negative organisms includes an outer membrane (OM) which consists of an outer lipopolysaccharide leaflet over an inner phospholipid leaflet which hinders penetration of many antimicrobials into the periplasmic space [115]. Embedded within the OM are outer membrane porins (OMPs) which function as channels that allow for the ingress of small molecules (< 600 Daltons in *Escherichia coli*), while

excluding larger molecules such as vancomycin (~1446 Daltons) [116-118]. *E. coli* mutants with mutations in OMPs or porin assembly that lead to increased OM permeability demonstrate significant increases in susceptibility to large antimicrobials, including vancomycin [119-121]. Krishnamoorthy *et al.* [122] demonstrated that vancomycin susceptibility was increased in *E. coli* constructs overexpressing a modified *fhuA* OMP lacking the N-terminal plug domain, allowing free diffusion of hydrophilic substances across the OM. They further demonstrated that disruption of *tolC*, which produces a periplasmic channel that works in concert with instrinsic antimicrobial efflux pumps, led to no discernable changes in vancomycin MICs. These results suggest that vancomycin susceptibility in *E. coli* is governed OM permeability alone.

In addition, Zhou *et al.* [123] found that both nitrofurantoin and trimethoprim displayed synergy with vancomycin against *E. coli* growth. These authors also hypothesized that since other cell wall biosynthesis inhibitors demonstrated antagonism with nitrofurantoin or trimethoprim, that vancomycin may be acting on pathways other than peptidoglycan biosynthesis. Intriguingly, Kang *et al*. [124] reported that the vancomycin MIC of an *E. coli* mutant defective in the synthesis of thymidine through the deletion of the deoxycytidine deaminase gene *dcd* decreased 8-fold when compared to the parent strain. This increase in vancomycin susceptibility was further enhanced by the addition of cytidine but could be reversed by the addition of thymine to the growth medium, and the authors speculate that small amounts of vancomycin may penetrate to the cytoplasm causing oxidative damage to DNA [124, 125]. These findings raise the possibility that vancomycin may act on Gram-negative cells outside peptidoglycan

biosynthesis inhibition and underscores the importance of understanding how vancomycin interacts with Gram-negative cells such as *Elizabethkingia*.

1.3.2 Transcriptional profiling of cells challenged with vancomycin

While to the best of our knowledge no transcriptional profiling has been done for Gram-negative organisms challenged with vancomycin, the transcriptional response of Gram-positive cells has been studied. Vancomycin challenge significantly upregulates the two component sensor system *vraRS,* which functions as the primary sensor of cell wall stress in Gram-positive organisms [126]. Other genes that are found to be significantly upregulated during vancomycin exposure include components of the phosphotransferase system, members of the proline/glycine – betaine transport system, amino acid biosynthesis pathways including glutamate, cysteine, histidine, lysine, threonine, serine, and valine/isoleucine [127]. Genes encoding putative amino acid and oligopeptide transporters and the Krebs cycle components *citB*, *citC*, and *citZ* were also significantly upregulated [127-130]. Penicillin binding protein (PBP) 2 was found to be significantly upregulated in multiple studies [127-130], while other components the cell wall stress response stimulon were more variable [127-130]. Genes involved in cell division, replication, tRNA modification enzymes, autolysins, hemagglutinin proteins, and antigens *ssaA* and *isaA* were found to be downregulated in multiple studies [127-130].

1.4 Cell wall stress response in Gram-negative organisms

Gram-negative organisms are surrounded by a complex cellular envelope consisting of the asymmetric outer membrane, a thin peptidoglycan layer, and the inner membrane [131]. Some organisms also produce a polysaccharide capsule which covers the outer membrane and functions to protect the cell from harmful conditions encountered in the environment. The integrity of this envelope is critical to the survival of cells in the face of changing environmental factors, stressors, predation, and potential antimicrobial challenge. Of particular importance is the integrity of the peptidoglycan layer, as this is the primary structure that helps cells to resist osmotic pressure, and defines cell shape. Unlike the *vraRS* two component sensor system in Gram-positive bacteria [126] there is no known single stress response sensor system in Gram-negative cells with the primary function of detecting cell wall damage [132]. Instead, Gram-negative organisms have five main cell envelope stress sensor systems: (Cpx) [133, 134], bacterial adaptive response (Bae) [135], regulator of capsule synthesis (Rcs) [136], Rse, and phage shock protein (Psp) systems. Of these systems, the Cpx and Rcs systems appear to be the most responsive to peptidoglycan-associated stresses [133, 136]. The Cpx system is a classic two component sensor system, with *cpxA* encoding for the histidine sensor kinase component while *cpxR* encodes the response regulator [134, 137]. This system has two accessory genes: *cpxP* encodes a negative regulator of the *cpxRA* system, while *nlpE* encodes an outer membrane lipoprotein that aids in the detection of protein sorting and membrane associated protein defects [134]. This system is considered the primary cell envelope quality control system as CpxA and NlpE function to detect problems with protein folding in both the outer membrane and the periplasmic

space [133, 137]. CpxR is known to induce the production and transport into the periplasmic space of chaperones and proteases [133, 134, 137]. The Rcs system is more complex, with *rcsC* encoding the membrane associated sensor histidine kinase and *rcsB* encoding the primary response regulator [136, 138]. Activation of RcsB does not occur directly from RcsC, but is rather transduced through another membrane bound protein, RcsD [138, 139]. Both RcsC and RcsD are bound by another accessory protein IgaA which keeps these sensors in an inactive state and blocks the phosphorylation of RcsB [138-140]. A second sensor, RcsF, is located in the outer membrane and serves as the initiator of the signal cascade by binding to IgaA, which in turn releases RcsC and RcsD, which can then activate RcsB [139, 140]. RcsB can function as a homodimer, or it can dimerize with RcsA to form a heterodimer that is known to activate the expression of genes involved in the synthesis of capsular polysaccharides [138]. Other genes regulated by the Rcs system include genes for the production of lipopolysaccharide, flagella, fimbriae, and other cell wall structures, along with genes associated with virulence [140]. The Rcs system is thought to be the main cell wall stress detection system, and is the only response system that was consistently activated by β-lactam antibiotics or the destruction of the cell wall by lysozyme [136]. The Cpx and Bae systems were activated when the main penicillin binding proteins, PBP1a and 1b, along with PBP2, were inhibited by a combination of β-lactam antibiotics, but only under specific conditions [135]. There is evidence that activation of the Rcs system may be dependent in part on activation of the Cpx response system, however this has not been investigated in detail [135]. Unfortunately, which of these systems, if any, responds to cell wall damage caused by vancomycin challenge in Gram-negative organisms remains unknown.

1.5 Transcriptional profiling of *Elizabethkingia*

To the best of our knowledge the transcriptional profiling of *Elizabethkingia* is limited to two studies [75, 141]. Li *et al*. [75] investigated the stress response of *Elizabethkingia* following challenge with a sub-lethal concentration of hydrogen peroxide and found significant increases in the expression of iron uptake and iron utilization proteins, while several putative efflux systems were significantly downregulated [75]. Chen *et al.* [141] evaluated the transcriptional response of *Elizabethkingia* grown in high and low iron conditions to simulate conditions encountered by these organisms in the midgut of a mosquito during blood feeding. The authors reported that genes related to the electron transport chain, the TCA cycle, and iron-sulfur cluster protein synthesis were significantly upregulated, while iron uptake, genes related to translation, and amino acid metabolism were significantly downregulated [141].

1.6 Goals of the present studies

i. **Characterization of equine-associated *Elizabethkingia* isolates.**

Elizabethkingia have been isolated from companion animals [14], and it is known that pathogens can be transferred between these animals and humans [142]. Therefore, the objective of this work was to investigate the antimicrobial susceptibility profiles and phylogenetic relationships with known human pathogenic isolates of two *E. anophelis* horse isolates obtained from the local veterinary teaching hospital. This work has been published in PLoS ONE [74].

ii. **Evaluation of the impact of vancomycin on *Elizabethkingia*.** Vancomycin remains in use as an antibiotic used to treat *Elizabethkingia* infections, and the assessment of the efficacy of vancomycin treatment in the *Elizabethkingia* is complicated by the difficulties in determining susceptibility to this drug in confirmed *Elizabethkingia* species [105, 143]. This is further exacerbated by the lack of defined breakpoints for delineating susceptibility or resistance to vancomycin [105]. Therefore, the objective of this project was to evaluate the physiological impact of vancomycin on a collection of 21 characterized strains from six currently known genomospecies.

iii. **Elucidation of the transcriptomic response to vancomycin in *Elizabethkingia anophelis* R26.** We wanted to determine how vancomycin affects the transcriptome of *Elizabethkingia*. Due to the cell wall active nature of vancomycin, combined with the importance of outer membrane permeability in resisting the action of vancomycin I hypothesized that genes involved with cell wall stress, outer membrane permeability, and generalized stress response would be significantly altered in vancomycin-challenged cells. In order to test this hypothesis, I conducted RNASeq on *Elizabethkingia anophelis* $R26^T$ challenged with vancomycin, with the goal of using RNASeq to better understand how these organisms respond to vancomycin, and to expand our knowledge of the transcriptomics of this emerging opportunistic pathogen.

iv. **Isolation and characterization of *E. anophelis* R26 and *E. ursingii* G4122 isolates demonstrating vancomycin resistance.** As described in project ii above, I evaluated the physiological aspects of vancomycin challenge against *Elizabethkingia*. This study revealed that cultures challenged by vancomycin experienced an initial decrease in viable cell counts, while light microscopy confirmed that this decrease was the result of cell death. However, this decrease was followed by a rapid rebound to cell densities comparable to the unchallenged control cultures. This raised the prospect that mutants demonstrating increased resistance to vancomycin arose in normal laboratory media containing growth inhibitory concentrations of vancomycin. In this project I aimed to isolate mutants demonstrating vancomycin resistance by single step selection and to characterize the genomic mutations underlying this resistance along with the phenotypic consequences of these mutations.

CHAPTER 2

MATERIALS AND METHODS

2.1 Strains and working conditions

A list of all bacterial isolates used in this dissertation can be found in Table 1. All working stocks were maintained on heart infusion agar (HIA; Remel, San Diego, CA, USA) supplemented with 5% defibrinated rabbit blood (Hemostat Laboratories, Dixon, CA, USA). Overnight cultures were prepared by inoculating a single colony into heart infusion (HIB) or Mueller-Hinton (MHB) broth, followed by overnight incubation (37°C, 200 rpm).

2.2 Antimicrobial susceptibility testing

All antimicrobial susceptibility testing was performed following standardized protocols developed by the CLSI [144]. Relevant antimicrobial solvent controls were tested ensure that there was no growth inhibition caused by the solvent itself.

2.2.1 Minimal inhibitory/bactericidal concentration assays

For broth macrodilution assays master mixes (2 X the final desired concentration) were prepared for each concentration to be tested by adding an appropriate volume of sterilized antimicrobial stock solution to 9 ml sterile MHB. This was then vortexed at

Table 1. Sources and dates of isolation when available of bacterial isolates in this study. Isolates in bold were chosen for whole genome sequencing.

Isolate	Species	Source and Date	Reference
R26	*anophelis*	*Anopheles gambiae* G3, 2006	[7]
R26-VER1	***anophelis***	**Selected from R26**	**This study**
R26-VER2	***anophelis***	**Selected from R26**	**This study**
R26-VER3	***anophelis***	**Selected from R26**	**This study**
422	*anophelis*	Blood; Florida, USA; 1950	[145]
3375	*anophelis*	Spinal fluid and throat culture; South Carolina, USA; 1957	[145]
E6809	*anophelis*	Blood; California, USA; 1979	[145]
F3201	*anophelis*	Spinal fluid; Kuwait; 1982	[145]
F3543	*anophelis*	Spinal fluid; Florida, USA; 1982	[145]
OSUVM-1	***anophelis***	**Equine Endoscope; Oklahoma, USA, 2016**	**[74]**
OSUVM-2	***anophelis***	**Equine guttural pouch aspirate; Oklahoma, USA; 2016**	**[74]**
ATCC 33958	*bruuniana*	Contaminated commercial enzyme preparation; California, USA; 1982	[146]
G0146	*bruuniana*	Blood culture; Margate, England	[145]
G0153	*bruuniana*	Urine; Dublin, Ireland	[145]
G4075	*bruuniana*	Blood culture; Strasbourg, France; 1978	[145]
KC1913	*meningoseptica*	Spinal fluid; Massachusetts, USA; 1949	[145]
G4120	*meningoseptica*	Conjunctivitis; Nottingham, England	[145]
G4076	*meningoseptica*	Urine; St. Brieuc, France; 1983	[145]
G4071	*miricola*	Tracheal exudate; Strasbourg, France; 1978	[145]
G4074	*miricola*	Suction water; Reading, England	[145]
G4121	*miricola*	Water; Goteborg, Sweden; 1982	[145]
G4070	*occulta*	Sputum; Melbourne, Australia; 1977	[145]
G4122	*ursingii*	Soil; Odense, Denmark; 1964	[6]
G4122-VRS6	***ursingii***	**Selected from G4122**	**This study**
G4122-VRS7	*ursingii*	Selected from G4122	This study
G4122-VRS8	*ursingii*	Selected from G4122	This study
G4122-VRS9	*ursingii*	Selected from G4122	This study
G4122-VRS10	***ursingii***	**Selected from G4122**	**This study**
G4123	***ursingii***	Lung autopsy; Copenhagen, Denmark	[145]

maximum speed for at least 5 sec, and 1 ml was then transferred to a sterile screw-capped tube. Overnight cultures were then diluted to an optical density at 600nm (OD_{600nm}) = 0.01, and 1 ml of diluted culture was added to each tube. Typical final antimicrobial concentrations tested ranged from 256 mg/L to 0.25 mg/L following the addition of culture. Bleach and ethanol minimum inhibitory concentrations (MICs) were performed following this method, and final bleach concentrations ranged from 0.08% to 10% (v/v) with 0.01% increments from 0.08% to 1.5%, along with 2%, 5%, and 10%. Final ethanol concentrations ranged from 1% (v/v) to 12% in 1% increments. These tubes were then securely capped and incubated for 24 h without shaking at 37°C. The MIC was determined to be the lowest antimicrobial concentration with no visible turbidity following incubation.

Microdilution MIC assays were performed on 96 well microtiter plates by adding 100 µl sterile MHB to the first 11 columns of the 12 column microtiter plate. One-hundred µl of the appropriate antimicrobial was then added to columns 11 and 12. The solution in column 11 was mixed by tituration, and 100 µl was transferred to column 10. This solution was mixed by tituration, and 100 µl was transferred to column 9, and these steps repeated until column 2. Following tituration 100 µl was removed from column 2 and discarded. This yielded 2-fold serial dilutions at 2 X the desired final concentration. Overnight cultures were then diluted to an OD_{600nm} = 0.01, and 100 µl of diluted culture was added to each well. Plates were then incubated for 24 h at 37°C without shaking, and the MIC was determined as described above. Minimum bactericidal concentrations (MBCs) were determined by spreading 100 µl of culture starting with the highest

antimicrobial concentration demonstrating visible growth, and repeating until the highest tested concentration onto drug-free MHA. Plates were then incubated for 24 h at 37°C, and the MBC determined as the lowest concentration demonstrating no visible growth.

2.3 Characterization of equine-associated *Elizabethkingia* isolates

2.3.1 Isolate Identification

For bacterial identification, fresh colonies grown on tryptic soy agar containing 5% sheep blood were applied to a spot on the MALDI-TOF MS target plate and overlaid with freshly made matrix solution containing 70% formic acid and α-cyano-4-hydroxycinnamic acid following the manufacturer's recommendations. Bacterial identification was carried out using a Microflex LT MALDI-TOF mass spectrometer using default settings. Bacterial peptide spectra were collected using FlexControl software in positive linear mode with a mass range from 2 to 20 kDa and a laser frequency of 60 Hz (IS1 - 20 kV; IS2 - 18 kV; lens - 6 kV; extraction delay time of 100 ns) in automatic mode by accumulating a maximum of 240 profiles (40 laser shots from six different positions of the target spot). Microbial peptide mass spectra were then analyzed using the Biotyper RTC software version 3.1 using the default settings and database version 4.0.0.1. Both OSUVM-1 and OSUVM-2 were identified by MALDI-TOF MS as *E. meningoseptica*. This is consistent with the known insufficiency of MALDI-TOF MS default databases to correctly identify certain *Flavobacteriacae,* including species belonging to the *Chryseobacterium* and *Elizabethkingia* genera [147-149].

2.3.2 Genomic Sequencing and Analysis

Genomic DNA was isolated from 3 ml overnight cultures of OSUVM-1 and OSUVM-2 grown in HIB as described above using Qiagen Genomic-tip 100/g columns following the manufacturer's protocol. The resulting DNA samples were sent to Molecular Research LP where library preparation was performed using the Nextera DNA sample preparation kit. Genomic DNA was then sequenced using PacBio SMRT sequencing and Illumina MiSeq systems and assembled using SeqMan NGen® version 12.0 with paired end sequencing parameters on the default settings. The resulting assemblies were annotated using the Rapid Annotations Using Subsystems Technology (RAST) server [150-152] and the Prokaryote Genome Annotation Pipeline [153]. Both genomes were further analyzed using the nucleotide and protein Basic Local Alignment Search Tool (BLAST) [154, 155]. The draft genome sequences can be found under bioproject PRJNA397081. OSUVM-1 and OSUVM-2 are represented by biosamples SAMN08100548 and SAMN08100549 and nucleotide accession numbers PJMA00000000 and PJLZ00000000, respectively.

The OSUVM-1 and OSUVM-2 genomes were shared with the Special Bacteriology Reference Laboratory (SBRL) at the Centers for Disease Control and Prevention (CDC), where they were compared to the genomes of *E. anophelis* isolates derived from human clinical specimens which were obtained after the 2016 Wisconsin *Elizabethkingia* outbreak [4]. These genomes had been sequenced from cultures grown at 35°C on heart infusion agar supplemented with 5% rabbit blood. DNA was extracted using the Zymo ZR Fungal/Bacterial DNA Microprep kit, or the MasterPure™ Complete

DNA and RNA Purification Kit, according to the manufacturer's instructions. Libraries were prepared using the NEBNext Ultra DNA library prep kit (, then sequencing was done with an Illumina MiSeq instrument using a 2x250 paired-end protocol as described previously [37]. The *de Bruijn* graph *de novo* assembler in CLC Genomics Workbench version 9.0. was used on reads trimmed with a quality limit of 0.02 to produce draft genomes. Ambiguous nucleotides (N's) in the resulting contigs were resolved using read alignments, and contigs were split wherever N's could not be resolved. The accession numbers of these strains are NWMM00000000, NWMI00000000, and NWMH00000000. Genomes were aligned and single nucleotide polymorphism (SNP) trees produced using HarvestTools [156], and exported Newick files were edited using MEGA v6 [157].

2.4 Evaluation of the impact of vancomycin on *Elizabethkingia*

2.4.1 Vancomycin survival assay

Overnight cultures were diluted in MHB to an OD_{600nm} = 0.01, and 25 mL was aliquoted into 4 50 mL flasks containing no addition, and 1 X the MIC, 1.5 X the MIC, and 1 X the MBC of vancomycin. These flasks were incubated (200 rpm, 37°C) and the OD_{600nm} was measured over time. Colony forming units per 1 ml (CFUs) were also estimated by plating 10 µl of culture serial dilutions on drug-free Mueller-Hinton agar (MHA), followed by overnight incubation (37°C).

2.4.2 Antimicrobial and synergism testing

Synergy assays were performed for combinations of vancomycin + ciprofloxacin and vancomycin + rifampin by standard checkerboard assay and interpreted using the

fractional inhibitory concentration index (FICI) using the same criteria as Di Pentima *et al* [158]. Gradient plates were prepared as described previously [159]: 40 ml of drug free MHA was added to 90 X 90 mm square Petri plates. Plates were elevated 6 mm on one end and allowed to cool overnight. Subsequently, each plate was laid flat, 40 ml of MHA supplemented with the appropriate antibiotic concentration was added, and the plates were dried open faced for 4 h. Overnight cultures of each isolate were diluted in MHB to an OD_{600nm} = 0.1, spread onto each plate with a sterile cotton swab, and all plates were incubated for 48 h (37°C). The distance of confluent growth (mm) of three biological replicates for each isolate was measured and compared by one-way ANOVA followed by Tukey-Kramer *post hoc* testing in JMP 14Pro.

2.4.3 Scanning electron microscopy

Cells were prepared for SEM imaging by diluting a standard overnight culture to an OD_{600nm} = 0.01 in MHB followed by incubation to mid-exponential phase (OD_{600nm} = 0.70). The cells were then challenged with 12 mg/L vancomycin after which the cells were collected by centrifugation (5000 X g, 5 min). The pelleted cells were re-suspended in 2% glutaraldehyde solution in sodium cacodylate buffer for 20 min, followed by fixation to a glass coverslip coated in poly-L-lysine for 1 h, and washed 3 times in sodium cacodylate buffer (15 min per wash). Cells were subsequently fixed in 1% osmium tetroxide for 1 h, washed 3 times with sodium cacodylate (15 min per wash), and progressively dehydrated under increasing concentrations of ethanol (50%, 70%, 90%, 95%, and 3 x 100%; 15 min per treatment). Final solvent substitution was carried out by washing the slides twice with HMDS (20 min each). Lastly, the dried samples were

sputter coated with a gold-palladium mixture and visualized utilizing a FEI Quanta 600 field emission gun Environmental SEM.

Cell sizes were determined by imaging five random fields at 15,000 X magnification and length and width measurements taken using the acquisition software for each discreet cell in the field. As the distributions of measured cell sizes differed significantly from normal (Shaprio-Wilke test for normality, $P < 0.01$ for all comparisons) cell sizes were compared using the Mann-Whitney U-test in JMP 14Pro.

2.4.4 Live cell microscopy

Overnight cultures were diluted in MHB to an $OD_{600nm} = 0.01$ and incubated for 3 h (37°C, 200 rpm). Following incubation, vancomycin was added to a final concentration of 1.5 X the MIC for each isolate and a 1 µl aliquot was transferred to a sterile 1% agar pad at room temperature for visualization. Challenged cultures were then incubated for 4 h (37°C, 200 rpm), with 1 µl aliquots removed for imaging at 2 h and 4 h post challenge. Phase contrast images were collected on a NikonNi-E epifluorescent microscope equipped with a 100X/1.45 NA objective (Nikon), Zyla 4.2 plus cooled sCMOS camera (Andor), and NIS Elements software (Nikon). Three biological replicates were used for each strain and condition.

2.5 Elucidation of the transcriptomic response to vancomycin in *Elizabethkingia anophelis* R26

2.5.1 Sample preparation and RNA extraction

Overnight cultures for three biological replicates were diluted in 25 ml MHB to an OD_{600nm} = 0.01. Diluted cultures were transferred to 50 ml growth flasks and incubated with shaking (37°C, 200 rpm) until mid-exponential phase (OD_{600nm} = 0.7). Two 5 ml aliquots of mid-exponential phase cells were then transferred to overnight culture tubes where the treatment tube was challenged with 12 mg/L vancomycin (1.5 X the MIC), while the control tube received an equal amount of autoclaved diH_2O, and incubated with shaking for 30 min. Following incubation, RNA was stabilized in RNAProtect for 5 min at room temperature, and RNA was extracted using the RNeasy minikit following the manufacturer's protocol. Ribosomal RNAs were removed from each sample using the Ribo-Zero kit following the manufacturer's instructions. Libraries were then prepared for sequencing using the Illumina TruSeq Stranded mRNA Sample Preparation Kit following the manufacturer's protocol and the quality verified using an Agilent Technologies 2100 Bioanalyzer. Libraries were then sequenced at the Oklahoma State University Core Facility using an Illumina NextSeq sequencer.

2.5.2 Data analysis

All analysis was conducted on the Galaxy server, where sequencing data was initially subjected to adaptor sequence trimming and quality control using the Trimmomatic and Fast QC packages, respectively. Paired reads were then mapped to the R26 reference genome using Bowtie 2, and aligned reads counted for each predicted

feature using the featureCount package. Finally, feature counts were normalized and compared between control and treatment groups using the edgeR package. Genes were considered to be altered if there was a greater than 2-fold change and the false discovery rate was below 0.05.

2.6 Isolation and characterization of *E. anophelis* R26 and *E. ursingii* G4122 isolates demonstrating vancomycin resistance.

2.6.1 Selection of vancomycin-resistant mutants

Overnight HIB cultures were ten-fold serially diluted and 100 µl was plated on HIA plates supplemented with increasing concentrations of vancomycin ranging from 2 – 20 mg/L. Following overnight incubation (37°C), single isolated colonies were picked, and passaged 3 times on drug free HIA, before making HIB overnight cultures and 20% glycerol freezer stocks. Vancomycin MICs and MBCs for each isolate were determined by broth microdilution following standard CLSI guidelines [144].

2.6.2 Whole genome sequencing, mapping, annotation, and analysis of vancomycin-resistant mutants

Genomic DNA from *E. anophelis* R26 along with vancomycin-resistant mutants R26-VSR1, R26-VSR2, and R26-VSR3, along with *E. ursingii* vancomycin-resistant mutants G4122-VR6 and G4122-VR10 was extracted from 3 ml overnight cultures and sequenced as described previously [74]. Briefly, raw reads were trimmed to remove adapter sequences and for quality control using a quality threshold of 0.02 and 0 allowable ambiguous nucleotides. Trimmed reads were then mapped to the complete

reference genome of each parent strain using the default options and the consensus sequence for each isolate extracted. All reported mutations were verified by inspection of the raw reads. All trimming and mapping steps were performed using CLC Genomics Workbench v11.0.1. Consensus sequences were annotated using the Rapid Annotations Using Subsystems Technology (RAST) server [150-152]. Regulatory elements were predicted using the BPROM program [160] while the identity and putative functional domains of hypothetical proteins were investigated using nucleotide and protein Basic Local Alignment Search Tool (BLAST) [154, 155].

2.6.3 Quantitative polymerase chain reaction analysis

A 1% (v/v) inoculum of cells from standard *E. anophelis* R26, R26-VSR3, *E. ursingii* G4122, and G4122-VR6 overnight cultures were added to 3 ml MHB and incubated to mid-exponential phase, at which point cells were challenged with 1.5 X the vancomycin MIC for 2 h, and harvested by centrifugation (5000 X g, 5 min). Cells were lysed in 1 ml Trizol, followed by nucleic acid extraction in chloroform. Total RNA was precipitated from the aqueous layer by the addition of 0.5 volume isopropanol followed by centrifugation (12,000 X g, 5 min, 4°C). The resulting RNA was then washed with ice cold 70% (v/v) ethanol, dried at room temperature for 30 min, and resuspended in ultrapure diH_2O. RNA extractions were screened for DNA contamination by PCR using primers targeting the RNA polymerase β subunit (Table 2) and first strand cDNA synthesis was performed using the Agilent First Strand cDNA Synthesis Kit following the manufacturer's protocol using random hexamer primers. Gene specific amplification primers (Table 2) were validated by standard PCR. Quantitative PCR was conducted on

Table 2. Primers, target gene, and sequence of qPCR primers.

Primer Name	Isolate	Gene Target	Primer Sequence
mpF	R26/R26-VR3	ORF 552	CGTCGTTCTATGGAGCCTGA
mpR			CGGTGTACCGATAAGGGCAA
Rpo_ICF	R26/R26-VR3	*rpoB*	TGTACTGACCCGGAACATGA
Rpo_ICR			CGGTGAACGGTGTAACTGAG
EUVR6-Eam-Q-F	G4122/G4122-VR6	ORF 261	GCTGTTAGGAGGTGCAGTTAT
EUVR6-Eam-Q-R			CGGACGAATCCCTTCCATATT
EUVR6-M60-Q-F	G4122/G4122-VR6	ORF 723	CCTTAACTGGGACGGATATGAC
EUVR6-M60-Q-R			GGCTTTGTTGGTAGGGTAGAA
EUVR6-RpoB-Q-F	G4122/G4122-VR6	*rpoB*	CACGTTCAATCGGACCATACT
EUVR6-RpoB-Q-R			CAAATGCTTCTAGTGCCCAAAC

a LightCycler 96 instrument using SYBR-Green. Triplicate biological and technical replicates were used for all comparisons. Expression change was assessed using *rpoB* as the standard housekeeping gene for all comparisons. All expression data was found to be normally distributed (Shaprio-Wilke test for normality, $P > 0.05$ for all comparisons), and all statistical analyses were carried out using parametric statistics in JMP 14Pro. ΔΔCt values were compared by Student's t-test, with mean ΔΔCt values transformed to fold change ($2^{-\Delta\Delta Ct}$) for ease of presentation.

CHAPTER 3

RESULTS AND DISCUSSION

3.1 Characterization of equine associated *Elizabethkingia* isolates

Despite exhaustive investigation, the source(s) of the 2015 – 2016 Midwestern US *E. anophelis* outbreak remain elusive [4]. This outbreak is notable for several reasons, including the large number of community-acquired cases, and the absence of *E. anophelis* from sink taps and other water storage sources, which are frequently the sources for *Elizabethkingia* outbreaks [13, 19, 20, 34, 161, 162]. Both companion and food animals may serve as reservoirs for antibiotic-resistant bacterial pathogens [26-34], and the transmission of multiply-antibiotic resistant organisms between humans and these animals has been documented [142, 163, 164]. While there is no evidence that the 2015 – 2016 *E. anophelis* outbreak was one of these cases, instances of *Elizabethkingia* infection have been reported in several animal species [14-17]. Hu *et al*. [15] further reported that an *E. miricola* isolate responsible for a large outbreak in frogs was closely related to *E. miricola* isolated from humans. In 2016 the Oklahoma Animal Disease Diagnostic Laboratory isolated two confirmed *E. anophelis* strains that were associated with horses [74], and the objective of this project was to evaluate the genomic characteristics and antimicrobial susceptibility patterns of these isolates.

3.1.1 Sequencing and mass spectrometry analysis

The assembly of OSUVM-1 sequence data produced 7 contigs and a genome of 4,153,767 bp (%GC = 35.5). OSUVM-1 contained 3,850 putative coding sequences (CDS), of which 3,777 were protein CDS. RAST annotation assigned function to 2,421 (64%) predicted protein CDS and identified 75 rRNA and tRNA CDS. OSUVM-2 sequences were assembled into 10 contigs to produce a genome of 4,109,384 bp (%GC = 35.5). OSUVM-2 contained 3,814 CDS, of which 3,750 were protein CDS. RAST annotation assigned function to 2,404 (64%) predicted protein CDS and identified 64 rRNA and tRNA CDS.

Bacterial identification using MALDI-TOF indicated that both OSUVM-1 and OSUVM-2 were members of the *Elizabethkingia* genus. The *Elizabethkingia* are nonmotile [27] and RAST analysis of the draft genomes of OSUVM-1 and OSUVM-2 revealed no features supporting motility and chemotaxis. The subsystem feature count in both strains were identical for 16 of 25 subsystems identified in the draft genomes which differed in the feature count of the following subsystems: cell wall and capsule; virulence, disease, and defense; miscellaneous; membrane transport; iron acquisition and metabolism; protein metabolism; stress response; metabolism of aromatic compounds; and phages, prophages, and transposable elements (Table 3). This last finding is consistent with our expectation that the loci carried by mobile genetic elements will be better represented in a complete genome than a draft genome, since a draft genome will contain a single copy of a transposon sequence (with coverage levels scaled to the

Table 3. Distribution in coding sequence function as identified by RAST. Subsystems with differences in the number of coding sequences in the two strains are highlighted in bold.

Subsystem	Coding Sequences in OSUVM-1	Coding Sequences in OSUVM-2
Cofactors, vitamins, prosthetic groups, pigments	201	201
Cell wall and capsule	**78**	**77**
Virulence, disease, and defense	**93**	**89**
Potassium metabolism	12	12
Miscellaneous	**28**	**27**
Phages, prophages, and transposable elements	**8**	**7**
Membrane transport	**66**	**63**
Iron acquisition and metabolism	**25**	**24**
RNA metabolism	121	121
Nucleosides and nucleotides	64	64
Protein metabolism	**203**	**225**
Cell division and cell cycle	29	29
Regulation and cell signaling	48	48
Secondary metabolism	8	8
DNA metabolism	95	95
Fatty acids, lipids, and isoprenoids	101	101
Nitrogen metabolism	12	12
Dormancy and sporulation	4	4
Respiration	66	66
Stress response	**70**	**71**
Metabolism of aromatic compounds	**19**	**18**
Amino acids and derivatives	325	325
Sulfur metabolism	15	15
Phosphorus metabolism	21	21
Carbohydrates	263	263

number of copies of the transposon in the genome) while a complete genome will allow each gene in multiple copies to be identified.

3.1.2 Core genome and phylogenetic analysis

Nucleotide BLAST and phylogenetic analysis of the core genome of both isolates revealed that both strains were *E. anophelis*. Both OSUVM-1 and OSUVM-2 are part of a clade of strains resembling *E. anophelis* strain JM-87 [5, 30], which was isolated from *Zea mays* stem tissue and initially described as the type strain of *Elizabethkingia endophytica* before whole genome sequence analysis revealed it to belonged to the *E. anophelis* species (Figure 2) [5, 7]. Using the HarvestTools v1.1.2 module ParSNP, we determined that both OSUVM-1 and OSUVM-2 are closely related to *E. anophelis* isolates derived from human clinical specimens in Minnesota, Illinois, and Tennessee (Figure 2). A second analysis limited to OSUVM-1, OSUVM-2, and the three human clinical isolates, revealed an 87% core genome among the five strains. Once ambiguous nucleotides were excluded only 198 SNP positions were located, scattered throughout the core genome of the five strains, and OSUVM-1 and OSUVM-2 differed by only 6 SNPs in the core genome, suggesting that OSUVM-1 and OSUVM-2 are clonal.

These results indicate that these five strains are highly related and that the two OSUVM isolates share commonalities with strains isolated from human *Elizabethkingia* infections. Similar findings were reported by Hu *et al.* [15] who isolated an *E.*

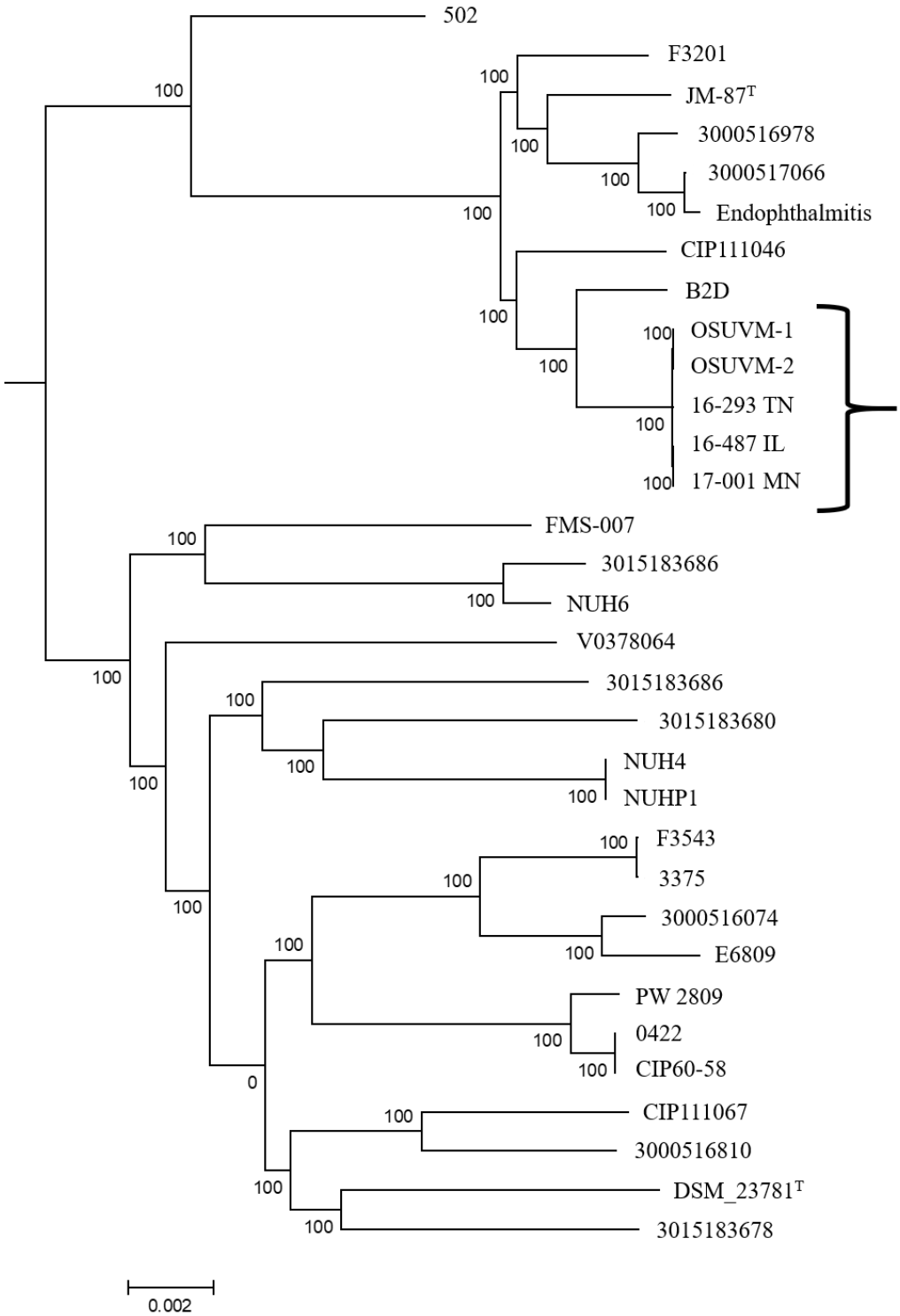

Figure 2. Core genome single nucleotide polymorphism tree showing the position of OSUVM-1 and OSUVM-2 compared to *E. anophelis* strains reported by Nicholson *et al.*[29]**.** Type strains are denoted by a superscript T, and the location of the isolates from this study is denoted by a bracket. Reprinted from Johnson *et al*. [74] under Creative Commons Attribution License.

miricola strain responsible for a contagious disease resulting in black-spotted frog losses at farms in China and was highly related to an *E. miricola* isolate isolated from a human case in China. Collectively these findings suggest that *Elizabethkingia* are not host-specific, which raises the possibility that *Elizabethkingia* might have the potential to move between humans and animals in a similar manner to known zoonotic pathogens.

3.1.3 β-lactamases

Genomic analysis of *Elizabethkingia* spp. consistently identifies multiple β-lactamases, including three characterized β-lactamases [72, 73, 165], along with a varying number of putative β-lactamases [4, 5, 9, 10, 12, 37, 76, 77, 79-81]. The 19 putative β-lactamase CDS in both OSUVM-1 and OSUVM-2 included the previously characterized class A serine β-lactamase (SBL) bla_{CME-1} [73], and metallo-β-lactamases (MBL) class B1 bla_{B14} [165] and class B3 bla_{GOB18} [72]. Of the remaining 16 putative β-lactamases, one is similar to the previously characterized class A SBL bla_{CIA-1} from *Chryseobacterium indologenes* (67% amino acid identity) [166], 11 are similar to class C SBLs, and the remaining 7 were classified as putative MBLs.

3.1.4 Multidrug efflux pumps

Efflux pumps are a key component of the intrinsic antibiotic-resistance mechanism of many bacteria and function by transporting antibiotics from within the cell to the outside [90-92]. Genomic annotation of all *Elizabethkingia spp.* reveals the presence of several drug efflux pumps, yet none of these transporters has been phenotypically characterized [4, 5, 9, 10, 12, 37, 76, 77, 79-81]. RAST annotation

revealed 32 CDS related to antibiotic efflux in both OSUVM-1 and OSUVM-2: 18 of the 32 CDS (56%) were identified by RAST analysis as components of RND efflux operons, 12 CDS (38%) as components of MFS operons, while the remaining 2 CDS (6%) were identified as MATE efflux pumps.

We are interested in the RND pumps in the draft genomes of OSUVM-1 and OSUVM-2 since RND efflux pumps can be a major factor contributing to clinically-relevant resistance to certain antibiotics in Gram-negative organisms [90]. Tripartite RND efflux pumps consist of an inner membrane pump attached to an outer membrane porin by way of a periplasmic adaptor protein [92, 97, 167, 168]. Although the arrangement of the genes that encode RND components varies among organisms, they can be found in a single operon in organisms such as *Pseudomonas aeruginosa* (e.g. *mexAB-oprM*) and *Campylobacter jejuni* (e.g. *cmeABC*) [97, 169]. When genes encoding the MexAB-OprM efflux pump in *P. aeruginosa* and the CmeABC efflux operon in *C. jejuni* are inactivated, a significant decrease in the MICs for various β-lactams, chloramphenicol, ciprofloxacin, erythromycin, nalidixic acid, and tetracycline is observed [168, 170-172].

The 18 CDS identified by RAST analysis as components of tripartite RND efflux pumps were all identical in OSUVM-1 and OSUVM-2 at the nucleotide level. These genes presented as six, three-gene operons, organized in the same manner as the *mexAB-oprM* and *cmeABC* operons. The OSUVM-1 and OSUVM-2 RND inner membrane pumps demonstrated 28 - 42% amino acid identity to MexB and CmeB, the periplasmic

adaptor proteins demonstrated 24 - 27% amino acid identity to MexA and CmeA, while the outer membrane porins demonstrated 25 - 29% amino acid identity to OprM and CmeC. These homologies only suggest a relationship between these operons and characterized RND efflux systems. It should be noted that when Schindler *et al.* [173] cloned and expressed 21 genes putatively identified as encoding efflux proteins in *S. aureus*, none resulted in increased MICs for any of the substrates tested, calling into question the function of these genes in drug efflux. As a result, it is important that the putative efflux genes from *Elizabethkingia* isolates be confirmed as drug resistance efflux pumps through biochemical analysis.

3.1.5 Antimicrobial susceptibility testing

Both OSUVM-1 and OSUVM-2 demonstrated high MICs for cefazolin, ceftazidime, ceftiofur, ampicillin, penicillin, ticarcillin, ticarcillin + clavulanic acid, imipenem, amikacin, gentamicin, chloramphenicol, fusidic acid, and tetracycline (Table 4). While the confirmed active β-lactamases in *Elizabethkingia* are known to contribute to resistance to a wide array of antibiotics that target penicillin-binding proteins [45-47], other mechanisms such as multidrug efflux, outer membrane alterations and penicillin-binding proteins that demonstrate reduced affinity for β-lactams can also contribute to β-lactam resistance, although these mechanisms remain untested in *Elizabethkingia* [91, 170, 171]. OSUVM-1 demonstrated an oxacillin MIC of 0.25 mg/l, while OSUVM-2 showed a higher oxacillin MIC (≥ 4 mg/l), and overall OSUVM-2 displayed higher MICs for 11 of the antibiotics tested (Table 4). Since the genes associated with resistances are

Table 4. Minimum inhibitory concentrations for select antibiotics determined by the Sensititre system or broth microdilution method. Antibiotics displaying different MICs are highlighted in bold.

Antibiotic	OSUVM-1 MIC (mg/L)	OSUVM-2 MIC (mg/L)
Amikacin	**16**	**32**
Ampicillin	> 32	> 32
Azithromycin	**2**	**4**
Cefazolin	> 16	> 16
Ceftazidime	64	64
Ceftiofur	4	4
Chloramphenicol	**8**	**32**
Ciprofloxacin[a]	0.25	0.25
Clarithromycin	**≤ 1**	**4**
Clindamycin[a]	1	1
Doxycycline	≤ 2	≤ 2
Enrofloxacin	≤ 0.25	≤ 0.25
Erythromycin	**1**	**8**
Fusidic acid[a]	16	16
Gentamicin	**4**	**> 8**
Imipenem	> 8	> 8
Oxacillin + 2% NaCl	**≤ 0.25**	**> 4**
Penicillin	> 8	> 8
Rifampin	≤ 1	≤ 1
Tetracycline	**8**	**> 8**
Ticarcillin	**64**	**> 64**
Ticarcillin + clavulanic acid	64	64
Trimethoprim + sulfamethoxazole	**≤ 0.5**	**4**
Vancomycin[a]	**8**	**32**

[a] Tested by broth macrodilution

identical in both strains, these MIC differences may be attributed to unidentified SNPs or specific gene content differences outside the core genome.

Both OSUVM-1 and OSUVM-2 demonstrated low MICs to ciprofloxacin and enrofloxacin, suggesting they are susceptible to these fluoroquinolones (Table S2). Ciprofloxacin resistance in Gram-negative bacteria is driven primarily by mutations in the gene encoding the DNA gyrase A subunit (*gyrA*), and resistance is enhanced in both cases by mutations in *gyrB*, *parC*, and *parE* [174-179]. The *E. anophelis gyrA* encodes a predicted protein of 858 amino acids, and Perrin *et al.* [4] identified a Ser83Ile mutation in the *gyrA* of an *E. anophelis* strain isolated during the 2016 Wisconsin outbreak that displayed an increased ciprofloxacin MIC. Lin *et al.* [76] subsequently identified the same mutation in another *E. anophelis* strain which also demonstrated an elevated ciprofloxacin MIC. Thus, it is probable that the *gyrA* mutation Ser83Ile imparts ciprofloxacin resistance in *E. anophelis,* as it does for *E. coli* [180-185]. Both OSUVM-1 and OSUVM-2 contain the wild-type serine at position 83, along with two mutations when compared to *E. anophelis* R26, Val841Ala and Ala842Ile. Positions 841 and 842 lie outside of the region of *gyrA* thought to be responsible for fluoroquinolone resistance [174, 175, 180, 182] and the low fluoroquinolone MICs demonstrated by both strains are consistent with the expectation that these mutations would not convey fluoroquinolone resistance.

Vancomycin is used extensively for treating Gram-positive infections, in particular infections caused by MRSA and *Clostridum difficile* [186, 187]. Gram-

negative organisms are normally intrinsically refractory to the action of vancomycin and exhibit MICs > 64 mg/L [122, 124, 188, 189], except *Elizabethkingia*, which have been reported to exhibit vancomycin MICs as low as 1 mg/L [77, 87, 89, 107, 143, 158]. Vancomycin has been used singly or in combination therapies to treat *Elizabethkingia* infections with mixed success (reviewed in [143]). Furthermore, Hazuka *et al*. [190] reported that when an isolate of *E. meningoseptica* was exposed to vancomycin for 6 days, the MIC increased from 8 mg/l to 64 mg/l. Vancomycin dosing recommendations suggest that a serum trough concentration of between 15 to 20 mg/L should be reached and maintained to kill susceptible organisms, but this guidance requires that the target organism has a vancomycin MIC < 1 mg/L [186, 187, 191]. Using this standard, OSUVM-1 and OSUVM-2 (vancomycin MICs = 8 and 32 mg/L, respectively) would be resistant to vancomycin.

Here we report the first two draft genomes from *Elizabethkingia* associated with horses, and that these two isolates are closely related to isolates derived from human infections, although to date no direct evidence for transmission of *Elizabethkingia* between humans and animals has been observed. We further demonstrated that both isolates display low MICs for ciprofloxacin and that both isolates display vancomycin MICs that are within the range of those reported for other *E. anophelis* isolates [19, 44, 86, 87, 143, 192]. These comparatively low vancomycin MICs piqued our interest, and we initiated preliminary investigations into the impact of vancomycin on *Elizabethkingia.*

3.2 Evaluation of the impact of vancomycin on *Elizabethkingia*

While vancomycin is utilized as a treatment for *Elizabethkingia* infection, to date there are no studies that have investigated the physiological effects of vancomycin on the *Elizabethkingia* [143]. It is critical to understand these effects in order to better inform the use of this antibiotic for treatment of these infections, and to understand how vancomycin interacts with Gram-negative organisms. Therefore, we assayed cell survival in the face of vancomycin challenge by kill curve assay, and expanded on the previous work of Di Pentima *et al*. [158] by evaluating vancomycin synergy for our collection of 21 genomically-characterized isolates representing six *Elizabethkingia* species.

3.2.1 Vancomycin kills *Elizabethkingia* in a species-dependent manner

Exponential phase cultures of *E. bruuniana, E. miricola,* and *E. ursingii* experienced no decrease in viable cell counts for the first 16 h of exposure at any vancomycin concentration (Figure 3). Two isolates, *E. bruuniana* ATCC 33958 and *E. ursingii* G4122 showed a decrease in viable cells at 24 h post vancomycin challenge, although it is unclear if this decrease is due to the action of vancomycin or other factors such as depletion of nutrients. In contrast, *E. anophelis*, *E. meningoseptica*, and *E. occulta* cultures all demonstrated decreases in viable cell counts at vancomycin concentrations 1.5 X the MIC and at the MBC (Figure 3). Viable cell counts began to decline 2 h after exposure to vancomycin and continued until 6 to 8 h post challenge. In all cases the cultures then rebounded over the next 16 h, nearly reaching the control

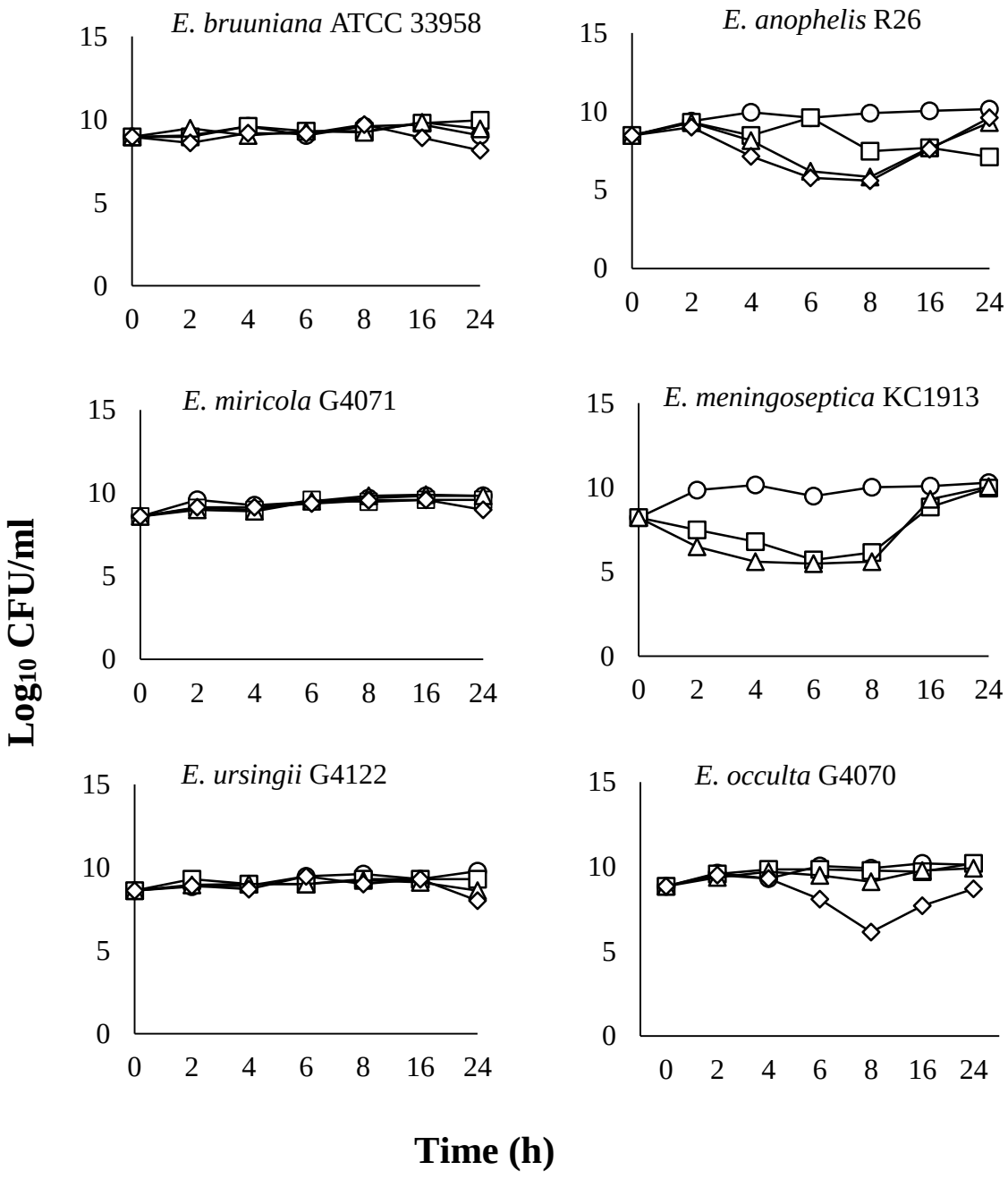

Figure 3. Kill curves for the *Elizabethkingia* type strains exposed to vancomycin in mid exponential phase. The growth control is denoted by open circles, while increasing concentrations of vancomycin (1 X MIC, 1.5 X MIC, and 1 X MBC) are denoted by squares, triangles, and diamonds, respectively.

cultures by 24 h post exposure. This data suggests that vancomycin resistance in the *Elizabethkingia* could readily emerge at bactericidal concentrations that were subsequently used to select for vancomycin-resistant mutants of *E. anophelis* and *E. ursingii* in section 3.4.

3.2.2 Vancomycin challenge leads to cell death

While the kill curve data shows that there is a reduction in the number of viable cells, and therefore indirectly suggests that vancomycin is causing cell death, it was important that we obtain direct evidence that vancomycin exposure was leading to cell death. Therefore, live cell microscopy was used to directly visualize *E. anophelis* cells challenged with vancomycin, and revealed alterations in cell morphology that are consistent with disruption of the cell wall, along with debris in the viewing fields that were consistent with cell death [131, 132, 137, 193, 194]. Maintenance of the integrity of the peptidoglycan cell wall is a tightly regulated competition between peptidoglycan biosynthesis and peptidoglycan removal through remodeling and recycling of aging or damaged areas of the peptidoglycan layer [194]. Inhibition of peptidoglycan biosynthesis leads to weaknesses in the peptidoglycan layer as the peptidoglycan recycling systems continue to function normally. In turn, weaknesses will emerge in the peptidoglycan layer and eventually the integrity of the peptidoglycan layer will fail at these weak points, at which point the turgor pressure within the cell will push the cytoplasmic membrane and contents through the breach [194]. This phenotype was observed in both *E. anophelis* R26 and *E. ursingii* G4122 cells challenged with vancomycin (Figures 4 and 5), which suggests that vancomycin is targeting cell wall biosynthesis, leading to

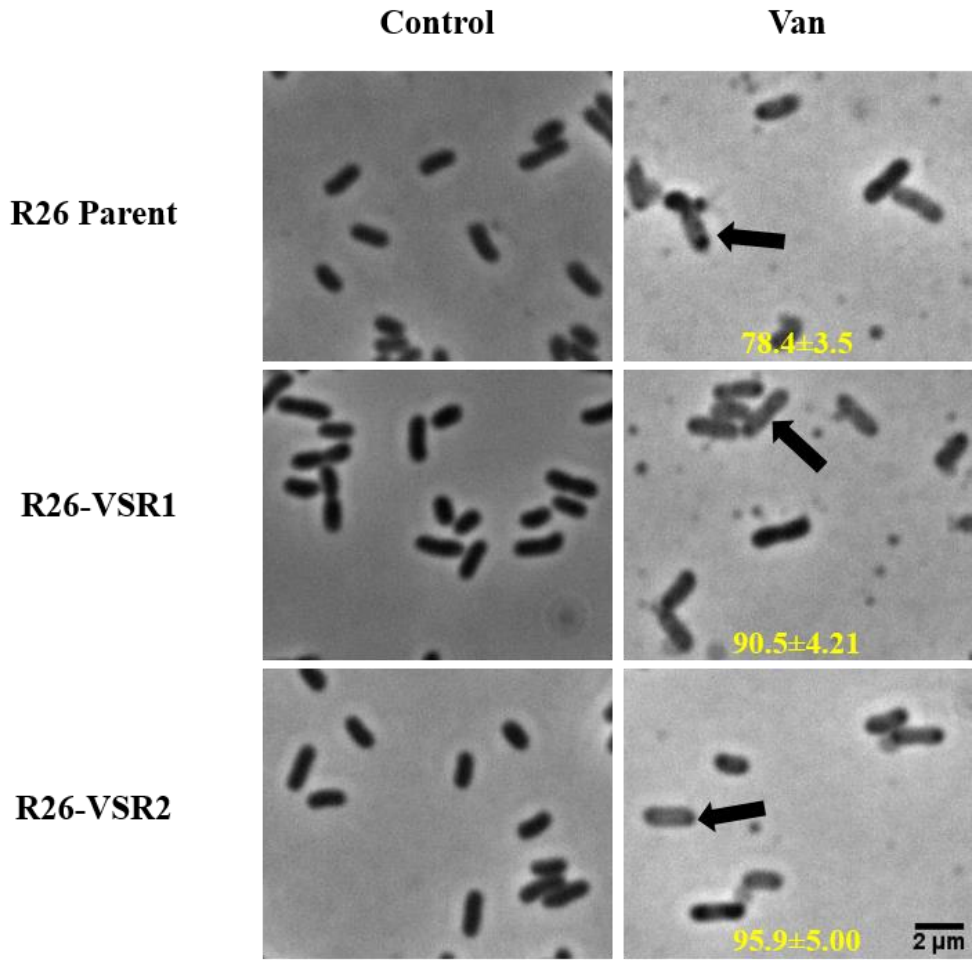

Figure 4. Phase contrast images of *Elizabethkingia* R26 and vancomycin-resistant mutant strains after 4 h incubation in MHB with 1.5 X the minimum inhibitory concentration of vancomycin. Arrows point to representative cells displaying the dying phenotype. Round phenotypes were not seen for R26 parent and mutant strains. Percent of dying cells is indicated with Poisson error to one standard deviation.

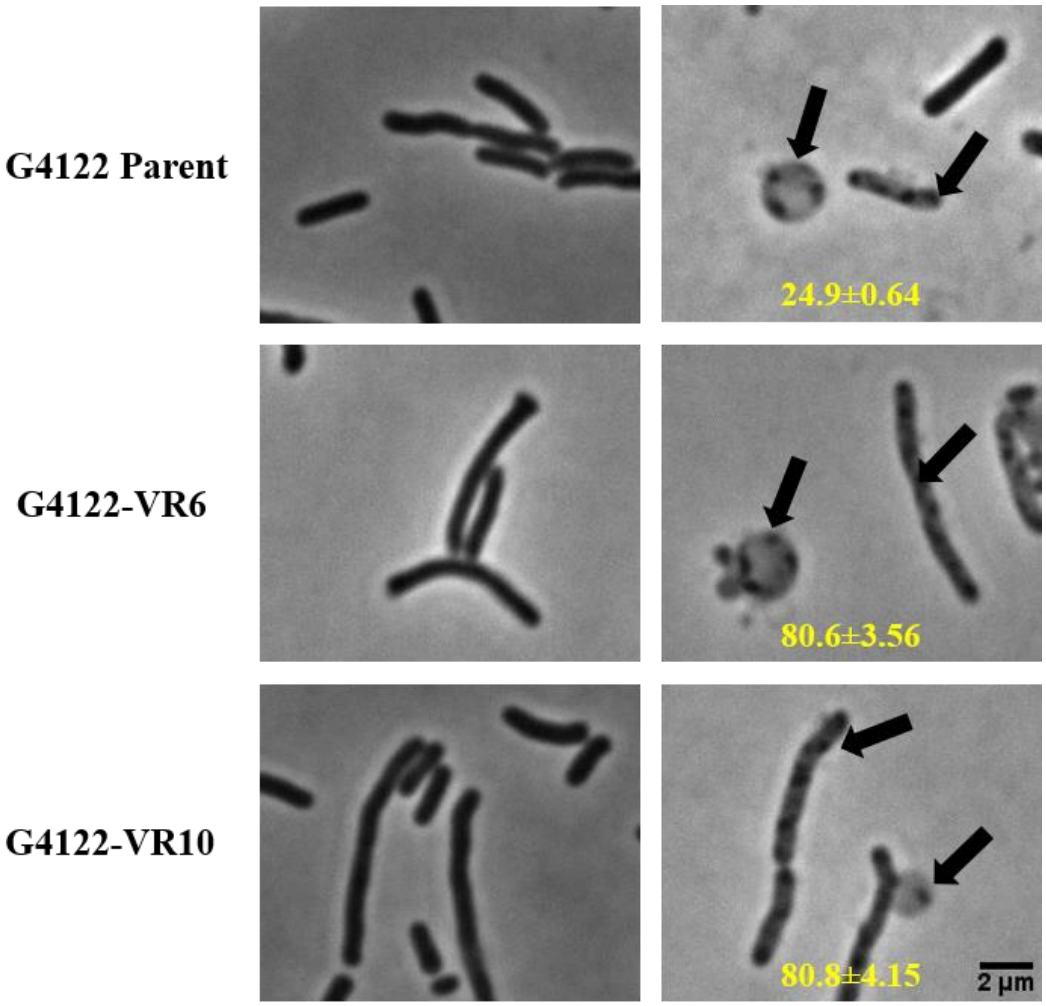

Figure 5. Phase contrast images of *Elizabethkingia* G4122 and vancomycin resistant mutant strains after 4 h incubation in MHB with 1.5 X the minimum inhibitory concentration of vancomycin. Arrows point to representative cells with dying phenotype. Percent of cells is indicated with Poisson error to one standard deviation.

weakening of the cell wall and death. These results are similar to those reported by Huang *et al.* [131] when they challenged *E. coli* mutants demonstrating susceptibility to vancomycin with 1 mg/L of vancomycin and noted abnormalities in cell morphology, followed by blebbing, and eventually rupture and release of the cytoplasm.

3.2.3 Vancomycin synergism is species-dependent

To date, only a single study has assessed vancomycin synergism in the *Elizabethkingia*, and unfortunately this work was done before accurate speciation was available [158]. In this study Di Pentima *et al.* tested vancomycin in combination with ciprofloxacin, linezolid, and rifampin. Vancomycin was found to be synergistic with rifampin for 3 of the 4 isolates tested, while all 4 isolates displayed additivity for vancomycin in combination with ciprofloxacin and linezolid.

Ciprofloxacin in combination with vancomycin displayed additivity for all *E. anophelis* isolates tested, and synergism for all *E. meningoseptica*, while this combination displayed indifference against all *E. bruuniana, E. miricola, E. occulta,* and *E. ursingii*. A similar pattern was found for rifampin in combination with vancomycin, with *E. anophelis* and *E. meningoseptica* displaying either synergistic or additive interactions, and the other four species being indifferent. There were two notable exceptions: *E. bruuniana* ATCC 33958^{T} displayed antagonism between rifampin and vancomycin, while *E. ursingii* G4123 displayed additivity between the two compounds (Table 5). The observed synergies of the *E. anophelis* and *E. meningoseptica* isolates are consistent with those reported by Di Pentima *et al*., while our results differ from those reported for *E.*

Table 5: Fractional inhibitory concentration indices (FICI) and interpretations for all 21 *Elizabethkingia* isolates.

Isolate	Species	Ciprofloxacin FICI	Interpretation[a]	Rifampin FICI	Interpretation[a]
R26	*anophelis*	0.52	Additive	0.25	Synergistic
F3543	*anophelis*	0.56	Additive	0.53	Additive
F3201	*anophelis*	0.53	Additive	0.25	Synergistic
3375	*anophelis*	0.63	Additive	0.31	Synergistic
422	*anophelis*	0.52	Additive	0.25	Synergistic
333	*anophelis*	0.63	Additive	0.26	Synergistic
514	*anophelis*	0.51	Additive	0.52	Additive
E6809	*anophelis*	0.56	Additive	0.25	Synergistic
ATCC 33958	***bruuniana***	**1.00**	**Indifferent**	**3.00**	**Antagonistic**
G0146	*bruuniana*	1.00	Indifferent	2.00	Indifferent
G0153	*bruuniana*	1.50	Indifferent	2.00	Indifferent
G4075	*bruuniana*	0.27	Synergistic	2.00	Indifferent
KC1913	*meningoseptica*	0.28	Synergistic	0.14	Synergistic
G4076	*meningoseptica*	0.25	Synergistic	0.25	Synergistic
G4120	*meningoseptica*	0.19	Synergistic	0.14	Synergistic
G4071	*miricola*	1.00	Indifferent	1.00	Indifferent
G4074	*miricola*	1.50	Indifferent	2.00	Indifferent
G4121	*miricola*	1.00	Indifferent	2.00	Indifferent
G4070	*occulta*	1.50	Indifferent	1.00	Indifferent
G4122	*ursingii*	1.00	Indifferent	1.00	Indifferent
G4123	***ursingii***	**1.00**	**Indifferent**	**0.63**	**Additive**

[a] As determined by Di Pentima *et al*.

bruuniana, *E. miricola*, *E. occulta* and *E. ursingii*, all of which displayed indifference to vancomycin in combination with both ciprofloxacin and rifampin. This suggests that there are important species dependent interactions *in vitro*, and highlight the importance of determining the species of the infecting *Elizabethkingia* isolate before initiating combination therapy. Having demonstrated that vancomycin exposure leads to cell death, we wanted to further investigate the impact of vancomycin exposure on a transcriptional level within *Elizabethkingia*.

3.3 Transcriptional profiling of vancomycin challenge

The transcriptional response of Gram-negative organisms such as *Elizabethkingia* to vancomycin challenge remains poorly understood, but has the potential to reveal important information about how vancomycin is disrupting the cell, and leading to cell death. Due to the cell wall active nature of vancomycin, combined with the importance of outer membrane permeability in resisting the action of vancomycin, I hypothesized that genes involved with cell wall stress and outer membrane permeability would be significantly altered in vancomycin challenged cells. To evaluate this hypothesis *E. anophelis* R26 cells were challenged with 12 mg/L (1.5 X vancomycin MIC) for 30 min and gene expression was probed by RNAseq. *E. anophelis* R26 was picked for this experiment because this isolate is the type strain of *E. anophelis*, which are the most common clinically isolated species, and for the complete genome that is available for this organism.

3.3.1 Assembly and mapping

Assembled Illumina reads mapped to all 3,704 predicted non-rRNA coding sequences, of which 114 were significantly upregulated (≥ 2-fold change, FDR ≤ 0.05, Table 6), while 111 were significantly downregulated (Table 6). A complete list of all significantly altered genes can be found in Appendix B. These 225 genes represented 11 major functional categories, of which the most upregulated functional categories were hypothetical genes, genes related to amino acid and protein metabolism, central metabolism, and genes related to transport, while amino acid and protein metabolism, hypothetical genes, transport genes, central metabolism, and cell envelope metabolism represented the most down regulated functional categories (Table 6).

3.3.2 Cell envelope metabolism

Genes related to the cell envelope were poorly represented among significantly altered genes, with only 4 significantly upregulated, while 10 were significantly downregulated. Two of these significantly downregulated genes were related to peptidoglycan turnover: a putative polysaccharide deactylase that shares a conserved domain with a poorly characterized *Helicobacter pylori* gene that is thought to modify peptidoglycan by converting (S)-allantoin into allantoic acid [195], which may function to conceal the highly immunogenic moieties of the cell wall from the host immune response [195], and a muramidase similar to the flagellum specific hydrolase *flgJ* [196]. This peptidoglycan hydrolase is known to be involved in the remodeling of the peptidoglycan layer in motile organisms to allow for the insertion and assembly of the flagellar motor assembly [196]. It is curious that a gene with this type of conserved domain is altered in *E. anophelis*,

Table 6. Functional categories and number of significantly altered genes.

Gene functional category	Up-regulated	Down-regulated
Amino acid and protein metabolism	21	36
• Amino acid metabolism	12	8
• Protein fate	3	2
• Protein synthesis	6	26
Antimicrobial resistance	3	3
Cell envelope metabolism	4	10
• Cell envelope	1	4
• Peptidoglycan biosynthesis	2	4
• Peptidoglycan turnover and remodeling	1	2
Central metabolism	18	11
• Carbohydrate metabolism	2	0
• Cofactors and secondary metabolites	4	4
• Energy production and conversion	10	1
• Nucleotide metabolism	1	6
• Sulfur metabolism	1	0
DNA replication, recombination, repair	3	1
Fatty Acid Metabolism	4	2
Hypothetical/Unknown Function	37	28
Stress response	8	3
Transcription and Regulation	3	1
Transport	10	13
• Amino acids	0	0
• Anions	2	1
• Carbohydrates	3	2
• Cofactors and secondary metabolites	0	2
• Metal ions	5	6
• Osmotic regulation	1	0
• Protein secretion	0	1
• Indeterminate[a]	0	1
Virulence factors	2	3
Total	114	111

[a] – Insufficient evidence to determine the exact functions of these genes

considering that these organisms are non-motile, and there is no evidence to date that these organisms express any flagella [27, 29]. It is a possibility that this protein is serving instead as peptidoglycan hydrolase involved in remodeling the peptidoglycan layer in preparation for cell division and it is known that enzymes bearing similar conserved domains serve this purpose in *Lactococcus lactis* [197], and *Streptococcus faecalis* [198]. The remaining 8 genes were evenly distributed between peptidoglycan biosynthesis, where two putative glycosyltransferase genes, along with the aspartate racemase gene *murI* and a putative septum formation inhibitor protein were significantly downregulated, and genes associated with the cell envelope. These genes included 3 porin family proteins, and a low molecular weight phosphotyrosine protein phosphatase.

The 4 upregulated cell envelope metabolism genes consisted of a linear amide C-N hydrolase with a poorly defined function, a putative *motB* flagella related protein, outer membrane porin (OMP) W, and a gene annotated as an ATP binding protein, but identified by conserved domain search as the stress response protease *ftsH*. The putative *motB*, *ompW*, and *ftsH* genes all are induced in response to cell wall stress stimuli, specifically the Cpx and Rcs systems [117, 119, 122, 129, 132, 133, 135-137, 139, 199-202]. Alterations in *ompW* expression are widely reported under a variety of environmental stressors including osmotic [203], oxidative [200, 204], temperature stress [202], and iron limited growth conditions [201]. OmpW is also associated with resistance to ampicillin and ceftriaxone, which are cell wall active β-lactam antibiotics, along with tetracycline, where it is speculated to partner with multidrug efflux pumps to facilitate removal of these drugs [205]. It has been demonstrated that vancomycin is not

a substrate recognized by known multidrug efflux pumps [122], and as a result it is unlikely that OmpW is functioning as a partner in the efflux of vancomycin, although this possibility cannot be ruled out. The *ftsH* protease is induced in Gram-negative organisms by the Cpx misfolded protein periplasmic stress response, while the putative *motB* is induced by the Rcs stress response system [133, 135-137, 139, 199]. The upregulation of these genes related to cell wall stress, combined with the downregulation the of 3 porin type genes suggests that we are observing the early stages of cell wall stress response in these organisms, and provide support for the hypothesis that vancomycin challenge induces cell wall stress responses.

3.3.3 Protein synthesis

Protein synthesis was significantly reduced in the presence of vancomycin challenge, and 26 out of 36 total downregulated genes in this category encoded proteins putatively associated with translation. Fifteen of these genes encoded for proteins that are structurally associated with the small or large ribosomal subunits, while two (the translational GTPase *typA*, and the ribosome-associated trigger factor) are involved in the translation and stabilization of the nascent polypeptide [206]. Six genes were involved in the modification of bases in tRNAs, including the highly conserved modifications at positions 34 (the wobble position in the codon/anticodon pair) and position 37, which is required for accurate pairing and prevention of frameshifting [207]. These genes encode for a putative threonylcarbamoyl-AMP synthase, the S-adenosylmethionine (SAM) ribosyltransferase-isomerase gene *queA*, the threonylcarbamoyltransferase ATPase subunit *tsaE*, two SAM-dependent methyltransferases with putative tRNA modification

functions, and the tRNA guanosine methyltransferase *trmB*. The preprotein translocase subunit *secD* was also significantly downregulated, as was the redox-regulated ATPase *ychF*. In addition, the ribosome-associated inhibitor protein *raiA* was significantly upregulated. This protein is known to alter the structure of the ribosome to prevent translation, and leads to the formation of inactivated 100s ribosome super complexes [208].

These alterations suggest a global downregulation of translation which is a common feature of a diverse array of stress responses as the cell shifts resources away from energy intensive growth and translation towards survival and stressor specific responses, and likely represent a conserved basal stress response that is initiated in the early stages of cell stress.

3.3.4 Amino acid and central metabolism

Genes associated with central metabolism showed the greatest differential regulation, with 10 genes significantly upregulated, while only a single gene (ATP synthase F1 subunit γ) was significantly downregulated. Three subunits of the succinate dehydrogenase complex were significantly upregulated, along with malate dehydrogenase. The catabolism of phenylalanine was upregulated through the *paa* operon [209], 4 genes of which were upregulated. This operon degrades phenylalanine to acetyl-CoA and succinyl-CoA and is upregulated in response to oxidative stress [75].

These central metabolism alterations suggest that the cells are in the process of transitioning from aerobic growth to anaerobic growth. The upregulation of alcohol dehydrogenases along with the upregulation of the cytochrome c accessory protein *ccoG*, which is known to aid in the detoxification of reactive oxygen species [210] supports this, as this gene is upregulated during microaerobic and anaerobic growth [211], and it is possible that these enzymes may also help to deal with oxidative stress. The hypothesis that the cell is positioning itself to deal with oxidative stress potentially caused by disruption of energy production is further supported by the upregulation of genes involved in cysteine biosynthesis and phenolic acid breakdown. Both of these operons are known to be induced by oxidative stress [209, 212]. The metabolic and amino acid metabolism alterations do not appear to support the hypothesis that vancomycin challenge leads to osmotic stress, as genes for the synthesis of neither glycine/betaine nor proline were significantly altered, although due to the overlapping nature of many genes in the oxidative and osmotic stress response, this hypothesis cannot be discounted [213, 214]. The downregulation of the F_1 subunit of ATP synthase is consistent with cell wall stress, as accumulation of unbound subunits in the cytoplasmic membrane is known to be toxic to the cell, and serves as an inducer for the Cpx stress response [133].

3.3.5 Metal ion transport

Ten genes involved in metal ion transport were significantly altered by vancomycin challenge. Vancomycin is known to function as a chelator of Zn^{2+} and Cu^{2+} [110], and vancomycin challenge of *Streptomyces coulicor* was shown to induce genes related to the uptake of both ions [130]. In contrast, during vancomycin challenge of *E.*

anophelis R26 all 6 significantly downregulated metal ion transport genes were related to the uptake of Zn^{+2} and Cu^{+2}. Instead, the four significantly increased metal ion transporters were predicted to function in the uptake of Fe^{2+}, which is not strongly chelated by vancomycin [110].

3.3.6 Stress response

Nine total genes related to stress response were significantly altered, 6 up- and 3 downregulated. The 3 significantly downregulated genes consisted of a poorly characterized transcriptional accessory factor similar to the *tex* gene in *Bordetella pertussis* and *Pseudomonas aeruginosa* where it is thought to regulate toxin expression [215]. The second downregulated gene was a protein annotated to contain a META domain, which is thought to be involved in the heat shock response [216]. The final gene was an uncharacterized helix-turn-helix transcriptional regulator with a conserved domain similar to the xenobiotic response element family [155]. The stringent response is a starvation induced response that occurs when amino acids are limited [217], and is characterized by the cessation of translation along with the upregulation of amino acid biosynthesis pathways. This response is mediated by the synthesis of the alarmone (p)ppGpp by *relA* [218], and effects this response in part by binding to the RNA polymerase complex to inhibit transcription [218]. No genes related to starvation-induced stress response through (p)ppGpp production were significantly altered in *E. anophelis* R26 following vancomycin challenge, suggesting these changes are occurring independent of the stringent response.

Instead, genes involved with the osmotic or oxidative stress responses were upregulated, including aquaporin Z, all 3 genes from the tripartite DL-methionine ABC transporter, a lipid hydroperodixe peroxidase, and 3 putative membrane stress response proteins. While aquaporin Z and the DL-methionine ABC transporter are upregulated during osmotic stress in Gram-negative organisms [219], these genes are also upregulated during oxidative stress in *E. anophelis* NUHP1 and other Gram-negative organisms [75, 219]. This association, combined with the induction of the lipid hydroperoxide peroxidase, the induction of genes related to cysteine biosynthesis, and the lack of genes associated with glycine/betaine and proline biosynthesis argues in favor of an oxidative stress response. It should be noted, however, that superoxide dismutase was not significantly altered, which in turn argues that these genes are being induced as part of a general stress response. Finally, the acyl-CoA dehydrogenase gene *aidB* was also significantly induced. This gene is induced in response to DNA damage, and is thought to function by associating with double stranded DNA and destroying alkylating agents before they have the opportunity to damage the DNA [215].

3.3.7 The vancomycin stimulon displays features of both the cell wall and oxidative stress responses

It has been suggested that antimicrobial agents kill microorganisms in part by the induction of reactive oxygen species generated by disruption of central metabolism, although this hypothesis is controversial [125, 220-222]. On the one hand, live cell imaging showed evidence of cell wall damage characterized by blebbing and the formation of spheroblasts [131], and the transcriptome of *E. anophelis* R26 cells supports

this by revealing the upregulation of genes associated with both the Cpx and Rcs cell wall stress response systems [136, 137], along with the alteration of genes associated with cell wall synthesis and maintenance, although at 30 min the number of significantly altered cell envelope associated genes and it should be noted that no significant alteration was found in any genes in the putative capsular synthesis gene cluster (associated with Rcs response activation) [135] nor upregulation of the periplasmic stress response chaperone CpxP [133, 199], a primary effector of the Cpx pathway. Other genes unique to the Cpx response pathway include periplasmic regulator *spy*, which did not display significant alteration in the *E. anophelis* R26 RNAseq, and the OM associated complex *tolAB*, which was also not significantly altered [199].

Surprisingly, RNAseq revealed the alteration of several genes associated with the oxidative stress response, including genes associated with iron uptake, osmotic/oxidative shock, and a lipid hydroxyperoxidase thought to act on long chain fatty acid alkyl hydroperoxides [223], showing that the early stage stress response induced by vancomycin challenge shares many hallmarks of the oxidative stress response. These findings suggest there is some evidence that vancomycin challenge leads to oxidative damage along with disrupting peptidoglycan biosynthesis, although more investigation into this possibility is required. It should be noted that the vancomycin challenge only lasted for 30 min, and it is possible that this is insufficient time to fully induce stress responses related to vancomycin challenge.

3.4 Isolation and characterization of *E. anophelis* R26 and *E. ursingii* G4122 isolates demonstrating vancomycin resistance.

As described in project 3.2 above, I evaluated the physiological aspects of vancomycin challenge against *Elizabethkingia*. This study revealed that cultures challenged by vancomycin experienced an initial decrease in viable cell counts followed by a rapid rebound to cell densities comparable to the unchallenged control cultures. This raised the prospect that mutants demonstrating increased resistance to vancomycin arose in normal laboratory media containing growth inhibitory concentrations of vancomycin. In this project I aimed to isolate mutants demonstrating vancomycin resistance by selection on media containing vancomycin and to characterize the genomic mutations associated with this resistance along with the phenotypic consequences of these mutations. As with the transcriptiomic investigation in project 3.3, *E. anophelis* R26 was chosen for this experiment as it is the type strain for the most important of the *Elizabethkingia* species causing human disease, while *E. ursingii* G4122 was chosen for the selection of mutants due to the low MIC of this isolate (2 mg/L) compared to other species (Table 7).

3.4.1 Mutants demonstrating enhanced resistance were isolated after a single exposure to vancomycin

Both *E. anophelis* and *E. ursingii* mutants demonstrating elevated resistance to vancomycin were selected following exposure to growth inhibitory concentrations of vancomycin. All 8 *Elizabethkingia* mutants demonstrated elevated vancomycin resistance characterized by MICs between 32 mg/L and 256 mg/L. Vancomycin MBCs

Table 7. Vancomycin MICs and MBCs for parent and vancomycin-resistant mutants.

Isolate	Selection concentration[a]	Mutation frequency	MIC[a]	MBC[a]
$R26^T$	-	-	8	16
R26-VR1	16	4.33×10^{-4}	128	> 256
R26-VR2	16	4.33×10^{-4}	64	128
R26-VR3	16	4.33×10^{-4}	64	128
$G4122^T$	-	-	2	4
G4122-VR6	12	5.34×10^{-3}	64	> 256
G4122-VR7	14	4.28×10^{-4}	32	> 256
G4122-VR8	16	2.28×10^{-4}	32	> 256
G4122-VR9	18	5.58×10^{-5}	> 256	NT[b]
G4122-VR10	20	1.23×10^{-5}	> 256	NT[b]

[a] mg/L

[b] Not tested due to MIC > 256

for *E. anophelis* R26-VR1 (VR = vancomycin resistant) and all 5 *E. ursingii* G4122-VR mutants demonstrated MBCs > 256 mg/L, while E. *anophelis* R26-VSR2 and -VSR3 demonstrated MBCs of 128 mg/L. These MICs represent an increase over the MIC of the *E. anophelis* R26 and *E.ursingii* G4122 parent strains (MIC = 8 mg/L and 2 mg/L, respectively; Table 7). The mutation frequency for the 3 *E. anophelis* mutants was 4.33 x 10^{-4}, while the mutation frequencies for the 5 *E. ursingii* mutants ranged from 5.34 x 10^{-3} at a vancomycin concentration of 12 mg/L to 1.23 x 10^{-5} at 20 mg/L (Table 7). These mutation frequencies are considerably higher than those we have observed for mutants displaying ciprofloxacin (10^{-8}) and rifampin (10^{-9}) resistance (data not shown).

3.4.2 Temperature and MICs

Decreasing temperatures are hypothesized to decrease membrane fluidity leading to transient gaps in the outer membrane allowing the ingress of agents such as vancomycin that are normally excluded from the outer membrane [224]. Therefore, examining how vancomycin MICs vary across an array of temperatures for both *E. anophelis* R26 and *E. ursingii* G4122 and the vancomycin-resistant mutants derived from these isolates may provide additional evidence for the mechanisms of vancomycin resistance that have been altered in these mutants. If vancomycin resistance in the mutants is largely driven by alterations in outer membrane permeability we would expect that as temperature decreases and therefore membrane permeability increases, at low temperatures (i.e. 15°C) there should be very little difference in MICs between the parent and mutant isolates. On the other hand, if the mutation(s) underlying vancomycin resistance affect systems other than outer membrane permeability, by producing "decoy"

D-ala-D-ala stems [225], for example, then even at low temperatures we would expect to see some elevation of vancomycin MICs in mutants demonstrating accumulation of unbound D-ala-D-ala stems compared to mutants with mutations affecting membrane permeability due to the extra "protective" effect imparted by the excess of D-ala-D-ala stems. While low temperatures may impact vancomycin binding, it will do so in both types of mutant.

For most of the strains analyzed, all demonstrated the lowest vancomycin MIC at 4ºC. Most strains (R26, R26-VSR1, R26-VRS2, R26-VRS3, G4122, G4122-VR6, and G4122-VR7; Table 8) demonstrated the highest MICS at 21°C, 30°C and 35°C. Only strains G4122-VR8 G4122-VR9 and G4122-VR10 demonstrated higher or equal MICs at 37°C compared to 21°C, 30°C, and 35°C (Table 8). This data demonstrates that reducing temperature does indeed alter vancomycin MIC levels, in an isolate specific manner.

3.4.3 Gradient plate analysis

It is often demonstrated that the selection for resistance to a single antimicrobial, alters the expression of resistance to mechanistically unrelated antimicrobials [226, 227]. Often this results from the activation of intrinsic antimicrobial resistance mechanisms that result in relatively low levels of resistance expression [227]. Therefore, we applied the gradient plate technique, which is used to determine minor alterations in resistance (less than 2-fold [228]) to investigate resistance expression to other antimicrobials in our vancomycin-resistant mutants. All vancomycin-resistant isolates grew significantly further on the vancomycin gradients than the respective parent isolates (Table 9). All

Table 8. Vancomycin MICs for parent and mutant *Elizabethkingia* isolates at different temperatures.

Isolate	Species	15°C	21°C	30°C	35°C	37°C
R26^{T}	*anophelis*	4	32	64	64	8
R26-VR1	*anophelis*	8	64	64	64	128
R26-VR2	*anophelis*	8	32	32	32	64
R26-VR3	*anophelis*	8	128	128	128	64
G4122^{T}	*ursingii*	4	8	16	16	2
G4122-VR6	*ursingii*	4	32	32	32	64
G4122-VR7	*ursingii*	4	32	64	64	32
G4122-VR8	*ursingii*	4	16	32	32	32
G4122-VR9	*ursingii*	32	64	64	128	> 256
G4122-VR10	*ursingii*	32	128	256	128	> 256

Table 9. Mean distances grown by *E. anophelis* R26 and *E. ursingii* G4122 elevated vancomycin resistance mutants on gradient plates for select antibiotics.

Isolate	**Ciprofloxacin 0 → 0.5 mg/L**	**Clindamycin 0 → 1 mg/L**	**Rifampin 0 → 0.25 mg/L**	**Vancomycin 0 → 64 mg/L**
R26T	3.67 ± 0.33^{A}	31.00 ± 1.15^{A}	41.33 ± 1.76^{A}	6.33 ± 0.67^{NT}
R26-VR1	7.67 ± 0.67^{BC}	65.67 ± 1.45^{B}	63.67 ± 2.60^{B}	90.00 ± 0.00
R26-VR2	7.00 ± 0.58^{C}	52.67 ± 1.20^{C}	70.33 ± 2.03^{B}	89.00 ± 1.00
R26-VR3	9.67 ± 0.33^{B}	61.67 ± 2.19^{B}	80.33 ± 1.45^{C}	90.00 ± 0.00
Isolate	**0 → 0.25 mg/L**	**0 → 0.25 mg/L**	**0 → 0.125 mg/L**	**0 → 64 mg/L**
G4122T	90.00 ± 0.00^{NT}	7.67 ± 1.53^{NT}	5.33 ± 1.53^{NT}	10.33 ± 0.88^{NT}
G4122-VR6	7.67 ± 1.03	90.00 ± 0.00	73.67 ± 2.33	24.00 ± 1.53
G4122-VR7	6.00 ± 0.00	90.00 ± 0.00	89.00 ± 1.00	15.00 ± 1.00
G4122-VR8	10.33 ± 2.03	90.00 ± 0.00	90.00 ± 0.00	18.00 ± 0.58
G4122-VR9	7.33 ± 1.00	90.00 ± 0.00	8.00 ± 0.00	90.00 ± 0.00
G4122-VR10	3.67 ± 2.44	90.00 ± 0.00	9.00 ± 1.00	90.00 ± 0.00

vancomycin resistant isolates also demonstrated significantly altered susceptibility to ciprofloxacin, clindamycin, and rifampin. All 3 R26 vancomycin-resistant mutants demonstrated significant decreases in susceptibility to all three drugs, while the 5 G4122 vancomycin-resistant mutants demonstrated increased susceptibility to ciprofloxacin compared to the parent strain G4122. All 5 G4122 vancomycin-resistant mutants demonstrated considerable decreases in susceptibility to both clindamycin and rifampin. Both of these antibiotics are known to be excluded by the outer membrane of Gram-negative cells, and this finding suggests that the acquisition of vancomycin resistance may also act to enhance the barrier function of the *Elizabethkingia* outer membrane. Alternatively, intrinsic drug efflux pumps are known to affect levels of ciprofloxacin resistance in Gram-negative organisms [92, 93, 168, 169, 174, 175, 183, 229-231] and these findings may also suggest that enhanced drug efflux might be playing a role with ciprofloxacin resistance, although it is less clear in the case of rifampin, which is not an efflux pump substrate [232].

3.4.4 Vancomycin synergism is altered in VR mutants

Antibiotic combinations are frequently used to empirically treat multiply-antibiotic resistant Gram-negative organisms in clinical practice [233], with the most common combination being a broad-spectrum β-lactam or related antibiotic in combination with an aminoglycoside or fluoroquinolone. These combinations may have the benefit of reducing the emergence of antibiotic resistance to either agent alone, although evidence for the clinical efficacy of these combinations when treating common Gram-negative pathogens is conflicting [234-236]. Vancomycin is frequently used in

combination with a second antibiotic, most commonly rifampin or ciprofloxacin, to treat *Elizabethkingia* infections. The ability of mutations conferring vancomycin resistance to alter susceptibility to other antimicrobials, raises the concern that these mutations may also impact the synergy between vancomycin and potential antibiotic partners. R26-VR2 and R26-VR3 demonstrated reduced synergy to vancomycin in combination with ciprofloxacin and rifampin, while R26-VR1 displayed no change to ciprofloxacin, and improved synergism to rifampin with vancomycin (Table 10). None of the R26-VR mutants demonstrated altered synergies to clindamycin. All 5 G4122-VR isolates demonstrated worse synergism between vancomycin and ciprofloxacin, while 2 isolates (VR6 and VR10) demonstrated worse synergy between vancomycin and clindamycin. Three isolates (VR7, 8, and 9) demonstrated more favorable synergy for vancomycin in combination with clindamycin. Only G4122-VR10 demonstrated altered synergy between vancomycin and rifampin, with this isolate demonstrating improved synergy between the two drugs. These results suggest that alterations to vancomycin susceptibility can also lead to alterations in the synergy between vancomycin and other antimicrobials through mechanisms that are specific to each isolate. The observed differences in susceptibility amongst mutants further demonstrates the need for rigorous antimicrobial testing, and caution when choosing antibiotics or antibiotic combinations to treat *Elizabethkingia* infections.

3.4.5 Effects of vancomycin on cell length

The inhibition of peptidoglycan biosynthesis, or the inactivation of genes that affect peptidoglycan biosynthesis, may lead to an alteration in overall cell morphology.

Table 10. Interpretation of vancomycin – antimicrobial synergies.

Isolate	Species	Ciprofloxacin		Clindamycin		Rifampin	
		FICI	**Interpretation**	**FICI**	**Interpretation**	**FICI**	**Interpretation**
R26^{T}	*anophelis*	0.500	Synergistic	0.31	Synergistic	0.500	Additive
R26-VSR1	*anophelis*	0.260	Synergistic	0.29	Synergistic	0.375	Synergistic
R26-VSR2	*anophelis*	1.000	Indifferent	0.50	Synergistic	2.250	Antagonistic
R26-VSR3	*anophelis*	1.250	Indifferent	0.38	Synergistic	2.063	Antagonistic
G4122^{T}	*ursingii*	1.125	Indifferent	0.75	Additive	1.250	Indifferent
G4122-VR6	*ursingii*	8.125	Antagonistic	1	Indifferent	1.063	Indifferent
G4122-VR7	*ursingii*	18.00	Antagonistic	0.20	Synergistic	1.016	Indifferent
G4122-VR8	*ursingii*	40.06	Antagonistic	0.19	Synergistic	1.125	Indifferent
G4122-VR9	*ursingii*	8.500	Antagonistic	0.25	Synergistic	1.001	Indifferent
G4122-VR10	*ursingii*	4.250	Antagonistic	2.03	Antagonistic	0.501	Additive

Therefore, we wanted to investigate the morphological consequences of mutations underlying vancomycin resistance. Because at least some of the mutations supporting vancomyin-resistance are expected to lead to alterations of either the peptidoglycan layer or the outer membrane above, we hypothesized that these mutations would lead to alterations in the morphology of the mutant isolates in the presence and absence of vancomycin. We challenged *E. anophelis* R26 and R26-VR1 with vancomycin for 30 min, and visualized the resulting cell morphologies by scanning electron microscopy.

No significant difference in cell length was observed between R26 (mean ± 1 standard error = 1.696 ± 0.04 µm, N = 152) and R26-VR1 (mean ± 1 SE = 1.628 ± 0.03 µm, N = 157) when grown in MHB alone (Mann-Whitney U-test, N = 309, DF = 308, P = 0.32; Table 11). Vancomycin challenged *E. anophelis* R26 cells were marginally shorter (mean ± 1 SE = 1.601 ± 0.04 µm, N = 155) than cells grown in MHB alone (Mann-Whitney U-test, N = 307, DF = 306, P = 0.07), while R26-VR1 cells were significantly longer (mean ±1 SE = 1.808 ± 0.05 µm, N = 105) than R26-VR1 cells grown in MHB alone (Mann-Whitney U-test, N = 262, DF = 261, P = 0.0002; Table 11). R26-VR1 cells exposed to vancomycin were significantly longer than *E. anophelis* R26 cells exposed to vancomycin (Mann-Whitney U-test, N = 260, DF = 259, $P < 0.0001$). No significant differences were observed in cell width under any condition (Mann-Whitney U-test, $P \geq 0.149$ for all comparisons; Table 11). While no significant differences were detected between *E. anophelis* R26 and R26-V1 isolates grown in MHB alone, *E. anophelis* R26 and *E. anophelis* R26-V1 displayed opposite changes in cell

Table 11. Mean sizes of *E. anophelis* R26 and *E. anophelis* R26-VR1 cells.

Isolate	Treatment	Mean cell length ± 1 SE[a]	P-value[b]	Mean cell width ± 1 SE[c]	P-value[b]
R26	MHB	1.696 ± 0.04 (152)	0.0712	635 ± 3.9 (152)	0.1491
R26	12 mg/L vancomycin	1.601 ± 0.04 (155)		629 ± 3.7 (155)	
R26-VR1	MHB	1.628 ± 0.03 (157)	0.0002	630 ± 6.4 (157)	0.2729
R26-VR1	256 mg/L vancomycin	1.808 ± 0.05 (105)		629 ± 9.8 (105)	

[a] In microns. Parenthesis indicate number of cells measured.
[b] Mann-Whitney U-test
[c] In nanometers. Parenthesis indicate number of cells measured.

morphology, with *E. anophelis* R26 demonstrating a marginally significant reduction in cell length, while *E. anophelis* R26-VR1 experienced a significant increase in length.

3.4.6 Identification of mutations leading to vancomycin resistance.

Antimicrobial resistance often emerges from chromosomal mutations. These mutations can affect the target genes of these antimicrobials, or may occur in genes that govern other aspects of antimicrobial susceptibility such as membrane permeability, antimicrobial efflux systems, or the production of capsule or biofilm formation [227]. While the systems governing the vancomycin susceptibility of Gram-negative organisms are not yet completely understood, accumulating evidence suggests that vancomycin resistance is driven primarily by the permeability of the outer membrane. It has also been demonstrated that vancomycin binds to the terminal D-ala-D-ala stem of the peptidoglycan of Gram-negative organisms in a similar manner as the peptidoglycan of Gram-positive organisms [131]. This suggests the possibility that mutations in systems other than those governing outer membrane permeability such as alterations in the thickness or composition of the peptidoglycan, or a reduction in peptidoglycan autolysis may have the potential to impact vancomycin susceptibility. Therefore, we sought to identify the mutations underlying the vancomycin-resistant phenotypes using whole genome sequencing of all 3 *E. anophelis* R26-VR mutants along with *E. ursingii* G4122-VR6 and G4122-VR10.

Whole genome sequencing of all 3 *E. anophelis* R26-VR mutants revealed a single identical insertion of a cytosine in a putative transcriptional regulator identified by

bioinformatics as a *padR* transcriptional regulator (Table 12). These are a large group of functionally diverse regulators that demonstrate a winged helix-turn-helix motif [237], and are structurally similar to the multiple antibiotic resistance MarR family of transcriptional regulators which regulate the expression of the well characterized multidrug efflux system AcrAB-TolC [167, 237] as well as other genes [238]. In Gram-positive organisms, a homologue of the *padR* regulator in *Streptococcus faecalis* controls expression of an operon with several putative membrane associated proteins, expression of which appears to control vancomycin tolerance. This novel *E. anophelis padR* regulator will from here out be referred to as "vancomycin susceptibility regulator-1" (*vsr1*). The mutation in the R26- VR mutants demonstrated the insertion of a cytosine, which resulted in a frameshift and caused amino acid substitutions R75T, Y77I, and Y78L, along with a premature stop codon at position 79. This truncation removes the final 34 amino acids of *vsr1* and truncated the predicted C-terminal dimerization domain [237]. This truncation will likely abolish the ability of Vsr1 to bind to DNA, and abolish the regulatory function of this protein.

In contrast, comparison of the G4122-VR6 and G4122-VR10 genomes to the G4122 parent genome revealed a total of 5 mutations between the three strains, of which 2 were unique to G4122-VR6, 1 to G4122-VR10, and the remaining 2 were found in both mutants (Table 12). Interestingly, both mutants carried a mutation in a putative endonuclease III gene resulting in a phenylalanine to cysteine substitution at position 136, which is located in the active site and is near both a conserved functionally critical aspartate residue at position 139 [239], and the catalytic lysine at position 120 [240].

Table 12. Location, identity, and sequence outcomes of SNPs.

Isolate	Mutation	Location[a]	Sequence outcome
All R26-VR	Insertion C	1,577,274^1,577,275	Frameshift truncating the last 34 amino acids of a putative PadR transcription factor, along with 3 amino acid substitutions: R75T, Y77I, and Y78L
All G4122-VR	A to C	1,196,035	Synonymous mutation in a putative thioredoxin protein
All G4122-VR	T to G	2,042,612	F136C amino acid substitution in a putative Endonuclease III gene predicted to be involved in base excision repair
G4122-VR6	Insertion A	452,179^452,180	Insertion between the predicted -35 box and -10 box for a putative S-layer surface protein-like M60 Peptidase domain containing hypothetical protein (ORF 723)
G4122-VR6	G to A	895,352	Located 36 bp downstream of a putative AraC family helix-turn-helix regulatory protein and 7 bp before a putative rteC tetracycline resistance element regulatory protein
G4122-VR10	G to A	2,454,961	Nonsense mutation resulting in a premature stop codon at position 256 of a putative β-lactamase/penicillin binding protein family ORF containing AmpC/penicillin binding protein 4A like domain.

[a] Base position in the relevant reference genome.

While the functional implications of this substitution have not been elucidated yet, a disruption in DNA repair resulting from this mutation in endonuclease III could set the stage for additional mutations that resulted in vancomycin resistance. Both mutants also carried a synonymous mutation at nucleotide position 725 in a putative thioredoxin reductase gene. It is unlikely that this mutation has any part in the vancomycin resistance phenotype displayed by the two mutants. Both of these mutations were detected following comparison with the closed *E. ursingii* G4122 genome that was completed by our collaborators at the CDC. At the time of writing we have not determined if these two mutations are present in our laboratory *E. ursingii* G4122 stocks, and we speculate that it is possible both of these mutations emerged during storage and growth in the laboratory.

G4122-VR6 also contains two mutations in intergenic regions (Table 12). The first of these is the insertion of an adenine in the intergenic region between two divergently encoded ORFs of 261 and 723 amino acids (Figure 6). ORF261 encodes a putative drug and metabolite transport protein that BLAST analysis revealed contains a putative EamA superfamily domain, a diverse and poorly characterized group of membrane spanning proteins found in both prokaryotic and eukaryotic organisms thought to participate in a wide array of metabolite transport functions, including transport of nucleotide and amino sugars [241, 242]. ORF723 encodes a product that is variously annotated as a histone acetyltransferase, wall protein precursor, or simply as a hypothetical protein in numerous *Elizabethkingia* genomes. BLAST analysis of ORF723 revealed two predicted domains: a M60 metalloprotease domain, and a *Fibrobacter*

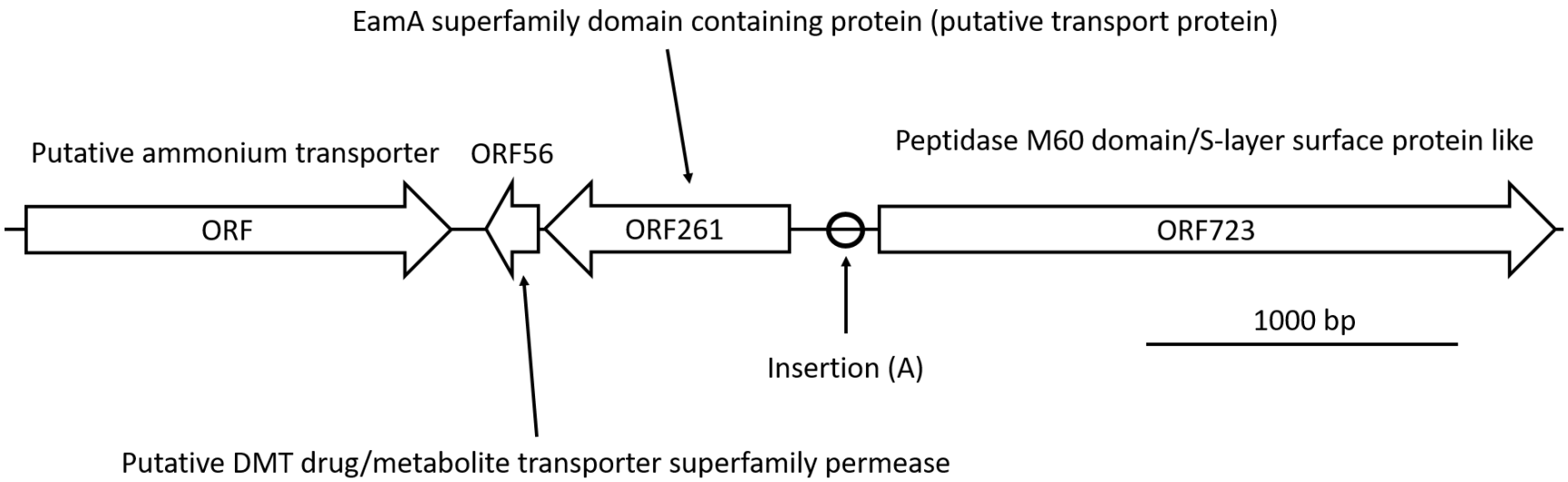

Figure 6. Adenine insertion in *E. ursingii* G4122-VR6.

succinogenes major domain. M60 metalloprotease domains are commonly found in extracellular proteins secreted by bacteria that colonize or invade the gut and are thought to be responsible for degrading complex glycoprotein matrices such as mucins [243], and may also be responsiblefor the formation of amyloid structures on the cell surface [244]. The *Fibrobacter succinogenes* major domain is another poorly characterized domain but is thought to participate in extracellular complex carbohydrate recognition and binding [245]. The bioinformatic information provided about these genes therefore does not help is trying to connect them to the vancomycin resistance mechanism.

The 236 bp intergenic region between ORF261 and ORF723 was analyzed using the BPROM promoter prediction software [160] to investigate the potential for this insertion to alter regulatory elements for one or both nearby ORFs. BPROM identified 13 potential binding sites for regulatory proteins on the plus strand, and 13 potential binding sites on the minus strand (Figures 7 and 8). Of the 26 predicted regulatory sequences, 4 predicted sequences on the minus strand, along with the predicted -35 box for ORF 261 contain the insertion, while two additional sequences are proximal to the insertion (Figure 7, Table 13). The second intergenic mutation in G4122-VR6 is an A>G transition in a 43 bp intergenic region between a putative AraC family transcriptional regulator, and *rteC*, a putative tetracycline response regulator. BPROM did not identify any putative regulatory elements in this region [246].

The unique SNP in G4122-VR10 leads to a nonsense mutation in a gene encoding a putative β-lactamase *ampC*/penicillin binding protein (PBP) 4A, truncating the final

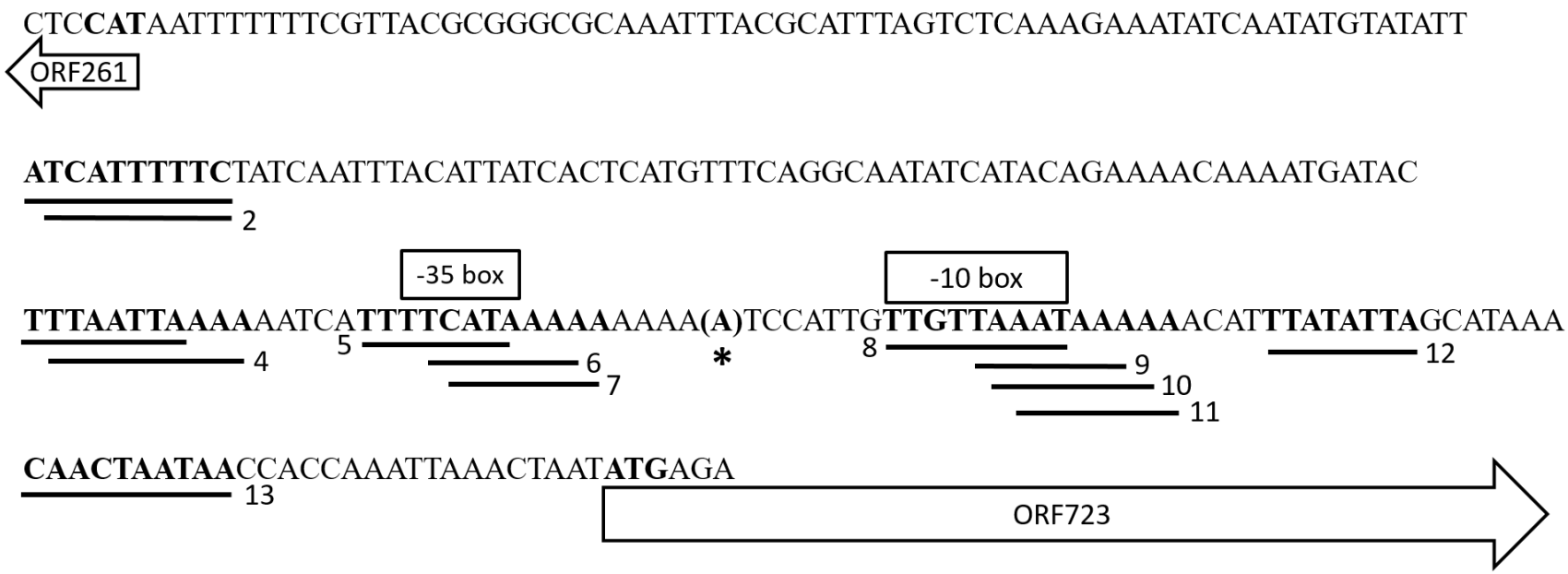

1.Fur 2. FlhA 3. PhoB 4. ArcA 5. PhoB 6. PhoB 7. ArgR 8. PdhR 9. TyrR 10. Ihf 11. ArcA 12. RpoS 13. MarR

Figure 7. Plus-strand genomic context of the insertion in *E. ursingii* G4122-VRS6. Regulatory elements predicted by BPROM are shown by solid lines and identified by a corresponding number. 452,179_452,180insA is indicated by an asterisk.

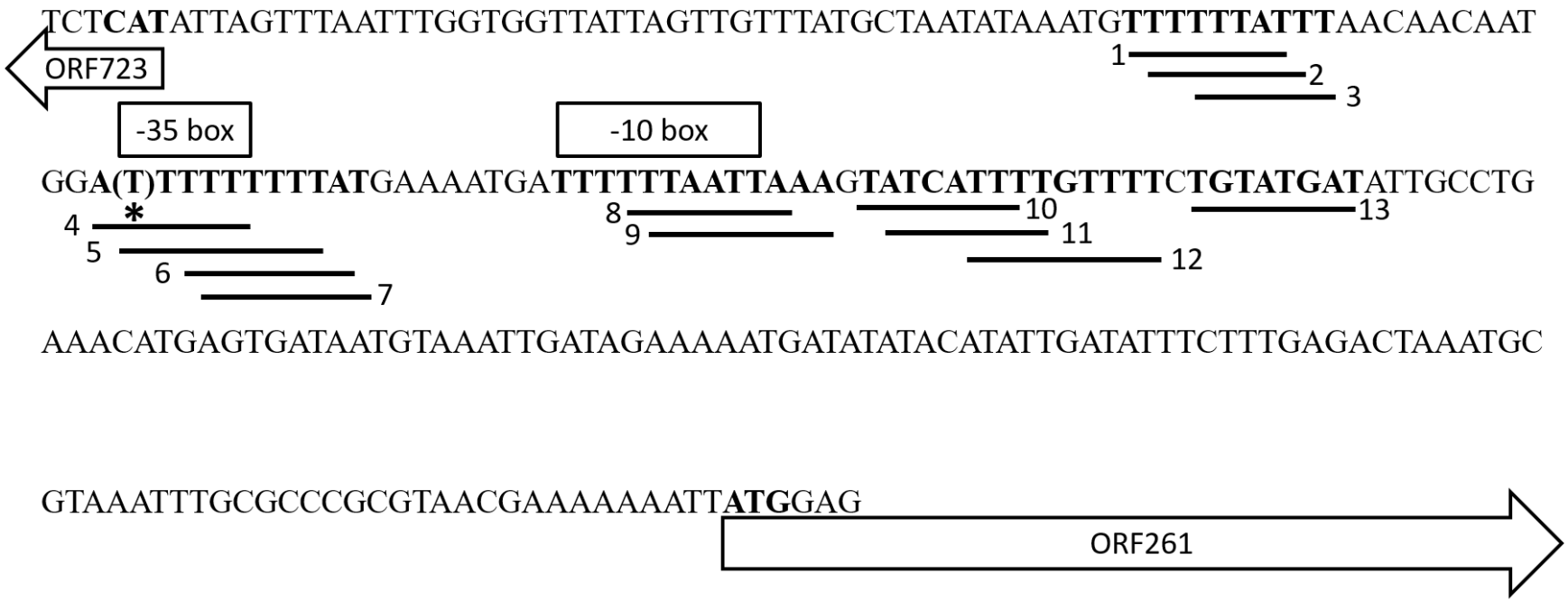

1. ArgR 2. ArgR 3. Ihf 4. Lrp 5. RpoH2 6. LexA 7. ArgR 8. PhoB 9. ArcA 10. SoxS 11. Fur 12. RpoD 13. RpoD

Figure 8. Minus-strand genomic context of the insertion in *E. ursingii* G4122-VRS6. Regulatory elements predicted by BPROM are shown by solid lines and identified by a corresponding number. 452,179_452,180insA is indicated by an asterisk.

Table 13. Potential regulatory sequences directly impacted by the insertion of a thymine in the intergenic region between ORF261 and ORF723.

Transcription Factor	Predicted target sequence[a]	Regulatory function
-35 box	(T)TTTTT	Binding site for σ^{70} mediated RNA polymerase binding
Lrp	A(T)TTTTTTT	Regulator of amino acid metabolism and pili synthesis [247]
RpoH2	(T)TTTTTTT	Heat and oxidative stress response [248]
LexA	TTTTTTTA	Stress response regulator, particularly DNA breakage SOS response [249]
ArgR	TTTTTTAT	Regulation of arginine metabolism, and may activate expression of pili and adhesins [250, 251]

[a] The inserted thymine is indicated by parentheses

120 amino acids in the vanomycin-resistant mutant (Table 12). Differentiating between β-lactamases and PBPs is complicated by the considerable sequence and domain conservation between the two enzyme classes [252]. The PBPs are critical enzymes for cell wall biosynthesis, remodeling, and maintenance, and PBP 4A is thought to function in the maintenance of cell shape and is known to possess DD-carboxypeptidase activity [253], which removes the terminal D-ala residue from the pentapeptide stem on peptidoglycan polymers. Both terminal D-ala residues are required for vancomycin to bind peptidoglycan [222] and therefore it is possible that the truncation of ORF376 in G4122-VR10 may lead to the accumulation of unbound D-ala-D-ala stems binding vancomycin away from the site of active cell wall biosynthesis in a similar mechanism to that proposed for vancomycin-intermediate *S. aureus* [126, 127].

3.4.7 qPCR analysis of vancomycin resistant mutants

Whole genome analysis of the three *E. anophelis* R26-VR mutants, along with *E. ursingii* G4122-VR6, revealed the presence of mutations that had the potential to impact the expression of genes around them. Therefore, the expression of three genes, ORF552 in *E. anophelis* R26 and R26-VR3 along with ORF261 and ORF723 in *E. ursingii* G4122 and G4122-VR6 in the presence and absence of vancomycin was quantified by qPCR.

ORF552 was significantly upregulated in the absence of vancomycin in *E. anophelis* R26-VR3 compared to R26 (mean fold-change ± 1 SE = 11.77 ± 2.25, P = 0.02; Student's t-test, N = 3, DF = 2 for all comparisons) (Table 14). This upregulation increased when the respective isolates were challenged with vancomycin (87.22 ± 1.27; P

Table 14. Quantitative PCR analysis of ORF552 in *E. anophelis* R26-VR3 and ORF261 and ORF723 in *E. uringii* G4122-VR6.

Isolate	Gene	Treatment	Mean Fold Change ± 1SE	P-value[a]
R26	ORF552	Control	-	-
		Vancomycin	1.61 ± 1.28	0.193
R26-VR1	ORF552	Control	11.77 ± 2.25[b]	0.02
		Vancomycin	87.22 ± 1.27[c]	0.002
G4122	ORF261	Control	-	-
		Vancomycin	1.09 ±0.09[b]	1.000
G4122-VR6	ORF261	Control	5.86 ±0.66[b]	0.041
		Vancomycin	-1.33 ±0.73[c]	0.436
G4122^T	ORF723	Control	-	-
		Vancomycin	-15.99 ±0.67[b]	0.047
G4122-VR6	ORF723	Control	0.96 ±0.33[b]	0.976
		Vancomycin	24.27 ±0.67[c]	0.006

[a] Student's t-test
[b] Compared to expression levels in the parent isolate MHB only control
[c] Compared to expression levels for the parent isolate challenged with vancomycin

= 0.002). ORF552 expression was not significantly altered in the presence of vancomycin for neither *E. anophelis* R26 (1.61 ± 1.28; P = 0.193) nor *E. anophelis* R26-VR3 (1.16 ± 1.27; P = 0.680). This suggests that the truncation of *vsr1* in *E. anophelis* R26-VR3 has led to de-repression of ORF552 in this isolate, resulting in significantly increased basal expression levels. The lack of significant change in ORF552 in *E. anophelis* R26-VR3 is consistent with this hypothesis, as the major source of repression, *vsr1*, remains unable to regulate this gene due to the truncation. More interesting is the lack of significant change in *E. anophelis* R26. The potential importance of ORF552 in vancomycin resistance is suggested by the putative phage shock protein A/C domain that was detected in this protein [254]. This domain is one of the major sensor and effector proteins for the phage shock protein response [254], and the greater expression of this gene in *E. anophelis* R26-VR3 may increase the ability of this organism to detect vancomycin damage early, and activate survival responses that are thus more effective.

Quantitative PCR analysis demonstrated that in the absence of vancomycin ORF261 was significantly upregulated in G4122-VR6 compared to G4122 (5.86 ±0.68; P = 0.041), but was not significantly altered between the two isolates in the presence of vancomycin (-1.33 ± 0.73; P = 0.463). ORF261 was not significantly altered by vancomycin challenge in G4122 (1.09 ± 0.09; P = 1.000) but was significantly downregulated in G4122-VR6 (-4.09 ± 0.73; P = 0.016). Conversely, ORF723 was not significantly altered in G4122-VR6 compared to G4122 in the absence of vancomycin (0.96 ± 0.33; P = 0.976,) but was significantly upregulated during vancomycin challenge (24.27 ± 0.67; P = 0.006). Vancomycin challenge resulted in a significant

downregulation of ORF723 in G4122 (-15.99 ± 0.47; P = 0.047) but not G4122-VR6 (1.58 ± 0.67; P = 0.082). These results suggest two possibilities: that the downregulation of ORF261 in *E. ursingii* G4122-VR6 may reduce the permeability of the outer membrane by reducing the number of pore proteins inserted into the membrane. There is no evidence to date that vancomycin is capable of passing through the pores of transport proteins, but this has not been tested in the case of EamA-like proteins [122]. Secondly, it is possible that the adenine insertion in *E. ursingii* G4122-VR6 has disrupted the regulation of ORF723, preventing the downregulation of this ORF during vancomycin challenge. While the specific function of ORF723 is unclear, extracellular metalloproteases such as *ftsH* are upregulated during cell envelope stress, and it is possible that ORF723 is functioning in a similar manner.

3.5 Conclusions

We have demonstrated that *Elizabethkingia* isolates with significant genomic similarity to human isolates are found in horses, although to date no direct evidence for transmission of *Elizabethkingia* between humans and animals has been observed [74]. We further demonstrated that both isolates display low MICs for ciprofloxacin and that both isolates display MICs for vancomycin consistent with those reported for *E. anophelis* isolates from human infections [19, 44, 86, 87, 105, 107, 143, 158, 188, 192, 255]. This work continues to build evidence that *E. anophelis* are widely distributed, and that additional environmental and epidemiological studies should be carried out to further elucidate the interplay and importance of this potential for cross species transmission.

We have also demonstrated that vancomycin displays a bactericidal effect on *Elizabethkingia*, and that these organisms demonstrate vancomycin MICs and MBCs that are considerably lower than those normally observed for Gram-negative organisms [188]. Our results further demonstrate that there are considerable differences between *Elizabethkingia* species to vancomycin in combination with ciprofloxacin and rifampin, and that efforts should therefore be made to speciate suspected *Elizabethkingia* isolates prior to the initiation of combination therapy. It is possible that there are compositional differences in the outer membrane of *Elizabethkingia* isolates, which in turn may lead to differences in permeability, and needs to be investigated further.

Vancomycin challenge appeared to induce genes from both the Cpx and Rcs stress response systems in *E. anophelis* R26 following 30 min of exposure. Vancomycin challenge further resulted in the upregulation of genes that have been implicated in the oxidative stress response, including upregulation of iron uptake genes, alterations to components of the TCA cycle, and suppression of translation [75]. It is possible that the similarities between these two stress response stimulons points to a conserved cross protective underlying stress response, with more specific stress response genes activated on top of this basal response. It should be noted again that a major caveat of this work is that vancomycin challenge only lasted for 30 min. While 30 min challenge is sufficient to generate cell wall stress responses in Gram-negative organisms challenged with other cell wall active microbials [131, 199], the slower action of vancomycin as evidenced by the 2 h lag time between challenge and cell death raises the possibility that a longer challenge time should be used in the future to more fully capture this response. Finally,

while it is unlikely that OmpW is functioning in concert with multidrug efflux systems to remove vancomycin [122], this possibility cannot be ruled out and should be investigated further.

Vancomycin resistance in the *Elizabethkingia* requires very few mutations to occur, and can have dramatic impacts on antimicrobial susceptibility to other antibiotics and combinations. Similar to Gram-positive organisms where vancomycin intermediate resistance is known to arise from a diverse array of mutations [109, 126-128, 256, 257], our results suggest that there are several different mechanisms for the development of vancomycin resistance in the *Elizabethkingia*. All 3 sequenced *E. anophelis* R26 vancomycin-resistant mutants displayed an identical mutation, however this mutation was different than the mutations identified in the two *E. ursingii* G4122 vancomycin-resistant mutants that were sequenced. A major caveat to this work is that the sequencing data was compared to reference genomes, rather than comparison by *de novo* assembly. It is possible that this method has resulted in other alterations in the genome, such as duplications or more significant insertions or deletions, being missed.

All told, we have demonstrated that vancomycin kills *Elizabethkingia* by inhibiting peptidoglycan biosynthesis, although the high mutation frequency of vancomycin-resistant mutants, along with the ability of vancomycin resistance to arise from mutations in multiple different systems raises concerns about the efficacy of this drug in the treatment of *Elizabethkingia* infections.

3.6 Future Directions

In vitro synergy assays are limited because they provide an ideal environment for the organism being challenged to grow in while eliminating potentially important host factors [258]. The behavior of microorganisms *in vitro* does not always translate *in vivo*, and it is possible that the impact of vancomycin on *Elizabethkingia* is a prime example. Therefore, to better understand both the role of vancomycin in *Elizabethkingia* treatment, and to better evaluate the impact of mutations conferring vancomycin resistance in a clinically relevant setting, it is of critical importance to develop and validate an animal model of *Elizabethkingia* infection. A functional animal model will allow the characterization of host factors (innate immune responses, for example), and will provide a better understanding of how these mutations impact fitness and antibiotic susceptibility.

While our microscopy data provides more direct evidence of cell death due to vancomycin, imaging does not provide direct evidence of the inhibition of peptidoglycan biosynthesis. Therefore, the inhibitory action of vancomycin should be investigated by isolating the peptidoglycan sacculus from cells grown in the presence of ^{14}C-labeled peptidoglycan precursors, and quantifying the incorporation of these precursors into the cell wall with and without the presence of vancomycin by liquid scintillation radiography. Furthermore, fluorescently labeled vancomycin should be utilized to directly visualize vancomycin to assess differences in accumulation between the various species, and in the mutants as well.

De novo assembly of the existing whole genome sequencing, along with sequencing of the remaining 3 *E. ursingii* G4122-VR isolates may identify other potential mutations, or confirm the known mutations. RNAseq of the vancomycin-resistant mutants is critical to understanding the alterations in these organisms that allow them to resist the action of vancomycin, and will allow for the investigation of genes that are more specifically involved in the vancomycin response. Additionally, many of the cell envelope stress responses in Gram-negative organisms rely on proteolytic activation of response regulators and may not be captured by qPCR or RNAseq assays. Therefore, proteomic analysis of cell wall stress sensors will provide a more detailed analysis of the vancomycin stress response in *Elizabethkingia*, and may help to identify potential targets for enhancing the effectiveness of vancomycin in these and other Gram-negative organisms.

Finally, the isolation and characterization of a wider collection of *E. anophelis* vancomycin- resistant mutants will help to better understand the prevalence of each of these mechanisms in the most clinically important of the *Elizabethkingia* species.

REFERENCES

1. Lau SK, Chow WN, Foo CH, Curreem SO, Lo GC, Teng JL, *et al*. *Elizabethkingia anophelis* bacteremia is associated with clinically significant infections and high mortality. Sci Rep. 2016;6:26045. Epub 2016/05/18. doi: 10.1038/srep26045. PubMed PMID: 27185741; PubMed Central PMCID: PMCPMC4868968.

2. Dziuban EJ, Franks J, So M, Peacock G, Blaney DD. *Elizabethkingia* in Children: A Comprehensive Review of Symptomatic Cases Reported from 1944-2017. Clin Infect Dis. 2017. Epub 2017/12/07. doi: 10.1093/cid/cix1052. PubMed PMID: 29211821.

3. Figueroa Castro CE, Johnson C, Williams M, VanDerSlik A, Graham MB, Letzer D, *et al. Elizabethkingia anophelis*: Clinical Experience of an Academic Health System in Southeastern Wisconsin. Open Forum Infect Dis. 2017;4(4):ofx251. Epub 2018/01/09. doi: 10.1093/ofid/ofx251. PubMed PMID: 29308406; PubMed Central PMCID: PMCPMC5751080.

4. Perrin A, Larsonneur E, Nicholson AC, Edwards DJ, Gundlach KM, Whitney AM, *et al*. Evolutionary dynamics and genomic features of the *Elizabethkingia anophelis* 2015 to 2016 Wisconsin outbreak strain. Nat Commun. 2017;8:15483. Epub 2017/05/26. doi: 10.1038/ncomms15483. PubMed PMID: 28537263; PubMed Central PMCID: PMCPMC5458099.

5. Kampfer P, Busse HJ, McInroy JA, Glaeser SP. *Elizabethkingia endophytica sp. nov*., isolated from *Zea mays* and emended description of *Elizabethkingia anophelis* Kampfer *et al*. 2011. Int J Syst Evol Microbiol. 2015;65(7):2187-93. Epub 2015/04/11. doi: 10.1099/ijs.0.000236. PubMed PMID: 25858248.

6. Olsen H. *Flavobacterium meningosepticum* isolated from outside hospital surroundings and during routine examination of patient specimens. Acta Pathol Microbiol Scand. 1969;75(2):313-22. Epub 1969/01/01. PubMed PMID: 5822968.

7. Kampfer P, Matthews H, Glaeser SP, Martin K, Lodders N, Faye I. *Elizabethkingia anophelis sp. nov*., isolated from the midgut of the mosquito *Anopheles gambiae*. Int J Syst Evol Microbiol. 2011;61(Pt 11):2670-5. Epub 2010/12/21. doi: 10.1099/ijs.0.026393-0. PubMed PMID: 21169462.

8. Jiang HY, Ma JE, Li J, Zhang XJ, Li LM, He N, *et al*. Diets Alter the Gut Microbiome of Crocodile Lizards. Front Microbiol. 2017;8:2073. Epub 2017/11/10. doi: 10.3389/fmicb.2017.02073. PubMed PMID: 29118742; PubMed Central PMCID: PMCPMC5660983.

9. Kukutla P, Lindberg BG, Pei D, Rayl M, Yu W, Steritz M, *et al*. Draft Genome Sequences of *Elizabethkingia anophelis* Strains R26T and Ag1 from the Midgut of the Malaria Mosquito *Anopheles gambiae*. Genome Announc. 2013;1(6). Epub 2013/12/07. doi: 10.1128/genomeA.01030-13. PubMed PMID: 24309745; PubMed Central PMCID: PMCPMC3853068.

10. Lee D, Kim YK, Kim YS, Kim TJ. Complete Genome Sequence of *Elizabethkingia sp.* BM10, a Symbiotic Bacterium of the Wood-Feeding Termite *Reticulitermes speratus* KMT1. Genome Announc. 2015;3(5). Epub 2015/10/10. doi: 10.1128/genomeA.01181-15. PubMed PMID: 26450743; PubMed Central PMCID: PMCPMC4599102.

11. Mee PT, Lynch SE, Walker PJ, Melville L, Duchemin JB. Detection of *Elizabethkingia spp*. in Culicoides Biting Midges, Australia. Emerg Infect Dis. 2017;23(8):1409-10. Epub 2017/07/21. doi: 10.3201/eid2308.161565. PubMed PMID: 28726605; PubMed Central PMCID: PMCPMC5547790.

12. Raygoza Garay JA, Hughes GL, Koundal V, Rasgon JL, Mwangi MM. Genome Sequence of *Elizabethkingia anophelis* Strain EaAs1, Isolated from the Asian Malaria Mosquito *Anopheles stephensi*. Genome Announc. 2016;4(2). Epub 2016/03/12. doi: 10.1128/genomeA.00084-16. PubMed PMID: 26966196; PubMed Central PMCID: PMCPMC4786652.

13. Kyritsi MA, Mouchtouri VA, Pournaras S, Hadjichristodoulou C. First reported isolation of an emerging opportunistic pathogen (*Elizabethkingia anophelis*) from hospital water systems in Greece. J Water Health. 2018;16(1):164-70. Epub 2018/02/10. doi: 10.2166/wh.2017.184. PubMed PMID: 29424730; PubMed Central PMCID: PMCwh_2017_184.

14. Bordelo J, Viegas C, Coelho C, Poeta P. First report of bacteremia caused by *Elizabethkingia meningoseptica* in a dog. Can Vet J. 2016;57(9):994. Epub 2016/09/03. PubMed PMID: 27587896; PubMed Central PMCID: PMCPMC4982576.

15. Hu R, Yuan J, Meng Y, Wang Z, Gu Z. Pathogenic *Elizabethkingia miricola* Infection in Cultured Black-Spotted Frogs, China, 2016. Emerg Infect Dis. 2017;23(12):2055-9. Epub 2017/11/18. doi: 10.3201/eid2312.170942. PubMed PMID: 29148374.

16. Lei XP, Yi G, Wang KY, OuYang P, Chen F, Huang XL, *et al. Elizabethkingia miricola* infection in Chinese spiny frog (*Quasipaa spinosa*). Transbound Emerg Dis. 2018. Epub 2018/12/17. doi: 10.1111/tbed.13101. PubMed PMID: 30554477.

17. Jacobs A, Chenia HY. Biofilm formation and adherence characteristics of an *Elizabethkingia meningoseptica* isolate from *Oreochromis mossambicus*. Ann Clin Microbiol Antimicrob. 2011;10:16. Epub 2011/05/07. doi: 10.1186/1476-0711-10-16. PubMed PMID: 21545730; PubMed Central PMCID: PMCPMC3112384.

18. Lin JN, Lai CH, Yang CH, Huang YH, Lin HH. *Elizabethkingia bruuniana* Infections in Humans, Taiwan, 2005-2017. Emerg Infect Dis. 2019;25(7):1412-4. Epub 2019/06/19. doi: 10.3201/eid2507.180768. PubMed PMID: 31211685; PubMed Central PMCID: PMCPMC6590768.

19. Breurec S, Criscuolo A, Diancourt L, Rendueles O, Vandenbogaert M, Passet V, *et al*. Genomic epidemiology and global diversity of the emerging bacterial pathogen *Elizabethkingia anophelis*. Sci Rep. 2016;6:30379. doi: 10.1038/srep30379. PubMed PMID: 27461509; PubMed Central PMCID: PMCPMC4961963.

20. Chawla K, Gopinathan A, Varma M, Mukhopadhyay C. *Elizabethkingia meningoseptica* outbreak in intensive care unit. J Glob Infect Dis. 2015;7(1):43-4. Epub 2015/02/28. doi: 10.4103/0974-777X.150890. PubMed PMID: 25722622; PubMed Central PMCID: PMCPMC4338452.

21. Choi MH, Kim M, Jeong SJ, Choi JY, Lee IY, Yong TS, *et al*. Risk Factors for *Elizabethkingia* Acquisition and Clinical Characteristics of Patients, South Korea. Emerg Infect Dis. 2019;25(1):42-51. Epub 2018/12/19. doi: 10.3201/eid2501.171985. PubMed PMID: 30561316; PubMed Central PMCID: PMCPMC6302585.

22. Frost F, Nazareth D. Case Report: First report of *Elizabethkingia miricola* infection in a patient with cystic fibrosis. F1000Res. 2018;7:440. Epub 2018/08/09. doi: 10.12688/f1000research.14441.2. PubMed PMID: 30079241; PubMed Central PMCID: PMCPMC6058470.

23. Green O, Murray P, Gea-Banacloche JC. Sepsis caused by *Elizabethkingia miricola* successfully treated with tigecycline and levofloxacin. Diagn Microbiol Infect Dis. 2008;62(4):430-2. Epub 2008/10/10. doi: 10.1016/j.diagmicrobio.2008.07.015. PubMed PMID: 18842380; PubMed Central PMCID: PMCPMC2650818.

24. Gupta P, Zaman K, Mohan B, Taneja N. *Elizabethkingia miricola*: A rare non-fermenter causing urinary tract infection. World J Clin Cases. 2017;5(5):187-90. doi: 10.12998/wjcc.v5.i5.187. PubMed PMID: 28560237; PubMed Central PMCID: PMCPMC5434319.

25. Han MS, Kim H, Lee Y, Kim M, Ku NS, Choi JY, *et al*. Relative Prevalence and Antimicrobial Susceptibility of Clinical Isolates of *Elizabethkingia* Species Based on 16S rRNA Gene Sequencing. J Clin Microbiol. 2017;55(1):274-80. Epub 2016/11/17. doi: 10.1128/JCM.01637-16. PubMed PMID: 27847376; PubMed Central PMCID: PMCPMC5228240.

26. Kenna DTD, Fuller A, Martin K, Perry C, Pike R, Burns PJ, *et al*. *rpoB* gene sequencing highlights the prevalence of an *E. miricola* cluster over other *Elizabethkingia* species among UK cystic fibrosis patients. Diagn Microbiol Infect Dis. 2017. Epub 2017/11/28. doi: 10.1016/j.diagmicrobio.2017.10.014. PubMed PMID: 29174734.

27. King EO. Studies on a group of previously unclassified bacteria associated with meningitis in infants. Am J Clin Pathol. 1959;31(3):241-7. Epub 1959/03/01. PubMed PMID: 13637033.

28. Ursing J, Bruun B. Genetic heterogeneity of *Flavobacterium meningosepticum* demonstrated by DNA-DNA hybridization. Acta Pathol Microbiol Immunol Scand B. 1987;95(1):33-9. Epub 1987/02/01. doi: 10.1111/j.1699-0463.1987.tb03084.x. PubMed PMID: 3565016.

29. Nicholson AC, Gulvik CA, Whitney AM, Humrighouse BW, Graziano J, Emery B, *et al*. Revisiting the taxonomy of the genus *Elizabethkingia* using whole-genome sequencing, optical mapping, and MALDI-TOF, along with proposal of three novel *Elizabethkingia* species: *Elizabethkingia bruuniana sp. nov., Elizabethkingia ursingii sp. nov., and Elizabethkingia occulta sp. nov*. Antonie Van Leeuwenhoek. 2017. Epub 2017/09/01. doi: 10.1007/s10482-017-0926-3. PubMed PMID: 28856455.

30. Doijad S, Ghosh H, Glaeser S, Kampfer P, Chakraborty T. Taxonomic reassessment of the genus *Elizabethkingia* using whole-genome sequencing: *Elizabethkingia endophytica* Kampfer et al. 2015 is a later subjective synonym of *Elizabethkingia anophelis* Kampfer et al. 2011. Int J Syst Evol Microbiol. 2016;66(11):4555-9. Epub 2016/08/09. doi: 10.1099/ijsem.0.001390. PubMed PMID: 27498788.

31. Liu KM, Chang HL, Hsu MH, Lin YZ, Lee YL, Chen YT. Complete Genome Sequencing of *Elizabethkingia* sp. Strain 2-6. Microbiol Resour Announc. 2019;8(44). Epub 2019/11/02. doi: 10.1128/MRA.00805-19. PubMed PMID: 31672739; PubMed Central PMCID: PMCPMC6953514.

32. Cheng YH, Perng CL, Jian MJ, Cheng YH, Lee SY, Sun JR, *et al*. Multicentre study evaluating matrix-assisted laser desorption ionization-time of flight mass spectrometry for identification of clinically isolated *Elizabethkingia* species and analysis of antimicrobial susceptibility. Clin Microbiol Infect. 2019;25(3):340-5. Epub 2018/04/25. doi: 10.1016/j.cmi.2018.04.015. PubMed PMID: 29689427.

33. Lin JN, Lai CH, Yang CH, Huang YH, Lin HF, Lin HH. Comparison of four automated microbiology systems with 16S rRNA gene sequencing for identification of *Chryseobacterium* and *Elizabethkingia* species. Sci Rep. 2017;7(1):13824. Epub 2017/10/25. doi: 10.1038/s41598-017-14244-9. PubMed PMID: 29062009; PubMed Central PMCID: PMCPMC5653830.

34. Agarwal S, Kakati B, Khanduri S, Gupta S. Emergence of Carbapenem Resistant Non-Fermenting Gram-Negative Bacilli Isolated in an ICU of a Tertiary Care Hospital. J Clin Diagn Res. 2017;11(1):DC04-DC7. Epub 2017/03/10. doi: 10.7860/JCDR/2017/24023.9317. PubMed PMID: 28273965; PubMed Central PMCID: PMCPMC5324410.

35. Jean SS, Lee WS, Chen FL, Ou TY, Hsueh PR. *Elizabethkingia meningoseptica*: an important emerging pathogen causing healthcare-associated infections. J Hosp Infect. 2014;86(4):244-9. Epub 2014/04/01. doi: 10.1016/j.jhin.2014.01.009. PubMed PMID: 24680187.

36. Mirza HC, Tuncer O, Olmez S, Sener B, Tugcu GD, Ozcelik U, *et al*. Clinical Strains of *Chryseobacterium* and *Elizabethkingia* spp. Isolated from Pediatric Patients in a University Hospital: Performance of MALDI-TOF MS-Based Identification, Antimicrobial Susceptibilities, and Baseline Patient Characteristics. Microb Drug Resist. 2018;24(6):816-21. Epub 2017/12/12. doi: 10.1089/mdr.2017.0206. PubMed PMID: 29227188.

37. Nicholson AC, Humrighouse BW, Graziano JC, Emery B, McQuiston JR. Draft Genome Sequences of Strains Representing Each of the *Elizabethkingia* Genomospecies Previously Determined by DNA-DNA Hybridization. Genome Announc. 2016;4(2). doi: 10.1128/genomeA.00045-16. PubMed PMID: 26966213; PubMed Central PMCID: PMCPMC4786648.

38. Anderson B, Abd-Elsayed A. Pain as the main presenting symptom in a patient with *Elizabethkingia* infection. J Clin Anesth. 2016;34:302. Epub 2016/10/01. doi: 10.1016/j.jclinane.2016.05.002. PubMed PMID: 27687396.

39. Chen CH, Lin CH, Lin JS. Bacteremia caused by *Elizabethkingia meningoseptica* in a mechanically ventilated patient successfully treated with imipenem-cilastatin and ciprofloxacin. Rev Inst Med Trop Sao Paulo. 2017;59:e26. Epub 2017/06/08. doi: 10.1590/S1678-9946201759026. PubMed PMID: 28591254; PubMed Central PMCID: PMCPMC5459533.

40. Dias M, Prashant K, Pai R, Scaria B. *Chryseobacterium meningosepticum* bacteremia in diabetic nephropathy patient on hemodialysis. Indian J Nephrol. 2010;20(4):203-4. Epub 2011/01/06. doi: 10.4103/0971-4065.73460. PubMed PMID: 21206682; PubMed Central PMCID: PMCPMC3008949.

41. Edelsberg J, Berger A, Weber DJ, Mallick R, Kuznik A, Oster G. Clinical and economic consequences of failure of initial antibiotic therapy for hospitalized patients with complicated skin and skin-structure infections. Infect Control Hosp Epidemiol. 2008;29(2):160-9. Epub 2008/01/09. doi: 10.1086/526444. PubMed PMID: 18179372.

42. Fodor AA, Klem ER, Gilpin DF, Elborn JS, Boucher RC, Tunney MM, *et al*. The adult cystic fibrosis airway microbiota is stable over time and infection type, and highly resilient to antibiotic treatment of exacerbations. PLoS One. 2012;7(9):e45001. Epub 2012/10/11. doi: 10.1371/journal.pone.0045001. PubMed PMID: 23049765; PubMed Central PMCID: PMCPMC3458854.

43. Hagiya H, Ogawa H, Takahashi Y, Hasegawa K, Iwamuro M, Otsuka F. A Nephrostomy-associated Urinary Tract Infection Caused by *Elizabethkingia meningoseptica*. Intern Med. 2015;54(24):3233-6. Epub 2015/12/17. doi: 10.2169/internalmedicine.54.4998. PubMed PMID: 26666619.

44. Hsu MS, Liao CH, Huang YT, Liu CY, Yang CJ, Kao KL, *et al*. Clinical features, antimicrobial susceptibilities, and outcomes of *Elizabethkingia meningoseptica* (*Chryseobacterium meningosepticum*) bacteremia at a medical center in Taiwan, 1999-2006. Eur J Clin Microbiol Infect Dis. 2011;30(10):1271-8. Epub 2011/04/05. doi: 10.1007/s10096-011-1223-0. PubMed PMID: 21461847.

45. Huang YC, Huang YW, Lin YT, Wang FD, Chan YJ, Yang TC. Risk factors and outcome of levofloxacin-resistant *Elizabethkingia meningoseptica* bacteraemia in adult patients in Taiwan. Eur J Clin Microbiol Infect Dis. 2017;36(8):1373-80. Epub 2017/03/08. doi: 10.1007/s10096-017-2942-7. PubMed PMID: 28265817.

46. Lin JN, Lai CH, Yang CH, Huang YH. Comparison of Clinical Manifestations, Antimicrobial Susceptibility Patterns, and Mutations of Fluoroquinolone Target Genes between *Elizabethkingia meningoseptica* and *Elizabethkingia anophelis* Isolated in Taiwan. J Clin Med. 2018;7(12). Epub 2018/12/14. doi: 10.3390/jcm7120538. PubMed PMID: 30545016; PubMed Central PMCID: PMCPMC6306790.

47. Lin JN, Lai CH, Yang CH, Huang YH, Lin HH. Clinical manifestations, molecular characteristics, antimicrobial susceptibility patterns and contributions of target gene mutation to fluoroquinolone resistance in *Elizabethkingia anophelis*. J Antimicrob Chemother. 2018;73(9):2497-502. Epub 2018/05/31. doi: 10.1093/jac/dky197. PubMed PMID: 29846598.

48. Lin PY, Chu C, Su LH, Huang CT, Chang WY, Chiu CH. Clinical and microbiological analysis of bloodstream infections caused by *Chryseobacterium meningosepticum* in nonneonatal patients. J Clin Microbiol. 2004;42(7):3353-5. Epub 2004/07/10. doi: 10.1128/JCM.42.7.3353-3355.2004. PubMed PMID: 15243115; PubMed Central PMCID: PMCPMC446307.

49. Lothuvachai T, Likittanasombat K, Milindankura S, Sakulsaengprapha A, Kitiyakara C. *Chryseobacterium meningosepticum* infection and cardiac tamponade in a long-term hemodialysis patient. Am J Kidney Dis. 2006;48(4):e49-53. Epub 2006/09/26. doi: 10.1053/j.ajkd.2006.07.010. PubMed PMID: 16997045.

50. Montrucchio G, Corcione S, Vaj M, Zaccaria T, Costa C, Brazzi L, *et al*. First case of *E. meningoseptica* in Italy in a patient with necrotic hemorrhagic pancreatitis. Infection. 2017. Epub 2017/08/05. doi: 10.1007/s15010-017-1055-7. PubMed PMID: 28776164.

51. Musalem HM, Honjol YN, Tuleimat LM, Al Abbad SI, Alsohaibani FI. *Elizabethkingia Meningoseptica* in a Case of Biliary Tract Infection Following Liver Transplantation. Am J Case Rep. 2017;18:1014-9. Epub 2017/09/22. PubMed PMID: 28931801; PubMed Central PMCID: PMCPMC5624779.

52. Navon L, Clegg WJ, Morgan J, Austin C, McQuiston JR, Blaney DD, *et al*. Notes from the Field: Investigation of *Elizabethkingia anophelis* Cluster - Illinois, 2014-2016. MMWR Morb Mortal Wkly Rep. 2016;65(48):1380-1. Epub 2016/12/10. doi: 10.15585/mmwr.mm6548a6. PubMed PMID: 27932784.

53. Nielsen HL, Tarpgaard IH, Fuglsang-Damgaard D, Thomsen PK, Brisse S, Dalager-Pedersen M. Rare *Elizabethkingia anophelis* meningitis case in a Danish male. JMM Case Rep. 2018;5(8):e005163. Epub 2018/10/17. doi: 10.1099/jmmcr.0.005163. PubMed PMID: 30323938; PubMed Central PMCID: PMCPMC6152398.

54. Ozkalay N, Anil M, Agus N, Helvaci M, Sirti S. Community-acquired meningitis and sepsis caused by *Chryseobacterium meningosepticum* in a patient diagnosed with thalassemia major. J Clin Microbiol. 2006;44(8):3037-9. Epub 2006/08/08. doi: 10.1128/JCM.00588-06. PubMed PMID: 16891537; PubMed Central PMCID: PMCPMC1594611.

55. Plotkin SA, McKitrick JC. Nosocomial meningitis of the newborn caused by a flavobacterium. JAMA. 1966;198(6):662-4. Epub 1966/11/07. PubMed PMID: 5953444.

56. Ranjan S, Veerappan I, Patil SP, Sethuraman R. *Elizabethkingia meningoseptica* peritonitis in continuous ambulatory peritoneal dialysis patient: A rare case report with diagnostic challenges. Indian J Pathol Microbiol. 2017;60(4):626-8. Epub 2018/01/13. doi: 10.4103/IJPM.IJPM_28_17. PubMed PMID: 29323100.

57. Rossati A, Kroumova V, Bargiacchi O, Brustia D, Luigi Garavelli P. *Elizabethkingia miricola* bacteriemia in a young woman with acute alcoholic pancreatitis. Presse Med. 2015;44(10):1071-2. Epub 2015/09/05. doi: 10.1016/j.lpm.2015.08.003. PubMed PMID: 26337359.

58. Sader HS, Jones RN, Pfaller MA. Relapse of catheter-related *Flavobacterium meningosepticum* bacteremia demonstrated by DNA macrorestriction analysis. Clin Infect Dis. 1995;21(4):997-1000. Epub 1995/10/01. PubMed PMID: 8645856.

59. Sebastiampillai BS, Luke NV, Silva S, De Silva ST, Premaratna R. Septicaemia caused by Elizabethkingia-sp in a 'healthy' Sri Lankan man. Trop Doct. 2018;48(1):62-3. Epub 2017/06/24. doi: 10.1177/0049475517717135. PubMed PMID: 28641481.

60. Sedigh Ebrahim-Saraie H, Heidari H, Khashei R, Nabavizadeh SH. A rare case of complicated pericardial effusion with *Elizabethkingia meningoseptica* from Iran. Cell Mol Biol (Noisy-le-grand). 2018;64(3):53-5. Epub 2018/03/07. doi: 10.14715/cmb/2018.64.3.9. PubMed PMID: 29506640.

61. Snesrud E, McGann P, Walsh E, Ong A, Maybank R, Kwak Y, *et al*. Clinical and Genomic Features of the First Cases of *Elizabethkingia anophelis* Infection in New York, Including the First Case in a Healthy Infant Without Previous Nosocomial Exposure. J Pediatric Infect Dis Soc. 2018. Epub 2018/08/15. doi: 10.1093/jpids/piy071. PubMed PMID: 30107596.

62. Tai IC, Liu TP, Chen YJ, Lien RI, Lee CY, Huang YC. Outbreak of *Elizabethkingia meningoseptica* sepsis with meningitis in a well-baby nursery. J Hosp Infect. 2017;96(2):168-71. Epub 2017/01/13. doi: 10.1016/j.jhin.2016.11.018. PubMed PMID: 28077242.

63. Zdziarski P, Pasciak M, Rogala K, Korzeniowska-Kowal A, Gamian A. *Elizabethkingia miricola* as an opportunistic oral pathogen associated with superinfectious complications in humoral immunodeficiency: a case report. BMC Infect Dis. 2017;17(1):763. Epub 2017/12/14. doi: 10.1186/s12879-017-2886-7. PubMed PMID: 29233117; PubMed Central PMCID: PMCPMC5727958.

64. Balm MN, Salmon S, Jureen R, Teo C, Mahdi R, Seetoh T, *et al*. Bad design, bad practices, bad bugs: frustrations in controlling an outbreak of *Elizabethkingia meningoseptica* in intensive care units. J Hosp Infect. 2013;85(2):134-40. Epub 2013/08/21. doi: 10.1016/j.jhin.2013.05.012. PubMed PMID: 23958153.

65. Weaver KN, Jones RC, Albright R, Thomas Y, Zambrano CH, Costello M, *et al*. Acute emergence of *Elizabethkingia meningoseptica* infection among mechanically ventilated patients in a long-term acute care facility. Infect Control Hosp Epidemiol. 2010;31(1):54-8. Epub 2009/11/26. doi: 10.1086/649223. PubMed PMID: 19929372.

66. Pereira GH, Garcia Dde O, Abboud CS, Barbosa VL, Silva PS. Nosocomial infections caused by *Elizabethkingia meningoseptica*: an emergent pathogen. Braz J Infect Dis. 2013;17(5):606-9. Epub 2013/09/24. doi: 10.1016/j.bjid.2013.02.011. PubMed PMID: 24055393.

67. Bush K, Jacoby GA, Medeiros AA. A functional classification scheme for beta-lactamases and its correlation with molecular structure. Antimicrob Agents Chemother. 1995;39(6):1211-33. Epub 1995/06/01. doi: 10.1128/aac.39.6.1211. PubMed PMID: 7574506; PubMed Central PMCID: PMCPMC162717.

68. Bush K. The ABCD's of beta-lactamase nomenclature. J Infect Chemother. 2013;19(4):549-59. Epub 2013/07/06. doi: 10.1007/s10156-013-0640-7. PubMed PMID: 23828655.

69. Ghuysen JM. Serine beta-lactamases and penicillin-binding proteins. Annu Rev Microbiol. 1991;45:37-67. Epub 1991/01/01. doi: 10.1146/annurev.mi.45.100191.000345. PubMed PMID: 1741619.

70. Bellais S, Poirel L, Naas T, Girlich D, Nordmann P. Genetic-biochemical analysis and distribution of the Ambler class A beta-lactamase CME-2, responsible for extended-spectrum cephalosporin resistance in *Chryseobacterium* (*Flavobacterium*) *meningosepticum*. Antimicrob Agents Chemother. 2000;44(1):1-9. Epub 1999/12/22. PubMed PMID: 10602714; PubMed Central PMCID: PMCPMC89619.

71. Rossolini GM, Franceschini N, Riccio ML, Mercuri PS, Perilli M, Galleni M, *et al*. Characterization and sequence of the *Chryseobacterium* (*Flavobacterium*) *meningosepticum* carbapenemase: a new molecular class B beta-lactamase showing a broad substrate profile. Biochem J. 1998;332 (Pt 1):145-52. Epub 1998/05/13. doi: 10.1042/bj3320145. PubMed PMID: 9576862; PubMed Central PMCID: PMCPMC1219462.

72. Moran-Barrio J, Lisa MN, Larrieux N, Drusin SI, Viale AM, Moreno DM, *et al*. Crystal Structure of the Metallo-beta-Lactamase GOB in the Periplasmic Dizinc Form Reveals an Unusual Metal Site. Antimicrob Agents Chemother. 2016;60(10):6013-22. doi: 10.1128/AAC.01067-16. PubMed PMID: 27458232; PubMed Central PMCID: PMCPMC5038331.

73. Rossolini GM, Franceschini N, Lauretti L, Caravelli B, Riccio ML, Galleni M, *et al*. Cloning of a *Chryseobacterium* (*Flavobacterium*) *meningosepticum* chromosomal gene (*blaA(CME)*) encoding an extended-spectrum class A beta-lactamase related to the *Bacteroides* cephalosporinases and the VEB-1 and PER beta-lactamases. Antimicrob Agents Chemother. 1999;43(9):2193-9. Epub 1999/09/03. PubMed PMID: 10471563; PubMed Central PMCID: PMCPMC89445.

74. Johnson WL, Ramachandran A, Torres NJ, Nicholson AC, Whitney AM, Bell M, *et al*. The draft genomes of *Elizabethkingia anophelis* of equine origin are genetically similar to three isolates from human clinical specimens. PLoS One. 2018;13(7):e0200731. Epub 2018/07/20. doi: 10.1371/journal.pone.0200731. PubMed PMID: 30024943; PubMed Central PMCID: PMCPMC6053191.

75. Li Y, Liu Y, Chew SC, Tay M, Salido MM, Teo J, *et al*. Complete Genome Sequence and Transcriptomic Analysis of the Novel Pathogen *Elizabethkingia anophelis* in Response to Oxidative Stress. Genome Biol Evol. 2015;7(6):1676-85. Epub 2015/05/29. doi: 10.1093/gbe/evv101. PubMed PMID: 26019164; PubMed Central PMCID: PMCPMC4494045.

76. Lin JN, Lai CH, Yang CH, Huang YH, Lin HH. Genomic features, phylogenetic relationships, and comparative genomics of *Elizabethkingia anophelis* strain EM361-97 isolated in Taiwan. Sci Rep. 2017;7(1):14317. Epub 2017/11/01. doi: 10.1038/s41598-017-14841-8. PubMed PMID: 29085032; PubMed Central PMCID: PMCPMC5662595.

77. Lin XH, Xu YH, Sun XH, Huang Y, Li JB. Genetic diversity analyses of antimicrobial resistance genes in clinical *Chryseobacterium meningosepticum* isolated from Hefei, China. Int J Antimicrob Agents. 2012;40(2):186-8. Epub 2012/05/23. doi: 10.1016/j.ijantimicag.2012.03.020. PubMed PMID: 22612901.

78. Matyi SA, Hoyt PR, Hosoyama A, Yamazoe A, Fujita N, Gustafson JE. Draft Genome Sequences of *Elizabethkingia meningoseptica*. Genome Announc. 2013;1(4). Epub 2013/07/13. doi: 10.1128/genomeA.00444-13. PubMed PMID: 23846266; PubMed Central PMCID: PMCPMC3709143.

79. Opota O, Diene SM, Bertelli C, Prod'hom G, Eckert P, Greub G. Genome of the carbapenemase-producing clinical isolate *Elizabethkingia miricola* EM_CHUV and comparative genomics with *Elizabethkingia meningoseptica* and *Elizabethkingia anophelis*: evidence for intrinsic multidrug resistance trait of emerging pathogens. Int J Antimicrob Agents. 2017;49(1):93-7. doi: 10.1016/j.ijantimicag.2016.09.031. PubMed PMID: 27913093.

80. Pei D, Nicholson AC, Jiang J, Chen H, Whitney AM, Villarma A, *et al*. Complete Circularized Genome Sequences of Four Strains of *Elizabethkingia anophelis*, Including Two Novel Strains Isolated from Wild-Caught *Anopheles sinensis*. Genome Announc. 2017;5(47). Epub 2017/11/24. doi: 10.1128/genomeA.01359-17. PubMed PMID: 29167265.

81. Teo J, Tan SY, Liu Y, Tay M, Ding Y, Li Y, *et al*. Comparative genomic analysis of malaria mosquito vector-associated novel pathogen *Elizabethkingia anophelis*. Genome Biol Evol. 2014;6(5):1158-65. Epub 2014/05/08. doi: 10.1093/gbe/evu094. PubMed PMID: 24803570; PubMed Central PMCID: PMCPMC4041001.

82. Massova I, Mobashery S. Kinship and diversification of bacterial penicillin-binding proteins and beta-lactamases. Antimicrob Agents Chemother. 1998;42(1):1-17. Epub 1998/02/04. PubMed PMID: 9449253; PubMed Central PMCID: PMCPMC105448.

83. Govindaswamy A, Bajpai V, Trikha V, Mittal S, Malhotra R, Mathur P. Multidrug resistant *Elizabethkingia meningoseptica* bacteremia - Experience from a level 1 trauma centre in India. Intractable Rare Dis Res. 2018;7(3):172-6. Epub 2018/09/06. doi: 10.5582/irdr.2018.01077. PubMed PMID: 30181936; PubMed Central PMCID: PMCPMC6119665.

84. Liu CE, Wong WW, Yang SP, Wang FD, Fung CP, You KW, *et al. Flavobacterium meningosepticum* bacteremia: an analysis of 16 cases. Zhonghua Yi Xue Za Zhi (Taipei). 1999;62(3):125-32. Epub 1999/05/01. PubMed PMID: 10222599.

85. Teo J, Tan SY, Tay M, Ding Y, Kjelleberg S, Givskov M, *et al*. First case of *E anophelis* outbreak in an intensive-care unit. Lancet. 2013;382(9895):855-6. Epub 2013/09/10. doi: 10.1016/S0140-6736(13)61858-9. PubMed PMID: 24012265.

86. Aber RC, Wennersten C, Moellering RC, Jr. Antimicrobial susceptibility of flavobacteria. Antimicrob Agents Chemother. 1978;14(3):483-7. Epub 1978/09/01. PubMed PMID: 708026; PubMed Central PMCID: PMCPMC352486.

87. Altmann G, Bogokovsky B. In-vitro sensitivity of *Flavobacterium meningosepticum* to antimicrobial agents. J Med Microbiol. 1971;4(2):296-9. Epub 1971/05/01. doi: 10.1099/00222615-4-2-296. PubMed PMID: 4105616.

88. Arbune M, Fotea S, Nechita A, Stefanescu V. Emerging Infection with *Elizabethkingia Meningoseptica* in Neonate. A Case Report. J Crit Care Med (Targu Mures). 2018;4(3):96-100. Epub 2018/12/26. doi: 10.2478/jccm-2018-0013. PubMed PMID: 30582002; PubMed Central PMCID: PMCPMC6294984.

89. Ceyhan M, Yildirim I, Tekeli A, Yurdakok M, Us E, Altun B, *et al*. A *Chryseobacterium meningosepticum* outbreak observed in 3 clusters involving both neonatal and non-neonatal pediatric patients. Am J Infect Control. 2008;36(6):453-7. Epub 2008/08/05. doi: 10.1016/j.ajic.2007.09.008. PubMed PMID: 18675153.

90. Li XZ, Plesiat P, Nikaido H. The challenge of efflux-mediated antibiotic resistance in Gram-negative bacteria. Clin Microbiol Rev. 2015;28(2):337-418. Epub 2015/03/20. doi: 10.1128/CMR.00117-14. PubMed PMID: 25788514; PubMed Central PMCID: PMCPMC4402952.

91. Poole K. Efflux-mediated antimicrobial resistance. J Antimicrob Chemother. 2005;56(1):20-51. Epub 2005/05/26. doi: 10.1093/jac/dki171. PubMed PMID: 15914491.

92. Du D, van Veen HW, Murakami S, Pos KM, Luisi BF. Structure, mechanism and cooperation of bacterial multidrug transporters. Curr Opin Struct Biol. 2015;33:76-91. Epub 2015/08/19. doi: 10.1016/j.sbi.2015.07.015. PubMed PMID: 26282926.

93. Lubelski J, Konings WN, Driessen AJ. Distribution and physiology of ABC-type transporters contributing to multidrug resistance in bacteria. Microbiol Mol Biol Rev. 2007;71(3):463-76. Epub 2007/09/07. doi: 10.1128/MMBR.00001-07. PubMed PMID: 17804667; PubMed Central PMCID: PMCPMC2168643.

94. Pao SS, Paulsen IT, Saier MH, Jr. Major facilitator superfamily. Microbiol Mol Biol Rev. 1998;62(1):1-34. Epub 1998/04/08. PubMed PMID: 9529885; PubMed Central PMCID: PMCPMC98904.

95. Saier MH, Jr., Beatty JT, Goffeau A, Harley KT, Heijne WH, Huang SC, et al. The major facilitator superfamily. J Mol Microbiol Biotechnol. 1999;1(2):257-79. Epub 2000/08/16. PubMed PMID: 10943556.

96. Kuroda T, Tsuchiya T. Multidrug efflux transporters in the MATE family. Biochim Biophys Acta. 2009;1794(5):763-8. Epub 2008/12/23. doi: 10.1016/j.bbapap.2008.11.012. PubMed PMID: 19100867.

97. Nikaido H. Structure and mechanism of RND-type multidrug efflux pumps. Adv Enzymol Relat Areas Mol Biol. 2011;77:1-60. Epub 2011/06/23. PubMed PMID: 21692366; PubMed Central PMCID: PMCPMC3122131.

98. Chung YJ, Saier MH, Jr. SMR-type multidrug resistance pumps. Curr Opin Drug Discov Devel. 2001;4(2):237-45. Epub 2001/05/31. PubMed PMID: 11378963.

99. Fairbrother RW, Williams BL. Two new antibiotics; antibacterial activity of novobiocin and vancomycin. Lancet. 1956;271(6954):1177-8. Epub 1956/12/08. PubMed PMID: 13377703.

100. George RM, Cochran CP, Wheeler WE. Epidemic meningitis of the newborn caused by flavobacteria. II. Clinical manifestations and treatment. Am J Dis Child. 1961;101:296-304. Epub 1961/03/01. PubMed PMID: 13704460.

101. Perera S, Palasuntheram C. *Chryseobacterium meningosepticum* infections in a dialysis unit. Ceylon Med J. 2004;49(2):57-60. Epub 2004/09/01. PubMed PMID: 15334801.

102. Soman R, Agrawal U, Suthar M, Desai K, Shetty A. Successful Management of *Elizabethkingia meningoseptica* Meningitis with Intraventricular Vancomycin. J Assoc Physicians India. 2016;64(10):98-9. Epub 2016/10/22. PubMed PMID: 27766817.

103. Tizer KB, Cervia JS, Dunn AM, Stavola JJ, Noel GJ. Successful combination vancomycin and rifampin therapy in a newborn with community-acquired *Flavobacterium meningosepticum* neonatal meningitis. Pediatr Infect Dis J. 1995;14(10):916-7. Epub 1995/10/01. PubMed PMID: 8584328.

104. Tseng MH, Diang LK, Su YC, Lin SH. Catheter-related *Chryseobacterium meningosepticum* bacteraemia in a haemodialysis patient. NDT Plus. 2009;2(5):433-4. Epub 2009/10/01. doi: 10.1093/ndtplus/sfp080. PubMed PMID: 25949372; PubMed Central PMCID: PMCPMC4421377.

105. Fraser SL, Jorgensen JH. Reappraisal of the antimicrobial susceptibilities of *Chryseobacterium* and *Flavobacterium* species and methods for reliable susceptibility testing. Antimicrob Agents Chemother. 1997;41(12):2738-41. Epub 1998/01/07. PubMed PMID: 9420049; PubMed Central PMCID: PMCPMC164199.

106. Bruun B. Antimicrobial susceptibility of *Flavobacterium meningosepticum* strains identified by DNA-DNA hybridization. Acta Pathol Microbiol Immunol Scand B. 1987;95(2):95-101. Epub 1987/04/01. PubMed PMID: 3591313.

107. Chang JC, Hsueh PR, Wu JJ, Ho SW, Hsieh WC, Luh KT. Antimicrobial susceptibility of flavobacteria as determined by agar dilution and disk diffusion methods. Antimicrob Agents Chemother. 1997;41(6):1301-6. Epub 1997/06/01. PubMed PMID: 9174188; PubMed Central PMCID: PMCPMC163904.

108. Jordan DC, Inniss WE. Selective inhibition of ribonucleic acid synthesis in *Staphylococcus aureus* by vancomycin. Nature. 1959;184(Suppl 24):1894-5. Epub 1959/12/12. PubMed PMID: 14407860.

109. Jordan DC. Effect of vancomycin on the synthesis of the cell wall mucopeptide of *Staphylococcus aureus*. Biochem Biophys Res Commun. 1961;6:167-70. Epub 1961/11/20. PubMed PMID: 14452426.

110. Reynolds PE. Studies on the mode of action of vancomycin. Biochim Biophys Acta. 1961;52:403-5. Epub 1961/09/16. PubMed PMID: 14491721.

111. Best GK, Grastie MK, McConnell RD. Relative affinity of vancomycin and ristocetin for cell walls and uridine diphosphate-N-acetylmuramyl pentapeptide. J Bacteriol. 1970;102(2):476-82. Epub 1970/05/01. PubMed PMID: 4986761; PubMed Central PMCID: PMCPMC247573.

112. Nieto M, Perkins HR. Modifications of the acyl-D-alanyl-D-alanine terminus affecting complex-formation with vancomycin. Biochem J. 1971;123(5):789-803. Epub 1971/08/01. PubMed PMID: 5124386; PubMed Central PMCID: PMCPMC1177079.

113. Nieto M, Perkins HR. Physicochemical properties of vancomycin and iodovancomycin and their complexes with diacetyl-L-lysyl-D-alanyl-D-alanine. Biochem J. 1971;123(5):773-87. Epub 1971/08/01. PubMed PMID: 5124385; PubMed Central PMCID: PMCPMC1177078.

114. Perkins HR, Nieto M. The preparation of iodinated vancomycin and its distribution in bacteria treated with the antibiotic. Biochem J. 1970;116(1):83-92. Epub 1970/01/01. PubMed PMID: 5411430; PubMed Central PMCID: PMCPMC1185327.

115. Nikaido H. Preventing drug access to targets: cell surface permeability barriers and active efflux in bacteria. Semin Cell Dev Biol. 2001;12(3):215-23. Epub 2001/06/29. doi: 10.1006/scdb.2000.0247. PubMed PMID: 11428914.

116. Sugawara E, Nikaido H. OmpA is the principal nonspecific slow porin of *Acinetobacter baumannii*. J Bacteriol. 2012;194(15):4089-96. Epub 2012/05/29. doi: 10.1128/JB.00435-12. PubMed PMID: 22636785; PubMed Central PMCID: PMCPMC3416538.

117. Kojima S, Nikaido H. Permeation rates of penicillins indicate that *Escherichia coli* porins function principally as nonspecific channels. Proc Natl Acad Sci U S A. 2013;110(28):E2629-34. Epub 2013/06/27. doi: 10.1073/pnas.1310333110. PubMed PMID: 23798411; PubMed Central PMCID: PMCPMC3710850.

118. Kwon HI, Kim S, Oh MH, Na SH, Kim YJ, Jeon YH, *et al*. Outer membrane protein A contributes to antimicrobial resistance of *Acinetobacter baumannii* through the OmpA-

like domain. J Antimicrob Chemother. 2017;72(11):3012-5. Epub 2017/10/06. doi: 10.1093/jac/dkx257. PubMed PMID: 28981866.

119. Sampson BA, Misra R, Benson SA. Identification and characterization of a new gene of *Escherichia coli* K-12 involved in outer membrane permeability. Genetics. 1989;122(3):491-501. Epub 1989/07/01. PubMed PMID: 2547691; PubMed Central PMCID: PMCPMC1203724.

120. Wu T, Malinverni J, Ruiz N, Kim S, Silhavy TJ, Kahne D. Identification of a multicomponent complex required for outer membrane biogenesis in *Escherichia coli*. Cell. 2005;121(2):235-45. Epub 2005/04/27. doi: 10.1016/j.cell.2005.02.015. PubMed PMID: 15851030.

121. Eggert US, Ruiz N, Falcone BV, Branstrom AA, Goldman RC, Silhavy TJ, *et al*. Genetic basis for activity differences between vancomycin and glycolipid derivatives of vancomycin. Science. 2001;294(5541):361-4. Epub 2001/08/25. doi: 10.1126/science.1063611. PubMed PMID: 11520949.

122. Krishnamoorthy G, Wolloscheck D, Weeks JW, Croft C, Rybenkov VV, Zgurskaya HI. Breaking the Permeability Barrier of *Escherichia coli* by Controlled Hyperporination of the Outer Membrane. Antimicrob Agents Chemother. 2016;60(12):7372-81. Epub 2016/10/05. doi: 10.1128/AAC.01882-16. PubMed PMID: 27697764; PubMed Central PMCID: PMCPMC5119019.

123. Zhou A, Kang TM, Yuan J, Beppler C, Nguyen C, Mao Z, *et al*. Synergistic interactions of vancomycin with different antibiotics against *Escherichia coli*: trimethoprim and nitrofurantoin display strong synergies with vancomycin against wild-type *E. coli*. Antimicrob Agents Chemother. 2015;59(1):276-81. Epub 2014/10/29. doi: 10.1128/AAC.03502-14. PubMed PMID: 25348521; PubMed Central PMCID: PMCPMC4291362.

124. Kang TM, Yuan J, Zhou A, Beppler C, Miller JH. Deoxycytidine deaminase-deficient *Escherichia coli* strains display acute sensitivity to cytidine, adenosine, and guanosine and increased sensitivity to a range of antibiotics, including vancomycin. J Bacteriol. 2014;196(11):1950-7. Epub 2014/03/19. doi: 10.1128/JB.01383-13. PubMed PMID: 24633874; PubMed Central PMCID: PMCPMC4010977.

125. Dwyer DJ, Collins JJ, Walker GC. Unraveling the physiological complexities of antibiotic lethality. Annu Rev Pharmacol Toxicol. 2015;55:313-32. Epub 2014/09/25. doi: 10.1146/annurev-pharmtox-010814-124712. PubMed PMID: 25251995.

126. Kuroda M, Kuroda H, Oshima T, Takeuchi F, Mori H, Hiramatsu K. Two-component system VraSR positively modulates the regulation of cell-wall biosynthesis pathway in *Staphylococcus aureus*. Mol Microbiol. 2003;49(3):807-21. Epub 2003/07/17. doi: 10.1046/j.1365-2958.2003.03599.x. PubMed PMID: 12864861.

127. McAleese F, Wu SW, Sieradzki K, Dunman P, Murphy E, Projan S, *et al*. Overexpression of genes of the cell wall stimulon in clinical isolates of *Staphylococcus aureus* exhibiting vancomycin-intermediate- *S. aureus*-type resistance to vancomycin. J Bacteriol. 2006;188(3):1120-33. Epub 2006/01/24. doi: 10.1128/JB.188.3.1120-1133.2006. PubMed PMID: 16428416; PubMed Central PMCID: PMCPMC1347359
.
128. Muthaiyan A, Silverman JA, Jayaswal RK, Wilkinson BJ. Transcriptional profiling reveals that daptomycin induces the *Staphylococcus aureus* cell wall stress stimulon and genes responsive to membrane depolarization. Antimicrob Agents Chemother. 2008;52(3):980-90. Epub 2007/12/19. doi: 10.1128/AAC.01121-07. PubMed PMID: 18086846; PubMed Central PMCID: PMCPMC2258546.

129. Russell JR, Cabeen MT, Wiggins PA, Paulsson J, Losick R. Noise in a phosphorelay drives stochastic entry into sporulation in *Bacillus subtilis*. EMBO J. 2017;36(19):2856-69. Epub 2017/08/26. doi: 10.15252/embj.201796988. PubMed PMID: 28838935; PubMed Central PMCID: PMCPMC5623841.

130. Zarkan A, Macklyne HR, Truman AW, Hesketh AR, Hong HJ. The frontline antibiotic vancomycin induces a zinc starvation response in bacteria by binding to Zn(II). Sci Rep. 2016;6:19602. Epub 2016/01/23. doi: 10.1038/srep19602. PubMed PMID: 26797186; PubMed Central PMCID: PMCPMC4726154.

131. Huang KC, Mukhopadhyay R, Wen B, Gitai Z, Wingreen NS. Cell shape and cell-wall organization in Gram-negative bacteria. Proc Natl Acad Sci U S A. 2008;105(49):19282-7. Epub 2008/12/04. doi: 10.1073/pnas.0805309105. PubMed PMID: 19050072; PubMed Central PMCID: PMCPMC2592989.

132. Rowley G, Spector M, Kormanec J, Roberts M. Pushing the envelope: extracytoplasmic stress responses in bacterial pathogens. Nat Rev Microbiol. 2006;4(5):383-94. Epub 2006/05/23. doi: 10.1038/nrmicro1394. PubMed PMID: 16715050.

133. Duguay AR, Silhavy TJ. Quality control in the bacterial periplasm. Biochim Biophys Acta. 2004;1694(1-3):121-34. Epub 2004/11/18. doi: 10.1016/j.bbamcr.2004.04.012. PubMed PMID: 15546662.

134. Surmann K, Cudic E, Hammer E, Hunke S. Molecular and proteome analyses highlight the importance of the Cpx envelope stress system for acid stress and cell wall stability in *Escherichia coli*. Microbiologyopen. 2016;5(4):582-96. Epub 2016/04/04. doi: 10.1002/mbo3.353. PubMed PMID: 27039284; PubMed Central PMCID: PMCPMC4985592.

135. Raffa RG, Raivio TL. A third envelope stress signal transduction pathway in *Escherichia coli*. Mol Microbiol. 2002;45(6):1599-611. Epub 2002/10/02. doi: 10.1046/j.1365-2958.2002.03112.x. PubMed PMID: 12354228.

136. Laubacher ME, Ades SE. The Rcs phosphorelay is a cell envelope stress response activated by peptidoglycan stress and contributes to intrinsic antibiotic resistance. J Bacteriol. 2008;190(6):2065-74. Epub 2008/01/15. doi: 10.1128/JB.01740-07. PubMed PMID: 18192383; PubMed Central PMCID: PMCPMC2258881.

137. May KL, Lehman KM, Mitchell AM, Grabowicz M. A Stress Response Monitoring Lipoprotein Trafficking to the Outer Membrane. mBio. 2019;10(3). Epub 2019/05/30. doi: 10.1128/mBio.00618-19. PubMed PMID: 31138744; PubMed Central PMCID: PMCPMC6538781.

138. Wall E, Majdalani N, Gottesman S. The Complex Rcs Regulatory Cascade. Annu Rev Microbiol. 2018;72:111-39. Epub 2018/06/14. doi: 10.1146/annurev-micro-090817-062640. PubMed PMID: 29897834.

139. Hussein NA, Cho SH, Laloux G, Siam R, Collet JF. Distinct domains of *Escherichia coli* IgaA connect envelope stress sensing and down-regulation of the Rcs phosphorelay across subcellular compartments. PLoS Genet. 2018;14(5):e1007398. Epub 2018/06/01. doi: 10.1371/journal.pgen.1007398. PubMed PMID: 29852010; PubMed Central PMCID: PMCPMC5978795.

140. Takeda S, Fujisawa Y, Matsubara M, Aiba H, Mizuno T. A novel feature of the multistep phosphorelay in *Escherichia coli*: a revised model of the RcsC --> YojN --> RcsB signalling pathway implicated in capsular synthesis and swarming behaviour. Mol Microbiol. 2001;40(2):440-50. Epub 2001/04/20. doi: 10.1046/j.1365-2958.2001.02393.x. PubMed PMID: 11309126.

141. Chen SJBKY, T.; Nelson B.N.; Walker, E.D. *Elizabethkingia anophelis* response to iron stress: physiologic, genomic, and transcriptomic analyses. Bioarxiv2019.

142. Guardabassi L, Schwarz S, Lloyd DH. Pet animals as reservoirs of antimicrobial-resistant bacteria. J Antimicrob Chemother. 2004;54(2):321-32. Epub 2004/07/16. doi: 10.1093/jac/dkh332. PubMed PMID: 15254022.

143. Jean SS, Hsieh TC, Ning YZ, Hsueh PR. Role of vancomycin in the treatment of bacteraemia and meningitis caused by *Elizabethkingia meningoseptica*. Int J Antimicrob Agents. 2017;50(4):507-11. Epub 2017/07/15. doi: 10.1016/j.ijantimicag.2017.06.021. PubMed PMID: 28705672.

144. Clinical and Laboratory Standards Institute. M100: Performance Standards for Antimicrobial Susceptibility Testing. 28th ed. Wayne, PA: Clinical and Laboratory Standards Institute; 2018.

145. Holmes B, Steigerwalt AG, Nicholson AC. DNA-DNA hybridization study of strains of *Chryseobacterium, Elizabethkingia* and *Empedobacter* and of other usually indole-producing non-fermenters of CDC groups IIc, IIe, IIh and IIi, mostly from human clinical sources, and proposals of *Chryseobacterium bernardetii* sp. nov.,

Chryseobacterium carnis sp. nov., Chryseobacterium lactis sp. nov., Chryseobacterium nakagawai sp. nov. and Chryseobacterium taklimakanense comb. nov. Int J Syst Evol Microbiol. 2013;63(Pt 12):4639-62. Epub 2013/08/13. doi: 10.1099/ijs.0.054353-0. PubMed PMID: 23934253; PubMed Central PMCID: PMCPMC4626006.

146. Elder JH, Alexander S. endo-beta-N-acetylglucosaminidase F: endoglycosidase from *Flavobacterium meningosepticum* that cleaves both high-mannose and complex glycoproteins. Proc Natl Acad Sci U S A. 1982;79(15):4540-4. Epub 1982/08/01. PubMed PMID: 6812050; PubMed Central PMCID: PMCPMC346710.

147. de Carvalho Filho EB, Marson FAL, Levy CE. Challenges in the identification of *Chryseobacterium indologenes* and *Elizabethkingia meningoseptica* in cases of nosocomial infections and patients with cystic fibrosis. New Microbes New Infect. 2017;20:27-33. doi: 10.1016/j.nmni.2017.09.002. PubMed PMID: 29062487; PubMed Central PMCID: PMCPMC5643076.

148. Mirza HC, Tuncer O, Olmez S, Sener B, Tugcu GD, Ozcelik U, *et al*. Clinical Strains of *Chryseobacterium* and *Elizabethkingia* spp. Isolated from Pediatric Patients in a University Hospital: Performance of MALDI-TOF MS-Based Identification, Antimicrobial Susceptibilities, and Baseline Patient Characteristics. Microb Drug Resist. 2017. doi: 10.1089/mdr.2017.0206. PubMed PMID: 29227188.

149. Nicholson AC, Gulvik CA, Whitney AM, Humrighouse BW, Graziano J, Emery B, *et al*. Revisiting the taxonomy of the genus *Elizabethkingia* using whole-genome sequencing, optical mapping, and MALDI-TOF, along with proposal of three novel *Elizabethkingia species: Elizabethkingia bruuniana sp. nov., Elizabethkingia ursingii sp. nov.,* and *Elizabethkingia occulta sp. nov*. Antonie Van Leeuwenhoek. 2018;111(1):55-72. doi: 10.1007/s10482-017-0926-3. PubMed PMID: 28856455.

150. Aziz RK, Bartels D, Best AA, DeJongh M, Disz T, Edwards RA, *et al*. The RAST Server: rapid annotations using subsystems technology. BMC Genomics. 2008;9:75. Epub 2008/02/12. doi: 10.1186/1471-2164-9-75. PubMed PMID: 18261238; PubMed Central PMCID: PMCPMC2265698.

151. Brettin T, Davis JJ, Disz T, Edwards RA, Gerdes S, Olsen GJ, *et al*. RASTtk: a modular and extensible implementation of the RAST algorithm for building custom annotation pipelines and annotating batches of genomes. Sci Rep. 2015;5:8365. Epub 2015/02/11. doi: 10.1038/srep08365. PubMed PMID: 25666585; PubMed Central PMCID: PMCPMC4322359.

152. Overbeek R, Olson R, Pusch GD, Olsen GJ, Davis JJ, Disz T, *et al*. The SEED and the Rapid Annotation of microbial genomes using Subsystems Technology (RAST). Nucleic Acids Res. 2014;42(Database issue):D206-14. Epub 2013/12/03. doi: 10.1093/nar/gkt1226. PubMed PMID: 24293654; PubMed Central PMCID: PMCPMC3965101.

153. Angiuoli SV, Gussman A, Klimke W, Cochrane G, Field D, Garrity G, *et al*. Toward an online repository of Standard Operating Procedures (SOPs) for (meta)genomic annotation. OMICS. 2008;12(2):137-41. Epub 2008/04/18. doi: 10.1089/omi.2008.0017. PubMed PMID: 18416670; PubMed Central PMCID: PMCPMC3196215.

154. Altschul SF, Gish W, Miller W, Myers EW, Lipman DJ. Basic local alignment search tool. J Mol Biol. 1990;215(3):403-10. Epub 1990/10/05. doi: 10.1016/S0022-2836(05)80360-2. PubMed PMID: 2231712.

155. Altschul SF, Madden TL, Schaffer AA, Zhang J, Zhang Z, Miller W, *et al*. Gapped BLAST and PSI-BLAST: a new generation of protein database search programs. Nucleic Acids Res. 1997;25(17):3389-402. Epub 1997/09/01. PubMed PMID: 9254694; PubMed Central PMCID: PMCPMC146917.

156. Treangen TJ, Ondov BD, Koren S, Phillippy AM. The Harvest suite for rapid core-genome alignment and visualization of thousands of intraspecific microbial genomes. Genome Biol. 2014;15(11):524. Epub 2014/11/21. doi: 10.1186/PREACCEPT-2573980311437212. PubMed PMID: 25410596; PubMed Central PMCID: PMCPMC4262987.

157. Tamura K, Stecher G, Peterson D, Filipski A, Kumar S. MEGA6: Molecular Evolutionary Genetics Analysis version 6.0. Mol Biol Evol. 2013;30(12):2725-9. Epub 2013/10/18. doi: 10.1093/molbev/mst197. PubMed PMID: 24132122; PubMed Central PMCID: PMCPMC3840312.

158. Di Pentima MC, Mason EO, Jr., Kaplan SL. In vitro antibiotic synergy against *Flavobacterium meningosepticum*: implications for therapeutic options. Clin Infect Dis. 1998;26(5):1169-76. Epub 1998/05/23. PubMed PMID: 9597247.

159. Price CT, O'Brien FG, Shelton BP, Warmington JR, Grubb WB, Gustafson JE. Effects of salicylate and related compounds on fusidic acid MICs in *Staphylococcus aureus*. J Antimicrob Chemother. 1999;44(1):57-64. Epub 1999/08/25. doi: 10.1093/jac/44.1.57. PubMed PMID: 10459810.

160. Solayev V, Salamov A. Automatic Annotation of Microbial Genomes and Metagenomic Sequences. In: Li RW, editor. Metagenomics and its Applications in Agriculture, Biomedicine and Environmental Studies. Hauppauge, New York, USA: Nova Science Pubkishers; 2011. p. 61-78.

161. de-Las-Casas-Camara G, Martin-Rios MD, Adillo-Montero MI, Munoz-Egea MC, Zapardiel-Ferrero J, Perez-Jorge Peremarch C. Under-utilization of taps in intensive care unit as a cause of reservoirs of nonfermenting gram-negative bacilli. Enferm Infecc Microbiol Clin. 2017. Epub 2017/03/16. doi: 10.1016/j.eimc.2017.01.008. PubMed PMID: 28291668.

162. Hoque SN, Graham J, Kaufmann ME, Tabaqchali S. *Chryseobacterium* (*Flavobacterium*) *meningosepticum* outbreak associated with colonization of water taps in a neonatal intensive care unit. J Hosp Infect. 2001;47(3):188-92. Epub 2001/03/15. doi: 10.1053/jhin.2000.0908. PubMed PMID: 11247678.

163. Guardabassi L, Loeber ME, Jacobson A. Transmission of multiple antimicrobial-resistant *Staphylococcus intermedius* between dogs affected by deep pyoderma and their owners. Vet Microbiol. 2004;98(1):23-7. Epub 2004/01/24. PubMed PMID: 14738778.

164. Bates J, Jordens JZ, Griffiths DT. Farm animals as a putative reservoir for vancomycin-resistant enterococcal infection in man. J Antimicrob Chemother. 1994;34(4):507-14. Epub 1994/10/01. PubMed PMID: 7868403.

165. Gonzalez LJ, Vila AJ. Carbapenem resistance in *Elizabethkingia meningoseptica* is mediated by metallo-beta-lactamase BlaB. Antimicrob Agents Chemother. 2012;56(4):1686-92. Epub 2012/02/01. doi: 10.1128/AAC.05835-11. PubMed PMID: 22290979; PubMed Central PMCID: PMCPMC3318372.

166. Matsumoto T, Nagata M, Ishimine N, Kawasaki K, Yamauchi K, Hidaka E, *et al*. Characterization of CIA-1, an Ambler class A extended-spectrum beta-lactamase from *Chryseobacterium indologenes*. Antimicrob Agents Chemother. 2012;56(1):588-90. Epub 2011/11/16. doi: 10.1128/AAC.05165-11. PubMed PMID: 22083470; PubMed Central PMCID: PMCPMC3256067.

167. Fralick JA. Evidence that TolC is required for functioning of the Mar/AcrAB efflux pump of *Escherichia coli*. J Bacteriol. 1996;178(19):5803-5. Epub 1996/10/01. PubMed PMID: 8824631; PubMed Central PMCID: PMCPMC178425.

168. Lin J, Michel LO, Zhang Q. CmeABC functions as a multidrug efflux system in *Campylobacter jejuni*. Antimicrob Agents Chemother. 2002;46(7):2124-31. Epub 2002/06/19. PubMed PMID: 12069964; PubMed Central PMCID: PMCPMC127319.

169. Okusu H, Ma D, Nikaido H. AcrAB efflux pump plays a major role in the antibiotic resistance phenotype of *Escherichia coli* multiple-antibiotic-resistance (Mar) mutants. J Bacteriol. 1996;178(1):306-8. Epub 1996/01/01. PubMed PMID: 8550435; PubMed Central PMCID: PMCPMC177656.

170. Poole K, Krebes K, McNally C, Neshat S. Multiple antibiotic resistance in *Pseudomonas aeruginosa*: evidence for involvement of an efflux operon. J Bacteriol. 1993;175(22):7363-72. Epub 1993/11/01. PubMed PMID: 8226684; PubMed Central PMCID: PMCPMC206881.

171. Pumbwe L, Piddock LJ. Identification and molecular characterisation of CmeB, a *Campylobacter jejuni* multidrug efflux pump. FEMS Microbiol Lett. 2002;206(2):185-9. Epub 2002/01/30. PubMed PMID: 11814661.

172. Mine T, Morita Y, Kataoka A, Mizushima T, Tsuchiya T. Expression in *Escherichia coli* of a new multidrug efflux pump, MexXY, from *Pseudomonas aeruginosa*. Antimicrob Agents Chemother. 1999;43(2):415-7. Epub 1999/01/30. PubMed PMID: 9925549; PubMed Central PMCID: PMCPMC89094.

173. Schindler BD, Frempong-Manso E, DeMarco CE, Kosmidis C, Matta V, Seo SM, *et al*. Analyses of multidrug efflux pump-like proteins encoded on the *Staphylococcus aureus* chromosome. Antimicrob Agents Chemother. 2015;59(1):747-8. Epub 2014/11/19. doi: 10.1128/AAC.04678-14. PubMed PMID: 25403665; PubMed Central PMCID: PMCPMC4291402.

174. Baquero F. Resistance to quinolones in gram-negative microorganisms: mechanisms and prevention. Eur Urol. 1990;17 Suppl 1:3-12. Epub 1990/01/01. PubMed PMID: 2162298.

175. Jacoby GA. Mechanisms of resistance to quinolones. Clin Infect Dis. 2005;41 Suppl 2:S120-6. Epub 2005/06/09. doi: 10.1086/428052. PubMed PMID: 15942878.

176. Ruiz J. Mechanisms of resistance to quinolones: target alterations, decreased accumulation and DNA gyrase protection. J Antimicrob Chemother. 2003;51(5):1109-17. Epub 2003/04/17. doi: 10.1093/jac/dkg222. PubMed PMID: 12697644.

177. Schmitz FJ, Higgins PG, Mayer S, Fluit AC, Dalhoff A. Activity of quinolones against gram-positive cocci: mechanisms of drug action and bacterial resistance. Eur J Clin Microbiol Infect Dis. 2002;21(9):647-59. Epub 2002/10/10. doi: 10.1007/s10096-002-0788-z. PubMed PMID: 12373497.

178. Smith JT. The mode of action of 4-quinolones and possible mechanisms of resistance. J Antimicrob Chemother. 1986;18 Suppl D:21-9. Epub 1986/11/01. PubMed PMID: 3542946.

179. Wolfson JS, Hooper DC. Bacterial resistance to quinolones: mechanisms and clinical importance. Rev Infect Dis. 1989;11 Suppl 5:S960-8. Epub 1989/07/01. PubMed PMID: 2549610.

180. Yoshida H, Kojima T, Yamagishi J, Nakamura S. Quinolone-resistant mutations of the *gyrA* gene of *Escherichia coli*. Mol Gen Genet. 1988;211(1):1-7. Epub 1988/01/01. PubMed PMID: 2830458.

181. Ruiz J, Marco F, Goni P, Gallardo F, Mensa J, Trilla A, *et al*. High frequency of mutations at codon 83 of the *gyrA* gene of quinolone-resistant clinical isolates of *Escherichia coli*. J Antimicrob Chemother. 1995;36(4):737-8. Epub 1995/10/01. PubMed PMID: 8591951.

182. Yoshida H, Bogaki M, Nakamura M, Nakamura S. Quinolone resistance-determining region in the DNA gyrase *gyrA* gene of *Escherichia coli*. Antimicrob Agents Chemother. 1990;34(6):1271-2. Epub 1990/06/01. PubMed PMID: 2168148; PubMed Central PMCID: PMCPMC171799.

183. Cambau E, Gutmann L. Mechanisms of resistance to quinolones. Drugs. 1993;45 Suppl 3:15-23. Epub 1993/01/01. PubMed PMID: 7689446.

184. Lewin CS, Allen RA, Amyes SG. Potential mechanisms of resistance to the modern fluorinated 4-quinolones. J Med Microbiol. 1990;31(3):153-62. Epub 1990/03/01. doi: 10.1099/00222615-31-3-153. PubMed PMID: 2156074.

185. Yoshida T, Muratani T, Iyobe S, Mitsuhashi S. Mechanisms of high-level resistance to quinolones in urinary tract isolates of *Pseudomonas aeruginosa*. Antimicrob Agents Chemother. 1994;38(7):1466-9. Epub 1994/07/01. PubMed PMID: 7979273; PubMed Central PMCID: PMCPMC284577.

186. Rybak MJ, Lomaestro BM, Rotschafer JC, Moellering RC, Jr., Craig WA, Billeter M, *et al*. Therapeutic monitoring of vancomycin in adults summary of consensus recommendations from the American Society of Health-System Pharmacists, the Infectious Diseases Society of America, and the Society of Infectious Diseases Pharmacists. Pharmacotherapy. 2009;29(11):1275-9. Epub 2009/10/31. PubMed PMID: 19873687.

187. Rybak MJ, Lomaestro BM, Rotschafer JC, Moellering RC, Craig WA, Billeter M, *et al*. Vancomycin therapeutic guidelines: a summary of consensus recommendations from the infectious diseases Society of America, the American Society of Health-System Pharmacists, and the Society of Infectious Diseases Pharmacists. Clin Infect Dis. 2009;49(3):325-7. Epub 2009/07/03. doi: 10.1086/600877. PubMed PMID: 19569969.

188. Fass RJ, Barnishan J. *In vitro* susceptibilities of nonfermentative gram-negative bacilli other than *Pseudomonas aeruginosa* to 32 antimicrobial agents. Rev Infect Dis. 1980;2(6):841-53. Epub 1980/11/01. PubMed PMID: 7012987.

189. Dorr T, Delgado F, Umans BD, Gerding MA, Davis BM, Waldor MK. A Transposon Screen Identifies Genetic Determinants of *Vibrio cholerae* Resistance to High-Molecular-Weight Antibiotics. Antimicrob Agents Chemother. 2016;60(8):4757-63. Epub 2016/05/25. doi: 10.1128/AAC.00576-16. PubMed PMID: 27216069; PubMed Central PMCID: PMCPMC4958186.

190. Hazuka BT, Dajani AS, Talbot K, Keen BM. Two outbreaks of *Flavobacterium meningosepticum* type E in a neonatal intensive care unit. J Clin Microbiol. 1977;6(5):450-55. Epub 1977/11/01. PubMed PMID: 925147; PubMed Central PMCID: PMCPMC274796.

191. Finch NA, Zasowski EJ, Murray KP, Mynatt RP, Zhao JJ, Yost R, *et al*. A Quasi-Experiment To Study the Impact of Vancomycin Area under the Concentration-Time Curve-Guided Dosing on Vancomycin-Associated Nephrotoxicity. Antimicrob Agents Chemother. 2017;61(12). Epub 2017/09/20. doi: 10.1128/AAC.01293-17. PubMed PMID: 28923869; PubMed Central PMCID: PMCPMC5700348.

192. Bruun B, Ursing J. Phenotypic characterization of *Flavobacterium meningosepticum* strains identified by DNA-DNA hybridization. Acta Pathol Microbiol Immunol Scand B. 1987;95(1):41-7. Epub 1987/02/01. PubMed PMID: 3565017.

193. Mengin-Lecreulx D, van Heijenoort J. Effect of growth conditions on peptidoglycan content and cytoplasmic steps of its biosynthesis in *Escherichia coli*. J Bacteriol. 1985;163(1):208-12. Epub 1985/07/01. PubMed PMID: 3891726; PubMed Central PMCID: PMCPMC219099.

194. Sobhanifar S, King DT, Strynadka NC. Fortifying the wall: synthesis, regulation and degradation of bacterial peptidoglycan. Curr Opin Struct Biol. 2013;23(5):695-703. Epub 2013/08/06. doi: 10.1016/j.sbi.2013.07.008. PubMed PMID: 23910891.

195. Ramazzina I, Cendron L, Folli C, Berni R, Monteverdi D, Zanotti G, *et al*. Logical identification of an allantoinase analog (*puuE*) recruited from polysaccharide deacetylases. J Biol Chem. 2008;283(34):23295-304. Epub 2008/06/14. doi: 10.1074/jbc.M801195200. PubMed PMID: 18550550.

196. Zaloba P, Bailey-Elkin BA, Derksen M, Mark BL. Structural and Biochemical Insights into the Peptidoglycan Hydrolase Domain of FlgJ from *Salmonella typhimurium*. PLoS One. 2016;11(2):e0149204. Epub 2016/02/13. doi: 10.1371/journal.pone.0149204. PubMed PMID: 26871950; PubMed Central PMCID: PMCPMC4752226.

197. Buist G, Kok J, Leenhouts KJ, Dabrowska M, Venema G, Haandrikman AJ. Molecular cloning and nucleotide sequence of the gene encoding the major peptidoglycan hydrolase of *Lactococcus lactis*, a muramidase needed for cell separation. J Bacteriol. 1995;177(6):1554-63. Epub 1995/03/01. doi: 10.1128/jb.177.6.1554-1563.1995. PubMed PMID: 7883712; PubMed Central PMCID: PMCPMC176772.

198. Joris B, Englebert S, Chu CP, Kariyama R, Daneo-Moore L, Shockman GD, *et al*. Modular design of the *Enterococcus hirae* muramidase-2 and *Streptococcus faecalis* autolysin. FEMS Microbiol Lett. 1992;70(3):257-64. Epub 1992/03/15. doi: 10.1016/0378-1097(92)90707-u. PubMed PMID: 1352512.

199. Bury-Mone S, Nomane Y, Reymond N, Barbet R, Jacquet E, Imbeaud S, *et al*. Global analysis of extracytoplasmic stress signaling in *Escherichia coli*. PLoS Genet. 2009;5(9):e1000651. Epub 2009/09/19. doi: 10.1371/journal.pgen.1000651. PubMed PMID: 19763168; PubMed Central PMCID: PMCPMC2731931.

200. Gil F, Hernandez-Lucas I, Polanco R, Pacheco N, Collao B, Villarreal JM, *et al*. SoxS regulates the expression of the *Salmonella enterica* serovar Typhimurium ompW gene. Microbiology. 2009;155(Pt 8):2490-7. Epub 2009/05/23. doi: 10.1099/mic.0.027433-0. PubMed PMID: 19460824.

201. Lin XM, Wu LN, Li H, Wang SY, Peng XX. Downregulation of Tsx and OmpW and upregulation of OmpX are required for iron homeostasis in *Escherichia coli*. J Proteome Res. 2008;7(3):1235-43. Epub 2008/01/29. doi: 10.1021/pr7005928. PubMed PMID: 18220334.

202. Sainz T, Perez J, Villaseca J, Hernandez U, Eslava C, Mendoza G, *et al*. Survival to different acid challenges and outer membrane protein profiles of pathogenic *Escherichia coli* strains isolated from pozol, a Mexican typical maize fermented food. Int J Food Microbiol. 2005;105(3):357-67. Epub 2005/09/20. doi: 10.1016/j.ijfoodmicro.2005.04.017. PubMed PMID: 16169107.

203. Ye Y, Ling N, Gao J, Zhang X, Zhang M, Tong L, *et al*. Roles of outer membrane protein W (OmpW) on survival, morphology, and biofilm formation under NaCl stresses in *Cronobacter sakazakii*. J Dairy Sci. 2018;101(5):3844-50. Epub 2018/02/27. doi: 10.3168/jds.2017-13791. PubMed PMID: 29477536.

204. Xiao M, Lai Y, Sun J, Chen G, Yan A. Transcriptional Regulation of the Outer Membrane Porin Gene *ompW* Reveals its Physiological Role during the Transition from the Aerobic to the Anaerobic Lifestyle of *Escherichia coli*. Front Microbiol. 2016;7:799. Epub 2016/06/16. doi: 10.3389/fmicb.2016.00799. PubMed PMID: 27303386; PubMed Central PMCID: PMCPMC4886647.

205. Hu WS, Li PC, Cheng CY. Correlation between ceftriaxone resistance of *Salmonella enterica* serovar Typhimurium and expression of outer membrane proteins OmpW and Ail/OmpX-like protein, which are regulated by BaeR of a two-component system. Antimicrob Agents Chemother. 2005;49(9):3955-8. Epub 2005/08/30. doi: 10.1128/AAC.49.9.3955-3958.2005. PubMed PMID: 16127081; PubMed Central PMCID: PMCPMC1195446.

206. Preissler S, Deuerling E. Ribosome-associated chaperones as key players in proteostasis. Trends Biochem Sci. 2012;37(7):274-83. Epub 2012/04/17. doi: 10.1016/j.tibs.2012.03.002. PubMed PMID: 22503700.

207. Agris PF, Narendran A, Sarachan K, Vare VYP, Eruysal E. The Importance of Being Modified: The Role of RNA Modifications in Translational Fidelity. Enzymes. 2017;41:1-50. Epub 2017/06/12. doi: 10.1016/bs.enz.2017.03.005. PubMed PMID: 28601219.

208. Prossliner T, Skovbo Winther K, Sorensen MA, Gerdes K. Ribosome Hibernation. Annu Rev Genet. 2018;52:321-48. Epub 2018/11/27. doi: 10.1146/annurev-genet-120215-035130. PubMed PMID: 30476446.

209. Fernandez C, Diaz E, Garcia JL. Insights on the regulation of the phenylacetate degradation pathway from *Escherichia coli*. Environ Microbiol Rep. 2014;6(3):239-50. Epub 2014/07/02. doi: 10.1111/1758-2229.12117. PubMed PMID: 24983528.

210. Koch HG, Winterstein C, Saribas AS, Alben JO, Daldal F. Roles of the *ccoGHIS* gene products in the biogenesis of the cbb(3)-type cytochrome c oxidase. J Mol Biol. 2000;297(1):49-65. Epub 2000/03/08. doi: 10.1006/jmbi.2000.3555. PubMed PMID: 10704306.

211. Fu H, Yuan J, Gao H. Microbial oxidative stress response: Novel insights from environmental facultative anaerobic bacteria. Arch Biochem Biophys. 2015;584:28-35. Epub 2015/09/01. doi: 10.1016/j.abb.2015.08.012. PubMed PMID: 26319291.

212. Mironov A, Seregina T, Nagornykh M, Luhachack LG, Korolkova N, Lopes LE, *et al*. Mechanism of H2S-mediated protection against oxidative stress in *Escherichia coli*. Proc Natl Acad Sci U S A. 2017;114(23):6022-7. Epub 2017/05/24. doi: 10.1073/pnas.1703576114. PubMed PMID: 28533366; PubMed Central PMCID: PMCPMC5468659.

213. Chiang SM, Schellhorn HE. Regulators of oxidative stress response genes in *Escherichia coli* and their functional conservation in bacteria. Arch Biochem Biophys. 2012;525(2):161-9. Epub 2012/03/03. doi: 10.1016/j.abb.2012.02.007. PubMed PMID: 22381957.

214. Kempf B, Bremer E. Uptake and synthesis of compatible solutes as microbial stress responses to high-osmolality environments. Arch Microbiol. 1998;170(5):319-30. Epub 1998/11/18. doi: 10.1007/s002030050649. PubMed PMID: 9818351.

215. Bowles T, Metz AH, O'Quin J, Wawrzak Z, Eichman BF. Structure and DNA binding of alkylation response protein AidB. Proc Natl Acad Sci U S A. 2008;105(40):15299-304. Epub 2008/10/03. doi: 10.1073/pnas.0806521105. PubMed PMID: 18829440; PubMed Central PMCID: PMCPMC2563087.

216. Ramos CS, Yokoyama-Yasunaka JK, Guerra-Giraldez C, Price HP, Mortara RA, Smith DF, *et al*. *Leishmania amazonensis* META2 protein confers protection against heat shock and oxidative stress. Exp Parasitol. 2011;127(1):228-37. Epub 2010/08/18. doi: 10.1016/j.exppara.2010.08.004. PubMed PMID: 20713053.

217. Chatterji D, Ojha AK. Revisiting the stringent response, ppGpp and starvation signaling. Curr Opin Microbiol. 2001;4(2):160-5. Epub 2001/04/03. doi: 10.1016/s1369-5274(00)00182-x. PubMed PMID: 11282471.

218. Zhu M, Pan Y, Dai X. (p)ppGpp: the magic governor of bacterial growth economy. Curr Genet. 2019;65(5):1121-5. Epub 2019/04/18. doi: 10.1007/s00294-019-00973-z. PubMed PMID: 30993414.

219. Calamita G. The *Escherichia coli* aquaporin-Z water channel. Mol Microbiol. 2000;37(2):254-62. Epub 2000/08/10. doi: 10.1046/j.1365-2958.2000.02016.x. PubMed PMID: 10931322.

220. Keren I, Wu Y, Inocencio J, Mulcahy LR, Lewis K. Killing by bactericidal antibiotics does not depend on reactive oxygen species. Science. 2013;339(6124):1213-6. Epub 2013/03/09. doi: 10.1126/science.1232688. PubMed PMID: 23471410.

221. Linares JF, Gustafsson I, Baquero F, Martinez JL. Antibiotics as intermicrobial signaling agents instead of weapons. Proc Natl Acad Sci U S A. 2006;103(51):19484-9. Epub 2006/12/07. doi: 10.1073/pnas.0608949103. PubMed PMID: 17148599; PubMed Central PMCID: PMCPMC1682013.

222. Perkins HR, Nieto M. The chemical basis for the action of the vancomycin group of antibiotics. Ann N Y Acad Sci. 1974;235(0):348-63. Epub 1974/05/10. PubMed PMID: 4369274.

223. Choi J, Choi S, Choi J, Cha MK, Kim IH, Shin W. Crystal structure of *Escherichia coli* thiol peroxidase in the oxidized state: insights into intramolecular disulfide formation and substrate binding in atypical 2-Cys peroxiredoxins. J Biol Chem. 2003;278(49):49478-86. Epub 2003/09/25. doi: 10.1074/jbc.M309015200. PubMed PMID: 14506251.

224. Stokes JM, French S, Ovchinnikova OG, Bouwman C, Whitfield C, Brown ED. Cold Stress Makes *Escherichia coli* Susceptible to Glycopeptide Antibiotics by Altering Outer Membrane Integrity. Cell Chem Biol. 2016;23(2):267-77. Epub 2016/02/09. doi: 10.1016/j.chembiol.2015.12.011. PubMed PMID: 26853624.

225. McGuinness WA, Malachowa N, DeLeo FR. Vancomycin Resistance in *Staphylococcus aureus*. Yale J Biol Med. 2017;90(2):269-81. Epub 2017/06/29. PubMed PMID: 28656013; PubMed Central PMCID: PMCPMC5482303.

226. Munita JM, Arias CA. Mechanisms of Antibiotic Resistance. Microbiol Spectr. 2016;4(2). Epub 2016/05/27. doi: 10.1128/microbiolspec.VMBF-0016-2015. PubMed PMID: 27227291; PubMed Central PMCID: PMCPMC4888801.

227. Martinez JL. General principles of antibiotic resistance in bacteria. Drug Discov Today Technol. 2014;11:33-9. Epub 2014/05/23. doi: 10.1016/j.ddtec.2014.02.001. PubMed PMID: 24847651.

228. Olsson-Liljequist B, Nord CE. Methods for susceptibility testing of anaerobic bacteria. Clin Infect Dis. 1994;18 Suppl 4:S293-6. Epub 1994/05/01. doi: 10.1093/clinids/18.supplement_4.s293. PubMed PMID: 8086578.

229. Hirai K, Mitsuhashi S. Mechanisms of resistance to quinolones. Prog Drug Res. 1992;38:107-20. Epub 1992/01/01. PubMed PMID: 1609109.

230. Ma D, Cook DN, Alberti M, Pon NG, Nikaido H, Hearst JE. Molecular cloning and characterization of *acrA* and *acrE* genes of *Escherichia coli*. J Bacteriol. 1993;175(19):6299-313. Epub 1993/10/01. PubMed PMID: 8407802; PubMed Central PMCID: PMCPMC206727.

231. Nikaido H. Multiple antibiotic resistance and efflux. Curr Opin Microbiol. 1998;1(5):516-23. Epub 1999/03/06. PubMed PMID: 10066525.

232. Goldstein BP. Resistance to rifampicin: a review. J Antibiot (Tokyo). 2014;67(9):625-30. Epub 2014/08/15. doi: 10.1038/ja.2014.107. PubMed PMID: 25118103.

233. Tamma PD, Cosgrove SE, Maragakis LL. Combination therapy for treatment of infections with gram-negative bacteria. Clin Microbiol Rev. 2012;25(3):450-70. Epub 2012/07/06. doi: 10.1128/CMR.05041-11. PubMed PMID: 22763634; PubMed Central PMCID: PMCPMC3416487.

234. Gerber AU, Vastola AP, Brandel J, Craig WA. Selection of aminoglycoside-resistant variants of *Pseudomonas aeruginosa* in an *in vivo* model. J Infect Dis. 1982;146(5):691-7. Epub 1982/11/01. doi: 10.1093/infdis/146.5.691. PubMed PMID: 6813385.

235. Pechere JC, Marchou B, Michea-Hamzehpour M, Auckenthaler R. Emergence of resistance after therapy with antibiotics used alone or combined in a murine model. J Antimicrob Chemother. 1986;17 Suppl A:11-8. Epub 1986/03/01. doi: 10.1093/jac/17.suppl_a.11. PubMed PMID: 3086276.

236. Johnson DE, Thompson B. Efficacy of single-agent therapy with azlocillin, ticarcillin, and amikacin and beta-lactam/amikacin combinations for treatment of *Pseudomonas aeruginosa* bacteremia in granulocytopenic rats. Am J Med. 1986;80(5C):53-8. Epub 1986/05/30. PubMed PMID: 3636060.

237. Fibriansah G, Kovacs AT, Pool TJ, Boonstra M, Kuipers OP, Thunnissen AM. Crystal structures of two transcriptional regulators from *Bacillus cereus* define the conserved structural features of a PadR subfamily. PLoS One. 2012;7(11):e48015. Epub 2012/11/29. doi: 10.1371/journal.pone.0048015. PubMed PMID: 23189126; PubMed Central PMCID: PMCPMC3506622.

238. Jordan S, Junker A, Helmann JD, Mascher T. Regulation of LiaRS-dependent gene expression in *Bacillus subtilis*: identification of inhibitor proteins, regulator binding sites, and target genes of a conserved cell envelope stress-sensing two-component system. J Bacteriol. 2006;188(14):5153-66. Epub 2006/07/04. doi: 10.1128/JB.00310-06. PubMed PMID: 16816187; PubMed Central PMCID: PMCPMC1539951.

239. Thayer MM, Ahern H, Xing D, Cunningham RP, Tainer JA. Novel DNA binding motifs in the DNA repair enzyme endonuclease III crystal structure. EMBO J.

1995;14(16):4108-20. Epub 1995/08/15. PubMed PMID: 7664751; PubMed Central PMCID: PMCPMC394490.

240. Kuo CF, McRee DE, Fisher CL, O'Handley SF, Cunningham RP, Tainer JA. Atomic structure of the DNA repair [4Fe-4S] enzyme endonuclease III. Science. 1992;258(5081):434-40. Epub 1992/10/16. PubMed PMID: 1411536.

241. Jack DL, Yang NM, Saier MH, Jr. The drug/metabolite transporter superfamily. Eur J Biochem. 2001;268(13):3620-39. Epub 2001/07/04. PubMed PMID: 11432728.

242. Vastermark A, Almen MS, Simmen MW, Fredriksson R, Schioth HB. Functional specialization in nucleotide sugar transporters occurred through differentiation of the gene cluster EamA (DUF6) before the radiation of Viridiplantae. BMC Evol Biol. 2011;11:123. Epub 2011/05/17. doi: 10.1186/1471-2148-11-123. PubMed PMID: 21569384; PubMed Central PMCID: PMCPMC3111387.

243. Luo Q, Kumar P, Vickers TJ, Sheikh A, Lewis WG, Rasko DA, *et al*. Enterotoxigenic *Escherichia coli* secretes a highly conserved mucin-degrading metalloprotease to effectively engage intestinal epithelial cells. Infect Immun. 2014;82(2):509-21. Epub 2014/01/31. doi: 10.1128/IAI.01106-13. PubMed PMID: 24478067; PubMed Central PMCID: PMCPMC3911403.

244. Belousov MV, Bondarev SA, Kosolapova AO, Antonets KS, Sulatskaya AI, Sulatsky MI, *et al*. M60-like metalloprotease domain of the *Escherichia coli* YghJ protein forms amyloid fibrils. PLoS One. 2018;13(1):e0191317. Epub 2018/01/31. doi: 10.1371/journal.pone.0191317. PubMed PMID: 29381728; PubMed Central PMCID: PMCPMC5790219.

245. Paradis FW, Zhu H, Krell PJ, Phillips JP, Forsberg CW. The *xynC* gene from *Fibrobacter succinogenes* S85 codes for a xylanase with two similar catalytic domains. J Bacteriol. 1993;175(23):7666-72. Epub 1993/12/01. doi: 10.1128/jb.175.23.7666-7672.1993. PubMed PMID: 8244936; PubMed Central PMCID: PMCPMC206924.

246. Park J, Salyers AA. Characterization of the *Bacteroides* CTnDOT regulatory protein RteC. J Bacteriol. 2011;193(1):91-7. Epub 2010/11/03. doi: 10.1128/JB.01015-10. PubMed PMID: 21037014; PubMed Central PMCID: PMCPMC3019952.

247. Brinkman AB, Ettema TJ, de Vos WM, van der Oost J. The Lrp family of transcriptional regulators. Mol Microbiol. 2003;48(2):287-94. Epub 2003/04/05. PubMed PMID: 12675791.

248. Barnett MJ, Bittner AN, Toman CJ, Oke V, Long SR. Dual RpoH sigma factors and transcriptional plasticity in a symbiotic bacterium. J Bacteriol. 2012;194(18):4983-94. Epub 2012/07/10. doi: 10.1128/JB.00449-12. PubMed PMID: 22773790; PubMed Central PMCID: PMCPMC3430346.

249. Kreuzer KN. DNA damage responses in prokaryotes: regulating gene expression, modulating growth patterns, and manipulating replication forks. Cold Spring Harb Perspect Biol. 2013;5(11):a012674. Epub 2013/10/08. doi: 10.1101/cshperspect.a012674. PubMed PMID: 24097899; PubMed Central PMCID: PMCPMC3809575.

250. Manias DA, Dunny GM. Expression of Adhesive Pili and the Collagen-binding Adhesin ACE is Activated by ArgR Family Transcription Factors in *Enterococcus faecalis*. J Bacteriol. 2018. Epub 2018/07/11. doi: 10.1128/JB.00269-18. PubMed PMID: 29986940.

251. Fulde M, Willenborg J, de Greeff A, Benga L, Smith HE, Valentin-Weigand P, *et al*. ArgR is an essential local transcriptional regulator of the *arcABC* operon in *Streptococcus suis* and is crucial for biological fitness in an acidic environment. Microbiology. 2011;157(Pt 2):572-82. Epub 2010/10/16. doi: 10.1099/mic.0.043067-0. PubMed PMID: 20947575.

252. Ozturk H, Ozkirimli E, Ozgur A. Classification of Beta-lactamases and penicillin binding proteins using ligand-centric network models. PLoS One. 2015;10(2):e0117874. Epub 2015/02/18. doi: 10.1371/journal.pone.0117874. PubMed PMID: 25689853; PubMed Central PMCID: PMCPMC4331424.

253. Duez C, Vanhove M, Gallet X, Bouillenne F, Docquier J, Brans A, *et al*. Purification and characterization of PBP4a, a new low-molecular-weight penicillin-binding protein from *Bacillus subtilis*. J Bacteriol. 2001;183(5):1595-9. Epub 2001/02/13. doi: 10.1128/JB.183.5.1595-1599.2001. PubMed PMID: 11160090; PubMed Central PMCID: PMCPMC95044.

254. Brissette JL, Russel M, Weiner L, Model P. Phage shock protein, a stress protein of *Escherichia coli*. Proc Natl Acad Sci U S A. 1990;87(3):862-6. Epub 1990/02/01. doi: 10.1073/pnas.87.3.862. PubMed PMID: 2105503; PubMed Central PMCID: PMCPMC53368.

255. Chang TY, Chen HY, Chou YC, Cheng YH, Sun JR. *In vitro* activities of imipenem, vancomycin, and rifampicin against clinical *Elizabethkingia* species producing BlaB and GOB metallo-beta-lactamases. Eur J Clin Microbiol Infect Dis. 2019. Epub 2019/07/29. doi: 10.1007/s10096-019-03639-3. PubMed PMID: 31352669.

256. Cameron DR, Lin YH, Trouillet-Assant S, Tafani V, Kostoulias X, Mouhtouris E, *et al*. Vancomycin-intermediate *Staphylococcus aureus* isolates are attenuated for virulence when compared with susceptible progenitors. Clin Microbiol Infect. 2017;23(10):767-73. Epub 2017/04/12. doi: 10.1016/j.cmi.2017.03.027. PubMed PMID: 28396035.

257. Gump DW. Vancomycin for treatment of bacterial meningitis. Rev Infect Dis. 1981;3 suppl:S289-92. Epub 1981/11/01. PubMed PMID: 6896243.

258. Gomara M, Ramon-Garcia S. The FICI paradigm: Correcting flaws in antimicrobial in vitro synergy screens at their inception. Biochem Pharmacol. 2019;163:299-307. Epub 2019/03/06. doi: 10.1016/j.bcp.2019.03.001. PubMed PMID: 30836058.

APPENDICES

Appendix A: Permission to use Supplementary Figure 3 (As Figure 1 in this work).

SPRINGER NATURE LICENSE

TERMS AND CONDITIONS

Mar 03, 2020

This Agreement William Johnson ("You") and Springer Nature ("Springer Nature") consists of your license details and the terms and conditions provided by Springer Nature and Copyright Clearance Center.

License Number	4781380773739
License date	Mar 03, 2020
Licensed Content Publisher	Springer Nature
Licensed Content Publication	Antonie van Leeuwenhoek

Licensed Content Title	Revisiting the taxonomy of the genus Elizabethkingia using whole-genome sequencing, optical mapping, and MALDI-TOF, along with proposal of three novel Elizabethkingia species: Elizabethkingia bruuniana sp. nov., Elizabethkingia ursingii sp. nov., and Elizabethkingia occulta sp. nov.
Licensed Content Author	Ainsley C. Nicholson *et al*
Licensed Content Date	Aug 30, 2017
Type of Use	Thesis/Dissertation
Requestor type	academic/university or research institute
Format	electronic
Portion	figures/tables/illustrations
Number of figures/tables/illustrations	1
Will you be translating?	no
Circulation/distribution	1 - 29
Author of this Springer Nature content	no

Title	Illuminating the black box: Impact of vancomycin challenge and mutations conferring vancomycin resistance on Elizabethkingia
Institution name	Oklahoma State University
Expected presentation date	Apr 2020
Portions	Figure S3
Requestor Location	4100 W. 19th Ave B202 STILLWATER, OK 74074 United States Attn: 4100 W. 19th Ave
Total	0.00 USD
Terms and Conditions	

Springer Nature Customer Service Centre GmbH

Terms and Conditions

This agreement sets out the terms and conditions of the licence (the **Licence**) between you and **Springer Nature Customer Service Centre GmbH** (the **Licensor**). By clicking 'accept' and completing the transaction for the material (**Licensed Material**), you also confirm your acceptance of these terms and conditions.

Grant of License

1. 1. The Licensor grants you a personal, non-exclusive, non-transferable, world-wide licence to reproduce the Licensed Material for the purpose specified in your order only. Licences are granted for the specific use requested in the order and for no other use, subject to the conditions below.

1. 2. The Licensor warrants that it has, to the best of its knowledge, the rights to license reuse of the Licensed Material. However, you should ensure that the material you are requesting is original to the Licensor and does not carry the copyright of another entity (as credited in the published version).

1. 3. If the credit line on any part of the material you have requested indicates that it was reprinted or adapted with permission from another source, then you should also seek permission from that source to reuse the material.

Scope of Licence

2. 1. You may only use the Licensed Content in the manner and to the extent permitted by these Ts&Cs and any applicable laws.

2. 2. A separate licence may be required for any additional use of the Licensed Material, e.g. where a licence has been purchased for print only use, separate permission must be obtained for electronic re-use. Similarly, a licence is only valid in the language selected and does not apply for editions in other languages unless additional translation rights have been granted separately in the licence. Any content owned by third parties are expressly excluded from the licence.

2. 3. Similarly, rights for additional components such as custom editions and derivatives require additional permission and may be subject to an additional fee.

Please apply to

Journalpermissions@springernature.com/bookpermissions@springernature.com for these rights.

2. 4. Where permission has been granted **free of charge** for material in print, permission may also be granted for any electronic version of that work, provided that the material is incidental to your work as a whole and that the electronic version is essentially equivalent to, or substitutes for, the print version.

2. 5. An alternative scope of licence may apply to signatories of the STM Permissions Guidelines, as amended from time to time.

Duration of Licence

3. 1. A licence for is valid from the date of purchase ('Licence Date') at the end of the relevant period in the below table:

	Duration of Licence
Post on a website	12 months
Presentations	12 months
Scope of Licence	
Books and journals Lifetime of the edition in the language purchased	

Acknowledgement

4. 1. The Licensor's permission must be acknowledged next to the Licenced Material in print. In electronic form, this acknowledgement must be visible at the same time as the figures/tables/illustrations or abstract, and must be hyperlinked to the journal/book's homepage. Our required acknowledgement format is in the Appendix below.

Restrictions on use

5. 1. Use of the Licensed Material may be permitted for incidental promotional use and minor editing privileges e.g. minor adaptations of single figures, changes of format, colour and/or style where the adaptation is credited as set out in Appendix 1 below. Any other changes including but not limited to, cropping, adapting, omitting material that affect the meaning, intention or moral rights of the author are strictly prohibited.

5. 2. You must not use any Licensed Material as part of any design or trademark.

5. 3. Licensed Material may be used in Open Access Publications (OAP) before publication by Springer Nature, but any Licensed Material must be removed from OAP sites prior to final publication.

Ownership of Rights

6. 1. Licensed Material remains the property of either Licensor or the relevant third party and any rights not explicitly granted herein are expressly reserved.

Warranty

IN NO EVENT SHALL LICENSOR BE LIABLE TO YOU OR ANY OTHER PARTY OR

ANY OTHER PERSON OR FOR ANY SPECIAL, CONSEQUENTIAL, INCIDENTAL

OR INDIRECT DAMAGES, HOWEVER CAUSED, ARISING OUT OF OR IN

CONNECTION WITH THE DOWNLOADING, VIEWING OR USE OF THE

MATERIALS REGARDLESS OF THE FORM OF ACTION, WHETHER FOR BREACH

OF CONTRACT, BREACH OF WARRANTY, TORT, NEGLIGENCE, INFRINGEMENT

OR OTHERWISE (INCLUDING, WITHOUT LIMITATION, DAMAGES BASED ON

LOSS OF PROFITS, DATA, FILES, USE, BUSINESS OPPORTUNITY OR CLAIMS OF

THIRD PARTIES), AND

WHETHER OR NOT THE PARTY HAS BEEN ADVISED OF THE POSSIBILITY OF

SUCH DAMAGES. THIS LIMITATION SHALL APPLY NOTWITHSTANDING ANY FAILURE OF ESSENTIAL PURPOSE OF ANY LIMITED REMEDY PROVIDED HEREIN.

Limitations

8. 1. ***BOOKS ONLY:***Where **'reuse in a dissertation/thesis'** has been selected the following terms apply: Print rights of the final author's accepted manuscript (for clarity, NOT the published version) for up to 100 copies, electronic rights for use only on a personal website or institutional repository as defined by the Sherpa guideline (www.sherpa.ac.uk/romeo/).

Termination and Cancellation

9. 1. Licences will expire after the period shown in Clause 3 (above).

9. 2. Licensee reserves the right to terminate the Licence in the event that payment is not received in full or if there has been a breach of this agreement by you.

Appendix 1 — Acknowledgements:

For Journal Content:

Reprinted by permission from [**the Licensor**]: [**Journal Publisher** (e.g.

Nature/Springer/Palgrave)] [**JOURNAL NAME**] [**REFERENCE CITATION** (Article name, Author(s) Name), [**COPYRIGHT**] (year of publication)

For **Advance Online Publication papers:**
Reprinted by permission from [**the Licensor**]: [**Journal Publisher** (e.g.

Nature/Springer/Palgrave)] [**JOURNAL NAME**] [**REFERENCE CITATION** (Article name, Author(s) Name), [**COPYRIGHT**] (year of publication), advance online publication, day month year (doi: 10.1038/sj.[JOURNAL ACRONYM].)

For Adaptations/Translations:
Adapted/Translated by permission from [**the Licensor**]: [**Journal Publisher** (e.g.

Nature/Springer/Palgrave)] [JOURNAL NAME] [REFERENCE CITATION

(Article name, Author(s) Name), [**COPYRIGHT**] (year of publication)

Note: For any republication from the British Journal of Cancer, the following credit line style applies:

Reprinted/adapted/translated by permission from [**the Licensor**]: on behalf of Cancer

Research UK: : [**Journal Publisher** (e.g. Nature/Springer/Palgrave)] [**JOURNAL**

NAME] [**REFERENCE CITATION** (Article name, Author(s) Name), [**COPYRIGHT]** (year of publication)

For **Advance Online Publication** papers:
Reprinted by permission from The [**the Licensor**]: on behalf of Cancer Research UK:

[**Journal Publisher** (e.g. Nature/Springer/Palgrave)] [**JOURNAL NAME**]

[**REFERENCE CITATION** (Article name, Author(s) Name), [**COPYRIGHT**] (year of publication), advance online publication, day month year (doi: 10.1038/sj.

[JOURNAL ACRONYM])

For Book content:
Reprinted/adapted by permission from [**the Licensor**]: [**Book Publisher** (e.g.

Palgrave Macmillan, Springer etc) [**Book Title**] by [**Book author**(s)]

[**COPYRIGHT**] (year of publication)

Other Conditions:
Version 1.2

Questions? customercare@copyright.com or +1-855-239-3415 (toll free in the US) or +1-978-646-2777.

Appendix B: Significantly altered genes in *Elizabethkingia anophelis* R26 with and without vancomycin.

GeneID	Function	Functional Group	logFC	logCPM	FDR
BAZ09_000165	AraC family transcriptional regulator	Amino acid and protein metabolism	0.869	6.610	0.005
BAZ09_000170	cytochrome c oxidase accessory protein CcoG	Central Metabolism	1.353	6.172	0.008
BAZ09_000310	hypothetical protein	Hypothetical	0.733	5.433	0.010
BAZ09_000560	hypothetical protein	Hypothetical	0.974	7.933	0.004
BAZ09_000565	hypothetical protein	Hypothetical	-0.774047	5.25075	0.0111
BAZ09_000630	hypothetical protein	Hypothetical	1.330	10.354	0.008
BAZ09_000790	HAD family hydrolase	Central Metabolism	1.357	6.199	0.004
BAZ09_000950	ketoacyl-ACP synthase III	Fatty Acid Metabolism	-0.947927	7.24609	0.0036
BAZ09_001110	SusC/RagA family TonB-linked outer membrane protein	Transport	-0.808883	7.22775	0.0079
BAZ09_001350	nicotinamidase/pyrazinamidase	Central Metabolism	-0.755537	5.99570	0.0211
BAZ09_001410	S1/P1 Nuclease	Central Metabolism	-0.771453	7.31162	0.0056
BAZ09_001445	hypothetical protein	Hypothetical	-0.945945	6.19428	0.0318
BAZ09_001450	threonylcarbamoyl-AMP synthase	Amino acid and protein metabolism	-0.995259	6.11190	0.0138
BAZ09_001490	isopentenyl-diphosphate Delta-isomerase	Fatty Acid Metabolism	-0.73563	6.77839	0.0463
BAZ09_001555	hypothetical protein	Hypothetical	1.294	7.714	0.004
BAZ09_001570	carbamoyl-phosphate synthase small subunit	Amino acid and protein metabolism	-1.047153	6.60463	0.0091
BAZ09_001720	hypothetical protein	Hypothetical	0.826	8.618	0.036

BAZ09_001755	DUF2029 domain-containing protein	Hypothetical	-0.920382	6.36301	0.0056
BAZ09_001760	glycosyltransferase	Cell envelope metabolism	-0.70611	5.38371	0.0165
BAZ09_001765	polysaccharide deacetylase	Cell envelope metabolism	-0.838623	5.05939	0.0053
BAZ09_001770	glycosyltransferase family 1 protein	Cell envelope metabolism	-0.820203	5.41120	0.0079
BAZ09_001910	molybdenum cofactor biosynthesis protein MoaE	Central Metabolism	0.698	5.259	0.026
BAZ09_002025	translational GTPase TypA	Amino acid and protein metabolism	-0.980508	9.37567	0.0046
BAZ09_002065	preprotein translocase subunit SecD	Amino acid and protein metabolism	-0.794689	10.6177	0.0052
BAZ09_002105	hemolysin	Virulence	-0.859617	4.41428	0.0096
BAZ09_002110	hypothetical protein	Hypothetical	-0.884213	8.95163	0.0039
BAZ09_002120	cytidine deaminase	Central Metabolism	-1.097429	5.32199	0.0064
BAZ09_002135	hypothetical protein	Hypothetical	0.739	6.205	0.043
BAZ09_002140	transcriptional regulator	Virulence	-0.764769	5.46500	0.0136
BAZ09_002190	AraC family transcriptional regulator	Transcription	-0.70241	4.51333	0.0175
BAZ09_002235	low molecular weight phosphotyrosine protein phosphatase	Cell envelope metabolism	-0.789002	5.74866	0.0202
BAZ09_002240	SAM-dependent methyltransferase	Amino acid and protein metabolism	-0.927054	6.04234	0.0131
BAZ09_002410	ABC transporter ATP-binding protein	Transport	-0.75842	5.00086	0.0091
BAZ09_002450	uridine kinase	Central Metabolism	-0.772424	6.76401	0.0136

BAZ09_002455	septum formation inhibitor	Cell envelope metabolism	-0.717961	5.51623	0.0337
BAZ09_002465	class I SAM-dependent methyltransferase	Amino acid and protein metabolism	-0.755596	5.60580	0.0136
BAZ09_002495	hypothetical protein	Hypothetical	-0.745491	6.64568	0.0173
BAZ09_002545	homoserine kinase	Amino acid and protein metabolism	1.210	5.851	0.006
BAZ09_002550	threonine synthase	Amino acid and protein metabolism	1.660	7.081	0.003
BAZ09_002620	hypothetical protein	Hypothetical	-0.926172	5.16849	0.0067
BAZ09_002625	thioredoxin	Amino acid and protein metabolism	-1.137691	5.27651	0.0083
BAZ09_002660	redox-regulated ATPase YchF	Amino acid and protein metabolism	-0.790291	8.07562	0.0091
BAZ09_002690	DUF4268 domain-containing protein	Hypothetical	-0.900568	5.76294	0.019
BAZ09_002845	SMI1/KNR4 family protein	Stress response	0.869	7.034	0.008
BAZ09_002895	transcriptional regulator	Stress response	-0.920982	5.12431	0.0204
BAZ09_002915	hypothetical protein	Hypothetical	-0.826425	5.49689	0.0089
BAZ09_002940	cytochrome D ubiquinol oxidase subunit II	Central Metabolism	0.923	5.727	0.005
BAZ09_003035	ATP-binding protein	Cell envelope metabolism	0.954	7.496	0.010
BAZ09_003080	META domain-containing protein	Stress response	-0.969999	5.67570	0.0046
BAZ09_003285	polyprenyl synthetase family protein	Transport	-0.822059	7.05617	0.0119
BAZ09_003295	23S rRNA (adenine(2503)-C(2))-methyltransferase RlmN	Amino acid and protein metabolism	-1.264548	6.78409	0.003

BAZ09_003300	tRNA preQ1(34) S-adenosylmethionine ribosyltransferase-isomerase QueA	Amino acid and protein metabolism	-0.731376	9.29714	0.0056
BAZ09_003345	PorT family protein	Cell envelope metabolism	-0.785203	11.2012	0.0275
BAZ09_003350	PorT family protein	Transport	-0.90356	12.1818	0.0155
BAZ09_003355	PorT family protein	Transport	-1.016941	7.52365	0.0176
BAZ09_003495	hypothetical protein	Hypothetical	-1.009329	5.57341	0.0336
BAZ09_003595	30S ribosomal protein S6	Amino acid and protein metabolism	-0.833909	10.4065	0.008
BAZ09_003600	30S ribosomal protein S18	Amino acid and protein metabolism	-0.970738	10.0473	0.0036
BAZ09_003615	histone H1	Hypothetical	-1.325895	10.0289	0.0096
BAZ09_003695	hypothetical protein	Hypothetical	-0.7761	9.38959	0.0323
BAZ09_003780	aminopeptidase	Amino acid and protein metabolism	-0.799386	7.79109	0.0081
BAZ09_003815	signal peptidase I	Hypothetical	0.745	5.690	0.018
BAZ09_003870	RNA-binding transcriptional accessory protein	Stress response	-0.774388	6.23684	0.0101
BAZ09_003980	50S ribosomal protein L19	Amino acid and protein metabolism	-0.926988	10.8218	0.0036
BAZ09_004015	EamA family transporter	Transport	-0.706752	6.6664	0.008
BAZ09_004025	30S ribosomal protein S1	Amino acid and protein metabolism	-1.039581	12.2027	0.0099
BAZ09_004295	muramidase	Cell envelope metabolism	-1.155155	7.60310	0.0044
BAZ09_004395	signal recognition particle sRNA small type	Transcription	1.235	4.198	0.025
BAZ09_004505	VOC family protein		1.109	5.031	0.011

BAZ09_004535	lipid hydroperoxide peroxidase	Stress response	0.979	11.293	0.021
BAZ09_004645	SusC/RagA family TonB-linked outer membrane protein	Transport	1.216	5.574	0.004
BAZ09_004650	RagB/SusD family nutrient uptake outer membrane protein	Transport	1.184	4.281	0.008
BAZ09_004710	TonB-dependent receptor	Transport	1.350	4.398	0.003
BAZ09_004715	MFS transporter	Antimicrobial Resistance	0.971	5.635	0.004
BAZ09_004720	peptidase M12	Virulence	1.384	4.820	0.004
BAZ09_004725	hypothetical protein	Hypothetical	0.886	4.147	0.017
BAZ09_005285	short chain dehydrogenase	Fatty Acid Metabolism	0.820	4.645	0.031
BAZ09_005325	vitellogenin ii	Hypothetical	0.718	7.102	0.039
BAZ09_005340	flagellar motor protein MotB	Cell envelope	0.878	7.388	0.008
BAZ09_005705	DUF2938 domain-containing protein	Hypothetical	1.010	4.155	0.025
BAZ09_005710	N-acetyltransferase	Indeterminate	1.009	5.270	0.010
BAZ09_005785	2-iminoacetate synthase ThiH	Central Metabolism	-0.778347	5.68189	0.0202
BAZ09_005805	phosphomethylpyrimidine synthase ThiC	Central Metabolism	-0.739214	7.32775	0.0258
BAZ09_005810	thiamine biosynthesis protein ThiS	Central Metabolism	-0.772944	4.47804	0.04
BAZ09_005880	tRNA (adenosine(37)-N6)-threonylcarbamoyltransferase complex ATPase subunit type 1 TsaE	Amino acid and protein metabolism	-0.780429	4.92320	0.0089
BAZ09_005885	alanine dehydrogenase	Amino acid and protein metabolism	-0.762286	7.18474	0.0167
BAZ09_005890	hypothetical protein	Hypothetical	-0.937976	5.23865	0.0127

BAZ09_005965	30S ribosomal protein S15	Amino acid and protein metabolism	-0.782633	10.4279	0.0376
BAZ09_006215	aspartate kinase	Amino acid and protein metabolism	-0.759832	5.69816	0.0167
BAZ09_006320	hypothetical protein	Hypothetical	0.898	6.072	0.006
BAZ09_006325	hypothetical protein	Hypothetical	0.997	3.242	0.020
BAZ09_006335	hypothetical protein	Hypothetical	0.945	4.958	0.005
BAZ09_006755	tRNA-Met	Amino acid and protein metabolism	0.830	6.529	0.047
BAZ09_006840	hypothetical protein	Hypothetical	1.091	4.731	0.008
BAZ09_006900	hypothetical protein	Hypothetical	0.711	4.027	0.032
BAZ09_007005	MerR family transcriptional regulator	Transcription	0.925	5.022	0.011
BAZ09_007030	DUF779 domain-containing protein	Hypothetical	1.581	6.008	0.003
BAZ09_007035	alcohol dehydrogenase AdhP	Amino acid and protein metabolism	1.627	7.083	0.006
BAZ09_007040	aldehyde dehydrogenase	Central Metabolism	1.817	8.599	0.004
BAZ09_007585	NADPH-dependent assimilatory sulfite reductase hemoprotein subunit	Central Metabolism	0.697	4.670	0.020
BAZ09_007595	uroporphyrinogen-III C-methyltransferase	Central Metabolism	1.331	4.513	0.005
BAZ09_007600	cysteine synthase A	Amino acid and protein metabolism	1.147	4.510	0.006
BAZ09_007605	serine acetyltransferase	Amino acid and protein metabolism	1.315	4.059	0.010
BAZ09_007610	sulfate adenylyltransferase	Amino acid and protein metabolism	1.027	4.643	0.008

BAZ09_007615	sulfate adenylyltransferase subunit CysD	Amino acid and protein metabolism	1.088	4.191	0.008
BAZ09_007665	SH3 domain-containing protein	Signal Transduction	0.903	10.374	0.005
BAZ09_007670	BON domain-containing protein	Stress response	0.913	10.144	0.005
BAZ09_007705	arginine decarboxylase	Amino acid and protein metabolism	-1.011218	8.57549	0.0079
BAZ09_007980	hypothetical protein	Hypothetical	1.039	5.519	0.004
BAZ09_008030	efflux RND transporter periplasmic adaptor subunit	Antimicrobial Resistance	-0.736008	5.37367	0.0079
BAZ09_008400	hypothetical protein	Hypothetical	0.897	5.321	0.039
BAZ09_008520	phenylacetic acid degradation bifunctional protein PaaZ	Amino acid and protein metabolism	0.694	6.877	0.008
BAZ09_008560	alpha/beta hydrolase	Central Metabolism	0.790	4.630	0.019
BAZ09_008565	phenylacetate-CoA oxygenase subunit PaaI	Amino acid and protein metabolism	0.772	4.883	0.032
BAZ09_008570	1,2-phenylacetyl-CoA epoxidase subunit B	Amino acid and protein metabolism	0.998	3.900	0.017
BAZ09_008575	phenylacetate-CoA oxygenase subunit PaaA	Amino acid and protein metabolism	1.105	5.635	0.007
BAZ09_008640	zinc metalloprotease	Amino acid and protein metabolism	1.269	6.334	0.003
BAZ09_008815	hypothetical protein	Hypothetical	0.699	4.538	0.017
BAZ09_008865	hypothetical protein	Hypothetical	-0.833656	3.77936	0.0258
BAZ09_009065	DUF3467 domain-containing protein	Hypothetical	-0.756382	9.90817	0.0091
BAZ09_009090	hypothetical protein	Hypothetical	-0.999246	5.14505	0.0052
BAZ09_009360	3-oxoacyl-ACP reductase	Fatty Acid Metabolism	0.768	5.363	0.010
BAZ09_009365	glucosidase	Central Metabolism	0.698	7.385	0.020

BAZ09_009755	30S ribosomal protein S7	Amino acid and protein metabolism	-0.783786	9.89100	0.0304
BAZ09_009920	RagB/SusD family nutrient uptake outer membrane protein	Transport	1.696	6.697	0.001
BAZ09_009925	TonB-dependent receptor	Transport	1.356	7.493	0.004
BAZ09_010135	TonB-dependent receptor	Transport	-0.717373	6.37521	0.0103
BAZ09_010395	TonB-dependent receptor	Transport	-1.191581	6.35431	0.0018
BAZ09_010420	acetylornithine carbamoyltransferase	Amino acid and protein metabolism	-1.060272	7.17606	0.0026
BAZ09_010425	aspartate aminotransferase family protein	Amino acid and protein metabolism	-0.87747	7.70306	0.0053
BAZ09_010430	N-acetyl-gamma-glutamyl-phosphate reductase	Amino acid and protein metabolism	-0.797647	6.80589	0.008
BAZ09_010435	argininosuccinate synthase	Amino acid and protein metabolism	-0.763415	8.02057	0.0178
BAZ09_010440	N-acetyltransferase	Hypothetical	-0.922193	5.28012	0.0079
BAZ09_010540	DoxX family membrane protein	Hypothetical	0.726	6.220	0.047
BAZ09_010575	hypothetical protein	Hypothetical	-0.719009	8.09780	0.0071
BAZ09_010655	AadS family aminoglycoside 6-adenylyltransferase	Antimicrobial Resistance	1.093	6.970	0.009
BAZ09_010700	HlyD family secretion protein	Antimicrobial Resistance	-0.760215	6.60335	0.0089
BAZ09_010705	TolC family protein	Cell envelope metabolism	-0.789704	6.76814	0.0056
BAZ09_010710	TetR/AcrR family transcriptional regulator	Virulence	-0.865637	5.56410	0.0065
BAZ09_010860	ribose-phosphate pyrophosphokinase	Central Metabolism	-0.842993	8.29742	0.0248
BAZ09_011525	hypothetical protein	Hypothetical	-0.877562	6.51976	0.0036

BAZ09_011540	GLPGLI family protein	Hypothetical	-0.98176	6.25304	0.0036
BAZ09_011710	50S ribosomal protein L21	Amino acid and protein metabolism	-0.878887	10.9004	0.0089
BAZ09_011715	50S ribosomal protein L27	Amino acid and protein metabolism	-0.793757	10.1351	0.0083
BAZ09_012080	hypothetical protein	Hypothetical	-0.792865	3.75641	0.0177
BAZ09_012085	hypothetical protein	Hypothetical	-0.819053	4.68752	0.0214
BAZ09_012365	uroporphyrinogen-III synthase	Central Metabolism	-0.707944	9.55557	0.0088
BAZ09_012675	tRNA (guanosine(46)-N7)-methyltransferase TrmB	Amino acid and protein metabolism	-0.954831	6.80264	0.0167
BAZ09_012760	50S ribosomal protein L13	Amino acid and protein metabolism	-0.965751	10.7949	0.012
BAZ09_012765	30S ribosomal protein S9	Amino acid and protein metabolism	-0.942313	9.72274	0.013
BAZ09_012770	30S ribosomal protein S2	Amino acid and protein metabolism	-1.162682	10.9153	0.0136
BAZ09_012860	acetyl-CoA carboxylase, biotin carboxyl carrier protein	Transport	-0.855035	8.61621	0.0304
BAZ09_013215	cysteine--tRNA ligase	Amino acid and protein metabolism	0.808	9.828	0.040
BAZ09_013290	30S ribosomal protein S21	Amino acid and protein metabolism	-1.196875	10.4165	0.0263
BAZ09_013295	integrase	DNA Replication, Recombination, Repair	1.014	8.748	0.020
BAZ09_013300	ribosomal subunit interface protein	Amino acid and protein metabolism	1.657	11.398	0.003
BAZ09_013305	tRNA-Thr	Amino acid and protein metabolism	1.350	8.406	0.003
BAZ09_013345	OmpW family protein	Cell envelope metabolism	3.280	9.509	0.011

BAZ09_013360	50S ribosomal protein L11	Amino acid and protein metabolism	-0.932828	10.3830	0.0058
BAZ09_013365	50S ribosomal protein L1	Amino acid and protein metabolism	-1.378914	10.5952	0.0138
BAZ09_013370	50S ribosomal protein L10	Amino acid and protein metabolism	-1.31409	10.6277	0.0045
BAZ09_013580	GlsB/YeaQ/YmgE family stress response membrane protein	Stress response	0.870	9.284	0.008
BAZ09_013625	trigger factor	Amino acid and protein metabolism	-0.704747	11.0179	0.0395
BAZ09_013640	DUF3109 domain-containing protein	Hypothetical	-0.787834	5.78976	0.0091
BAZ09_013780	HU family DNA-binding protein	DNA Replication, Recombination, Repair	0.865	13.362	0.022
BAZ09_014045	bacteriocin	Hypothetical	0.908	6.170	0.028
BAZ09_014055	hypothetical protein	Hypothetical	0.887	4.801	0.006
BAZ09_014170	recombinase RecA	DNA Replication, Recombination, Repair	0.728	10.041	0.008
BAZ09_014225	DUF423 domain-containing protein	Hypothetical	0.705	6.972	0.010
BAZ09_014250	TonB-dependent siderophore receptor	Transport	-0.810706	5.23232	0.0335
BAZ09_014275	5'(3')-deoxyribonucleotidase	Central Metabolism	0.808	8.261	0.012
BAZ09_014345	DUF2207 domain-containing protein	Hypothetical	0.741	7.468	0.010
BAZ09_014405	aquaporin Z	Transport	1.392	8.778	0.001
BAZ09_014540	aspartate racemase murI	Cell envelope metabolism	-1.088208	4.63129	0.0044

BAZ09_014645	TonB-dependent siderophore receptor	Transport	-0.69693	7.37241	0.0432
BAZ09_014690	malate dehydrogenase	Central Metabolism	0.839	9.591	0.014
BAZ09_014920	ATP synthase F1 subunit gamma	Central Metabolism	-0.695977	9.98959	0.0079
BAZ09_015030	oxidoreductase	Central Metabolism	1.308	6.163	0.001
BAZ09_015185	hypothetical protein	Hypothetical	1.192	6.100	0.008
BAZ09_015195	anion permease	Transport	2.714	8.052	0.003
BAZ09_015200	succinate dehydrogenase	Central Metabolism	2.713	6.107	0.004
BAZ09_015205	succinate dehydrogenase flavoprotein subunit	Central Metabolism	2.452	7.989	0.004
BAZ09_015210	succinate dehydrogenase/fumarate reductase iron-sulfur subunit	Central Metabolism	2.323	7.314	0.006
BAZ09_015335	hypothetical protein	Hypothetical	0.930	5.377	0.005
BAZ09_015360	acyl-CoA dehydrogenase	Stress response	1.248	6.492	0.003
BAZ09_015430	DUF4920 domain-containing protein	Hypothetical	0.895	6.917	0.010
BAZ09_015440	VOC family protein	Transport	0.730	4.376	0.040
BAZ09_015460	chloride channel protein	Transport	0.700	8.220	0.028
BAZ09_015500	DUF5074 domain-containing protein	Hypothetical	-0.937269	6.57341	0.0067
BAZ09_015760	ABC transporter ATP-binding protein	Stress response	0.950	7.174	0.003
BAZ09_015770	hypothetical protein	Hypothetical	1.047	4.053	0.006
BAZ09_015775	hypothetical protein	Hypothetical	1.527	4.094	0.003
BAZ09_015785	vitamin K epoxide reductase	Amino acid and protein metabolism	0.952	6.119	0.004

BAZ09_015790	peptidase	Amino acid and protein metabolism	1.196	8.332	0.004
BAZ09_015795	hypothetical protein	Hypothetical	0.860	6.859	0.034
BAZ09_015850	hypothetical protein	Hypothetical	0.705	4.020	0.038
BAZ09_015855	hypothetical protein	Hypothetical	0.925	6.157	0.011
BAZ09_016030	hypothetical protein	Hypothetical	-0.818784	6.76456	0.0202
BAZ09_016185	cytochrome C oxidase Cbb3	Central Metabolism	1.312	12.258	0.009
BAZ09_016610	hemolysin	Virulence	0.802	11.106	0.020
BAZ09_016625	hypothetical protein	Hypothetical	1.155	9.042	0.004
BAZ09_016690	DNA-binding protein	Hypothetical	-0.70618	6.01411	0.008
BAZ09_016930	glycosyl hydrolase	Central Metabolism	0.694	6.209	0.008
BAZ09_017025	hypothetical protein	Hypothetical	1.224	6.278	0.017
BAZ09_017070	ABC transporter ATP-binding protein	Antimicrobial Resistance	-0.726503	4.07636	0.0318
BAZ09_017115	VIT family protein	Transport	0.989	6.904	0.005
BAZ09_017395	TonB-dependent receptor	Transport	0.726	8.818	0.014
BAZ09_017615	4-hydroxyphenylpyruvate dioxygenase	Amino acid and protein metabolism	1.077	7.924	0.005
BAZ09_017620	4-hydroxybutyrate CoA-transferase	Central Metabolism	0.987	7.163	0.020
BAZ09_017675	integration host factor subunit beta	DNA Replication, Recombination, and Repair	-0.955912	8.77113	0.0082
BAZ09_017735	hypothetical protein	Hypothetical	-0.788288	9.51064	0.0082
BAZ09_017760	insulinase family protein	Central Metabolism	-0.970784	5.29352	0.0036
BAZ09_017785	MFS transporter	Transport	-0.72094	5.42479	0.0197
BAZ09_017800	hypothetical protein	Hypothetical	1.860	10.095	0.001
BAZ09_017805	polyisoprenoid-binding protein	Fatty Acid Metabolism	1.110	7.005	0.003

BAZ09_017910	1-(5-phosphoribosyl)-5-[(5-phosphoribosylamino)methylideneamino]imidazole-4-carboxamide isomerase	Amino acid and protein metabolism	0.775	6.799	0.047
BAZ09_018020	hypothetical protein	Hypothetical	0.780	10.108	0.005
BAZ09_018025	hypothetical protein	Hypothetical	-0.840981	9.02751	0.0307
BAZ09_018030	porin family protein	Cell envelope metabolism	-1.37215	7.69120	0.0053
BAZ09_018325	methionine ABC transporter substrate-binding protein MetQ	Transport	1.690	5.589	0.001
BAZ09_018330	D-methionine ABC transporter permease MetI	Transport	1.868	4.771	0.001
BAZ09_018335	DL-methionine transporter ATP-binding subunit	Transport	1.600	6.013	0.014
BAZ09_018400	inorganic phosphate transporter	Transport	-1.128711	7.68782	0.0025
BAZ09_018405	DUF47 domain-containing protein	Hypothetical	-1.287161	7.08201	0.003
BAZ09_018655	linear amide C-N hydrolase	Cell envelope metabolism	0.701	9.832	0.046

VITA

William L. Johnson

Candidate for the Degree of

Doctor of Philosophy

Thesis: ILLUMINATING THE BLACK BOX: ASPECTS OF *ELIZABETHKINGIA* EPIDEMIOLOGY AND ANTIMICROBIAL RESISTANCE

Major Field: Biochemistry and Molecular Biology

Biographical:

Education:

Completed the requirements for the Doctor of Philosophy in Biochemistry and Molecular Biology at Oklahoma State University, Stillwater, Oklahoma in May, 2020.

Completed the requirements for the Master of Public Health in Epidemiology at the University of Colorado-Denver, Denver, Colorado in 2016.

Completed the requirements for the Master of Science in Biology at New Mexico State University, Las Cruces, New Mexico in 2014.

Completed the requirements for the Bachelor of Science in Microbiology at New Mexico State University, Las Cruces, New Mexico in 2011.

Experience:

Teaching Assistant, Department of Biochemistry and Molecular Biology, Oklahoma State University, 2016 – 2020.

Teaching/Research Assistant, Department of Biology, New Mexico State University, 2011 – 2014.

Undergraduate Researcher, Department of Biology, New Mexico State University, 2008 – 2011.

Professional Memberships:

OSU Biochemistry and Molecular Biology Graduate Student Association, American Association for the Advancement of Science, American Society for Biochemistry and Molecular Biology, American Society of Microbiology, Phi Kappa Phi National Honor Society, NMSU Biology Graduate Student Organization.